WATER MOVEMENT IN A STRATIFIED AND INCLINED SNOWPACK: IMPLICATIONS FOR WET SLAB AVALANCHES

by

Erich Hans Peitzsch

A thesis submitted in partial fulfillment
of the requirements for the degree

of

Master of Science

in

Earth Sciences

MONTANA STATE UNIVERSITY
Bozeman, Montana

April 2009

APPROVAL

of a thesis submitted by

Erich Hans Peitzsch

This thesis has been read by each member of the thesis committee and has been found to be satisfactory regarding content, English usage, format, citation, bibliographic style, and consistency, and is ready for submission to the Division of Graduate Education.

Dr. Katherine Hansen

Dr. Karl Birkeland

Approved for the Department of Earth Sciences

Dr. Stephan Custer

Approved for the Division of Graduate Education

Dr. Carl A. Fox

STATEMENT OF PERMISSION TO USE

In presenting this thesis in partial fulfillment of the requirements for a Master's degree at Montana State University, I agree that the Library shall make it available to borrowers under rules of the Library.

If I have indicated my intention to copyright this thesis by including a copyright notice page, copying is allowable only for scholarly purposes, consistent with "fair use" as prescribed in the U.S. Copyright Law. Requests for permission for extended quotation from or reproduction of this thesis in whole or in parts may be granted only by the copyright holder.

Erich Hans Peitzsch

April 2009

ACKNOWLEDGEMENTS

Many thanks to my committee Karl Birkeland, Katherine Hansen, and Steve Custer for providing me guidance, patience, and encouragement throughout this process. I would also like to thank Eric Lutz for his time, effort, and patience in helping me with the SnowMicroPen portion of this project, and for general discussion and guidance. This research would have been much more difficult and lonely without the assistance of many individuals who helped in the field. I would also like to thank Dan Fagre and the USGS Northern Rocky Mountain Science Center for support with research in Glacier National Park, as well as Mark Dundas for his assistance with field work along the Going-to-the-Sun Road.

This work was made possible through funding from the University of Montana Rocky Mountain Cooperative Extension Unit/Crown of the Continent Research Learning Center Jerry O'Neal Fellowship for work in Glacier National Park, the Montana State University Barry Bishop scholarship, American Avalanche Association, American Alpine Club, Mazamas, and American Institute for Avalanche Research and Education.

Most importantly, I owe much gratitude to my family and friends, particularly my wife, Laura Fay.

TABLE OF CONTENTS

TABLE OF CONTENTS - CONTINUED

LIST OF TABLES

Table Page

LIST OF TABLES - CONTINUED

Table Page

LIST OF TABLES - CONTINUED

Table Page

LIST OF FIGURES

Figure Page

LIST OF FIGURES - CONTINUED

Figure Page

LIST OF FIGURES - CONTINUED

Figure Page

LIST OF FIGURES - CONTINUED

Figure Page

LIST OF FIGURES - CONTINUED

Figure Page

LIST OF FIGURES - CONTINUED

Figure Page

LIST OF FIGURES - CONTINUED

Figure Page

LIST OF FIGURES - CONTINUED

Figure Page

LIST OF FIGURES - CONTINUED

Figure Page

LIST OF FIGURES - CONTINUED

Figure Page

LIST OF FIGURES - CONTINUED

Figure Page

ABSTRACT

Wet snow avalanches are dangerous and can be particularly difficult to predict. The rate of change from safe snow conditions to dangerous snow conditions occurs rapidly in a wet snowpack, often in response to water production and movement. This research focused on the relationship between snow stratigraphy and water movement in an inclined snowpack. Concentrating on transitions that impede water and flow finger formation within the snowpack, dye tracer was mixed with water and applied to a stratified snowpack to observe and measure the movement of water in various snow grain types, sizes, densities, and temperatures. There were two types of layer transitions that impeded water. Water was impeded at capillary boundaries caused by fine grains over coarse grains. It was also impeded at hydraulic conductivity boundaries, such as ice layers. In layer transitions that impeded water, the grain size of the layer above was significantly smaller than the layer below. The layer above a transition that impeded water was also significantly less dense than the layer below the transition. A qualitative analysis of grain type showed that there was no relationship between grain types in the layer above or below a transition and whether they will or will not impede water.

A SnowMicroPen (SMP) was used to measure changes in structural element length to identify capillary boundaries. Results from SMP measurements indicate that microstructural analysis of the snowpack aids in characterizing capillary boundaries that impede water flow. The step change, rate of change, and percent increase were significantly larger in capillary boundaries than transitions that did not impede water for the entire dataset from all 8 sessions. When all transitions were ranked according to absolute change for each profile, capillary boundaries consistently ranked in the top two of all transitions evident within each SMP profile.

The amount of water needed to produce flow fingers was highly variable. There was no significant relationship between the amount of water necessary to form flow fingers and snow density, snow grain size, snow temperature, or grain type. Layer transitions that impeded vertical water movement and flow finger formation may both play a large role in wet slab avalanche formation.

CHAPTER 1

INTRODUCTION

Snow avalanches threaten life and property in mountainous areas worldwide. Most avalanche fatalities occur due to dry slab avalanches. However, wet snow avalanches are also dangerous and can be particularly difficult to predict because they are relatively poorly understood (Kattelmann, 1984; Reardon and Lundy, 2004; Baggi and Schweizer, 2008). Though most scientific literature addresses dry snow avalanches, nearly one in 10 (9 %) U.S. avalanche fatalities since 1950 have resulted from wet snow avalanches (Atkins, 2005; WWAN, 2006). Wet loose avalanches involve surficial layers in the snowpack and occur in response to increasing water content which disintegrates inter-grain bonds, while wet slab avalanches occur due to a failure at depth in the snowpack. Wet slab avalanches occur because of the presence of liquid water in the snowpack, but the water decreases the strength of an entire layer deeper in the snowpack (McClung and Schaerer, 1993). Of 30 individuals killed in wet slabs since 1950, 47 % were naturally triggered avalanches, 35 % were human triggered, and 17 % were unknown (Atkins, 2005). Thus, wet slab avalanche fatalities are more likely to involve natural avalanches than dry snow avalanche fatalities.

Wet snow avalanches impact recreationists, transportation corridors, and ski areas. Reardon and Lundy (2004) documented extensive wet slab activity on roads in Glacier National Park, USA, and reported several wet avalanche accidents in 71 seasons of clearing and opening the Going-to-the-Sun Road, including a 1964 wet slab that

carried a bulldozer and an operator off the road. In some ski areas, such as Bridger Bowl, Montana, poorly understood wet snow avalanches often create more difficulty for the ski patrol than better-understood dry snow avalanches because of unpredictability (Johnson, 2006). An increase in global mean temperature may also lead to a higher frequency of wet snow avalanches in the future. As snow may be precipitated at warmer temperatures, rain-on-snow events might become more frequent, and the snowpack itself might trend toward a wetter one. The above examples illustrate the need to achieve a more thorough understanding of wet slab avalanches.

The manner in which water flows through a snowpack has many implications for avalanche hazard. Forecasting wet slab avalanches requires considering the complexities of water percolation through the stratified snowpack, and the interaction of that water with various snowpack layers (Conway, 2004; Baggi and Schweizer, 2008). While research has focused on water flow in snow and wet snow metamorphism (Colbeck, 1973a, 1973b, 1974, 1976, 1978, 1979; Marsh and Woo, 1984), few studies exist investigating the movement of water and wet slab avalanches (Kattelmann, 1984; Reardon and Lundy, 2004; Techel et al., 2008). Water flow occurs because of melting within the snowpack or a rain-on-snow event (Heywood, 1988; Conway and Raymond, 1993; Conway and Benedict, 1994; Conway, 2004). Both situations, under optimal conditions, have the tendency to cause wet slab avalanches.

A dearth of research exists on the topic of forecasting for wet slab avalanches, which inherently involves water movement through the snowpack (Kattelmann, 1984; Reardon and Lundy, 2004). Most wet slab avalanche forecasting knowledge comes from

observational studies (Heywood, 1988; Reardon and Lundy, 2004). Thus, there is a need for simple tools and guidelines that aid avalanche practitioners (e.g. ski patrollers and avalanche forecasters) in forecasting wet slab avalanches during rain-on-snow events as well as during the transition from a dry snowpack to a wet one in the spring. This transition is critical in wet slab avalanche formation because often it is the rapid introduction of free water into a dry snowpack that causes wet slab release (Techel et al., 2008).

To achieve a comprehensive knowledge of wet slab avalanches it is important to understand the inputs in the process of wet slab formation. The interaction of water movement and snowpack stratigraphy is one such component that dictates the wet slab avalanche regime (Fig. 1) (Kattelmann, 1984; Waldner et al., 2004). Preferential flow of water and layer transitions that impede vertical water movement that result from this interaction are critical in understanding wet slab avalanche mechanics (Fig. 1, 2, and 3). The production of water from snowmelt or rainfall influences snow grain contact thus affecting snow stability (Kattelmann, 1987). Favorable snowpack conditions that can lead to a wet slab avalanche require two main components: change in strength of a buried weak layer in response to water and a cohesive slab above this weak layer that may be mostly dry or moist (McClung and Schaerer, 1993; Reardon and Lundy, 2004). Preferential flow (or flow fingering) allows water to penetrate to a buried weak layer without appreciably wetting the entire slab above (Colbeck, 1976). Once the entire slab above the weak layer becomes wet, then the regime of water flow and the resulting type of avalanche change (Fig. 1).

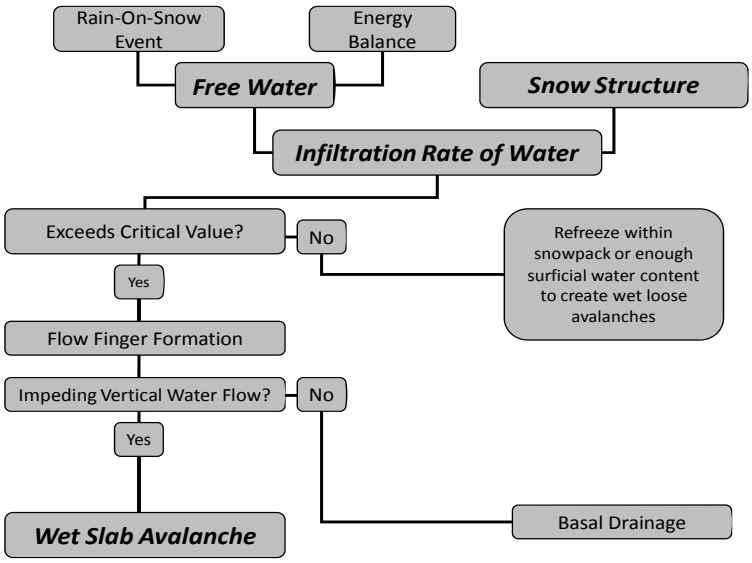

Figure 1: Schematic detailing factors leading to wet slab production. As water infiltrates at a certain rate through the snowpack it exceeds a critical value where it begins to flow preferentially. When this preferential movement of water reaches a capillary barrier that is also a weak layer a wet slab avalanche may occur.

Water can flow laterally in a snowpack based on stratigraphy in two major ways (Colbeck, 1973a; Wankiewicz, 1979; Waldner et al., 2004). Capillary boundaries force water to move along a potential weak layer and affect the bonds between the grain types and ultimately affect snowpack stability (Fig. 2). Capillary boundaries in a snowpack result from fine grains over coarse grains (e.g. rounded grains over depth hoar). The coarse grains have almost all larger pores relative to the layer of fine grains above, and the smaller diameter pores retain water against higher suctions than do larger pores because of capillary forces, and have a more negative capillary pressure. Thus, water is held within the layer of fine grains and cannot move through to the layer of coarse grains

until these capillary forces are overcome by the addition of more water (Hornberger et al. 1998).

A hydraulic conductivity boundary also impedes vertical water movement due to a change in hydraulic conductivity between adjacent layers (Fig. 3). Hydraulic conductivity is the ability of a porous medium to transmit liquid water (Hornberger et al. 1998). More porous media will conduct water more readily than less porous media. A layer of rounded grains over a melt-freeze crust is an example of a hydraulic conductivity boundary. A hydraulic conductivity boundary can also exist in the form of water reaching the ground/snow interface and moving downslope. This may lead to lubrication at the interface and plays a role in the formation of glide slab avalanches (McClung and Schaerer, 1993). Water movement in snow is complex, and needs to be addressed when considering wet slab processes. Thus, this research aimed to enhance this understanding of water movement through the investigation of water movement through an inclined and stratified snowpack.

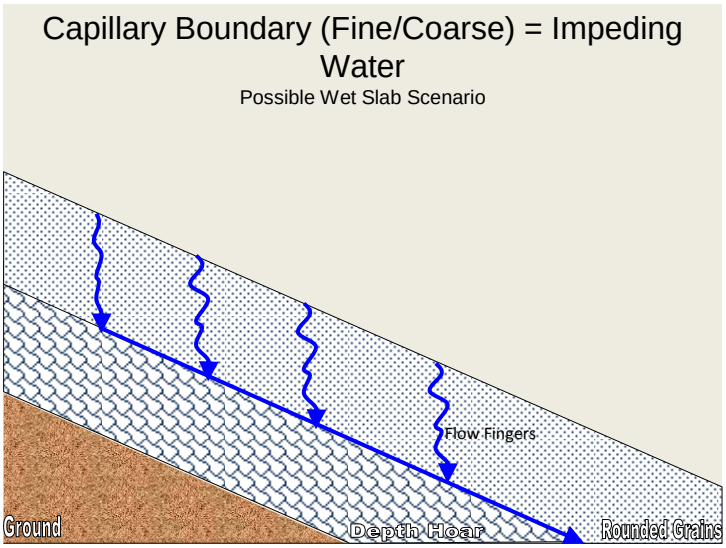

Figure 2: Schematic of snowpack and associated water movement that leads to wet slab avalanches. As water (blue lines) moves preferentially through the slab above (e.g. rounded grains) and reaches an impermeable layer below (e.g. depth hoar), it then moves laterally. As it moves laterally it decreases the contact between individual snow grains (Colbeck 1973) thus decreasing the strength of that layer and ultimately the stability.

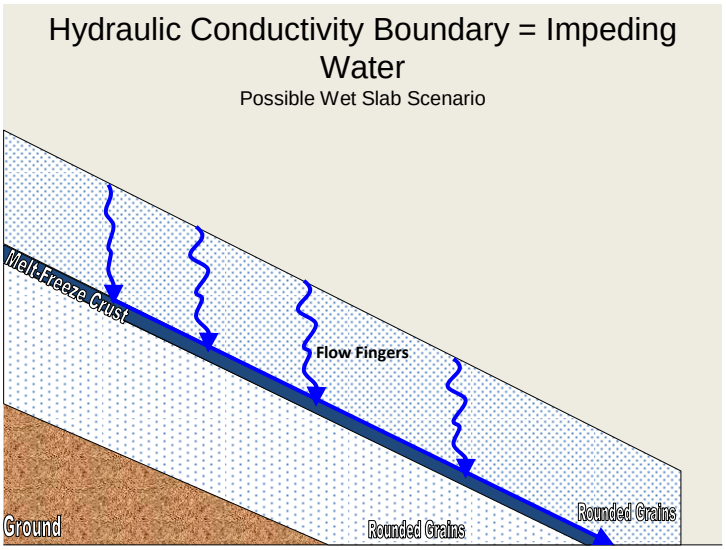

Figure 3: Schematic of snowpack and water movement that impedes vertical movement of water. An ice layer, in this case a melt-freeze crust, serves to impede vertical water movement because it has a lower hydraulic conductivity than the rounded grains above. Water moves laterally and may affect bonding between the rounded grains and the melt-freeze crust.

Since wet slab avalanches result from the interaction of specific snowpack composition and stratigraphy with free water in the snowpack, this research focused on the affect of composition and stratigraphy on water movement within the snowpack. It allowed me to follow the transport of free water in the upper snowpack through the lower portions of a stratified snowcover. The objective of this research was to identify measurable factors that might indicate wet slab conditions. I hypothesized that differences in snowpack stratigraphy influence preferential water flow within the snowpack, including flow fingering and vertical water movement impedance. The work focused on the following questions:

1. Do snow grain size, layer density, layer hand hardness, snow temperature, and snow grain type affect flow finger formation as free water is introduced to a dry and wet snowpack?
2. Do snow grain size, layer density, layer hand hardness, snow temperature, and snow grain type affect vertical water movement in a snowpack, and, if so, what are the characteristics of layer transitions that impede vertical water movement (including capillary boundaries and hydraulic conductivity boundaries)?
3. Can the SnowMicroPen (SMP) be used to aid in identifying potential layer capillary boundaries in the snowpack?

This research aims to enhance an understanding of and aid in forecasting for wet slab avalanches. Water movement in snow has been documented extensively through both laboratory experiments and field studies (Wakahama, 1968; Marsh and Woo, 1984;

Kattelmann, 1987; Illangasekare et al., 1990; Schneebeli, 1995; Pfeffer et al., 1996; Singh et al., 1997; Coleou et al., 1998; Williams et al., 1999; Waldner et al., 2004). However, investigating water movement in light of potential wet slab avalanche activity is limited (Kattelmann, 1984; Conway et al., 1988; Heywood 1988; Conway and Raymond, 1993; Techel et al., 2008). There is a need for an investigation into mechanisms driving this activity such as the characteristics of layer transitions that impede water flow and preferential flow. To my knowledge, this is the first work investigating layer transitions that impede water flow utilizing the SMP. These methods allowed me to examine relationships between snowpack structure and the behavior of water within the snowpack. I anticipated that certain layers in the snowpack, specifically capillary boundaries and hydraulic conductivity boundaries, would serve to impede vertical water flow and direct water laterally, and would also allow preferential flow to form depending on the amount of free water infiltrating through the snowpack. In general, the snow stratigraphy variables can be easily measured through simple snowpit measurements and observations thus allowing practitioners an easily accessible means to monitor snow conditions in the time leading up to possible wet slab avalanche cycles, and ultimately aiding in avalanche forecasting.

CHAPTER 2

LITERATURE REVIEW

Wet Slab Avalanche Processes

Wet slab avalanches occur less frequently than dry snow avalanches, but can be equally destructive (Kattelmann, 1984; McClung and Schaerer, 1993). The mechanism driving wet snow avalanches contrasts with that of dry slab avalanches. Wet snow avalanches depend upon the introduction of liquid water in the snowpack thus changing the shear strength and decreasing slope stability, whereas dry slab avalanches typically occur because of an increase in shear stress (Kattelmann, 1984). While a few studies have focused on shear strength and wet snow layers near the surface (Brun and Rey, 1986; Trautman et al., 2006), only one study in the Cascade Range, WA, USA, investigated the effect of a rain-on-snow event on shear strength in relation to wet slab avalanches (Conway and Raymond, 1993). They suggest that the immediate release of wet slabs ~30-50 cm deep during a rain-on-snow event results from one of the following mechanisms acting on the snow surface: downslope stress increase due to precipitation, inertial loading from smaller surficial avalanche activity, an increase in tensile stress deeper in the slab due to a decrease in tensile strength in the top 10-20 cm in the snowpack, and finally water weakening grain bonds thus causing an increase in tensile cracks in moist surface snow.

Similar mechanisms are thought to drive wet slab release after snowmelt events during the spring. Conway and Raymond (1993) showed that the introduction of free water in the snowpack causes melting and disintegration of bonds between snow grains thus affecting slope stability. Bond disintegration occurs because of lateral spreading along an impermeable boundary. They also observed increased vertical strain during periods of water infiltration through a horizontal snowpack. Thus, it is possible that as grains metamorphose due to the presence of water on a slope this vertical strain leads to slope instability. Heywood (1988) suggested a different mechanism where water moves laterally along an impermeable boundary for a length of time and the liquid water content increases within the upper layer, then creep and glide rates increase. This increase in velocity of the upper layer compared to the lower dry layer increases downslope shear stress and could result in a shear failure. The instability is released through an avalanche, refreezing of ponded water at the impermeable boundary, drainage out the bottom of the snowpack, or melting of the overlying slab itself thus reducing stress (Kattelmann, 1984). Thus, the movement of water within the snowpack clearly affects slope stability and illustrates the importance of understanding preferential flow and lateral water movement for wet slab avalanche forecasting.

Wet Slab Avalanche Forecasting

Wet slab avalanches can occur because of added stress during the onset of rain or a period of time after the onset of a rain-on-snow event. Conway and Raymond (1993) state

that forecasting for delayed wet slab avalanches is more difficult than forecasting for avalanches immediately after a rain-on-snow event. The occurrence of avalanches immediately after a rain-on-snow event can be forecasted using meteorological predictions to assess precipitation amounts for the incoming storm. Conversely, the accuracy of forecasting for delayed wet slab avalanche activity is far less accurate. Knowing the effects of the interaction between water movement and variable snow stratigraphy is essential (Conway and Raymond, 1993). Wet slab avalanches that occur during the transition from a dry snowpack to a wet spring snowpack are just as difficult to forecast as delayed avalanches after rain and pose a great concern for forecasters (Reardon and Lundy, 2004; Hartman and Borgeson, 2008).

For ski area managers, the use of artificial control methods such as explosives often proves ineffective in wet snow because shear fracture propagation in wet snow requires much more energy than in dry snow (McClung and Schaerer, 1993). This appears to be the circumstance in radiation-induced wet slab avalanches, but for rain-on-snow events, control work with explosives as reported in the literature seemed to have been effective. Avalanche forecasters along the Milford Road in New Zealand found that the timing of explosives was critical in rain-on-snow events (Conway, 2004). In the Sierra Nevada in California, Heywood (1988) also confirmed that the timing of control work using explosives was critical. He noted that explosives are effective only when utilized in the early stages of rainfall due to the immediate stresses acting on the upper layers of the snowpack. Improvement of our understanding of the relationship between water movement in snow and wet slab avalanches may improve forecasting decisions.

Seasonal Snowpack Transition

Slope stability in wet snow avalanches depends on the metamorphism of wet snow and the topic has received much attention (Wakahama, 1968; Colbeck, 1973, 1979; Denoth, 1980, 2003). The introduction of liquid water to a dry snowpack causes an increase in grain growth and a rounding of individual grains. As the liquid water content of snow layers change so do the mechanical processes (Colbeck, 1973b). When water saturation levels vary between zero to 20 %, two types of water regimes exist: pendular and funicular. Theoretical and experimental evidence shows that at around 7 % volumetric water content, a transition between these two types of water regimes takes place (Colbeck, 1973b; Denoth, 1980). The pendular, or low water content, regime exists between zero and 7 % and consists of air in contiguous space between individual snow grains (Colbeck, 1973b). In this regime, grains grow and cluster as they become more stable. As the volumetric water content increases to greater than 7 % the funicular regime becomes the dominant process. In this regime, water is continuous throughout the pore space and the increased amount of liquid water accelerates grain growth resulting in large grains with less grain-to-grain contacts between them than exists in their initial condition (Wakahama, 1968) (Fig. 4). This ultimately reduces contact between grains and can result in less mechanical strength in the snowpack as well (Kattelmann, 1984).

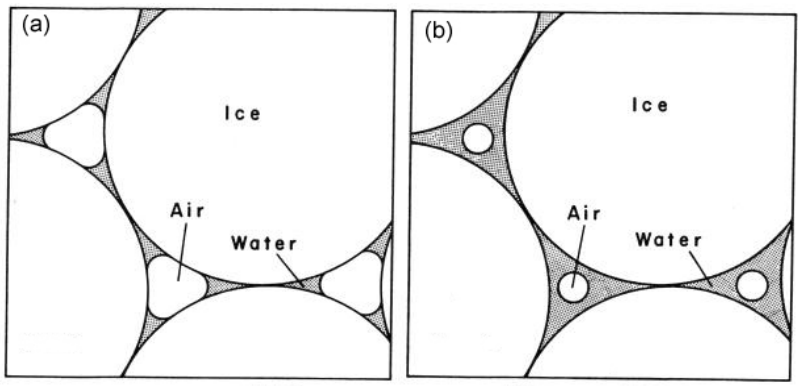

Figure 4: Two different regimes of liquid water content in snow: (a) The pendular regime exists when air is contiguous throughout the pore space between individual grains. This typically occurs up to 7 % water volume content. (b) The funicular regime exists when liquid water is continuous throughout the pore space, and air space is reduced. (Colbeck, 1973b, p. 1).

At the transition from pendular to funicular regimes in surface snow, water begins infiltrating deeper into the snowpack (Colbeck, 1973b). Increased avalanche activity can occur when volumetric liquid water content is greater than 7 % (Ambach and Howorka, 1965) illustrating the importance of this transition.

The rate of change from safe snow conditions to dangerous snow conditions can happen very rapidly in a wet snowpack. For example, Trautman et al. (2006) documented a case where conditions for wet, loose snow avalanches progressed from extremely stable to extremely unstable conditions in less than 20 minutes. By testing surficial shear strength and correlating it to avalanche activity, they found statistically significant gains and losses in shear strength in this very short time period. Shear strength values decreased significantly as the slope became exposed to increasing solar radiation and the water content in the snow surface increased.

In May 2005 a wet slab avalanche within Arapaho Basin Ski Area, Colorado claimed the life of a person skiing at the resort (WWAN, 2006). The subsequent investigation of the slide revealed the lack of useful tools available for avalanche professionals attempting to forecast wet slab avalanches. The rapid warming caused subsequent water flow through the snowpack leading to slope failure. Field experiments completed at Arapahoe Basin suggested a rapid warming and transition to a mostly wet snowpack over depth hoar led to wet slab avalanches (Hartman and Borgeson, 2008). For ski areas, highways, and recreational areas, this rapidity poses a serious problem.

Water Flow Within the Snowpack

Water percolation through snow has received much attention within the last half century (Colbeck, 1972, 1976, 1979; Wankiewicz, 1979; Jordan, 1995), and a sound understanding exists. Colbeck (1972) began the discussion with a theoretical framework using gravity flow as the primary driver of vertical flow within a snowpack. A modification of Darcian flow is derived for water flow in snow:

$$V = -K(d\psi / dz + 1)$$

where V is flux (m/s), which is proportional to ($d\psi / dz$), the capillary pressure gradient of a column where $d\psi$ is the change in pressure over dz, change in depth, plus the gravitational pressure gradient 1 (m/m), and K is hydraulic conductivity. During strong diurnal melt cycles gravitational flow is the predominant processes and capillary pressure gradients can essentially be ignored when examining the entire snowpack, but capillary head differences exist at certain layer interfaces resulting in barriers to vertical water

movement (Colbeck, 1974). Preferential flow and vertical water movement serve as two of the most intricate physical processes governing water flow and snow stability.

Preferential Flow

Extensive work concerning the topic of preferential flow paths through snow exists (Colbeck, 1976, 1979; Schneebeli, 1995; Kattelmann and Dozier, 1999; Williams et al., 1999; Trautman, 2007), but, again, the breadth of work within the context of wet slab avalanches is limited (Kattelmann, 1984; Techel et al., 2008). Schneebeli (1995) demonstrated that water flows vertically through preferential flow paths in the snowpack. These flow paths, or flow fingers, are highly variable throughout the snowpack and can change very quickly (Schneebeli, 1995). The terms flow fingers are similar to macropores that divert water through soils (Nieber, 1996), and the terms flow fingers and preferential flow are used interchangeably throughout this work. Sillolo and Tellam (2000) demonstrated the complexity of water movement and flow fingers in a multi-layered soil system. Their work is akin to water flow in a stratified snowpack and many of the concepts from soils can be easily transferred when working with snow as a porous medium.

It is suspected that flow fingers play a critical role in the formation of a wet slab within the snowpack (Reardon and Lundy, 2004). For instance, flow fingers transport water through the slab, leaving much of the slab unaffected by water flow, to a layer transition that impedes water and potential weak layer (Reardon and Lundy, 2004). On a plot scale of a few meters, preferential flow appears to have no spatial pattern

(Kattelmann and Dozier, 1999), yet on a slope scale there appears to be a correlation length of 5-7 m for preferential flow meaning that a pattern of flow fingers may exist on a larger scale (Williams et al., 1999). Williams et al. (1999) support previous work (Wankiewicz, 1979; Harrington and Bales, 1998) by demonstrating that preferential flow paths are used continuously throughout a snowmelt cycle or rain-on-snow event. They showed a spatial correlation length of flow fingers to be about 5 – 7 m. The laboratory experiments completed by Waldner et al. (2004) demonstrate that approximately 60% of the observed flow fingers remained at the same location for more than 100 minutes and new paths emerged mostly in areas previously wetted under a uniform (non-preferential) regime. This contrasts with the work of Schneebeli (1995) who suggested that flow fingers refroze and new flow paths emerged based on work done in the Swiss Alps over an entire winter season. However, Schneebeli's (1995) results are from multiple melt-freeze cycles, and since the introduction of liquid water enhances grain growth and reduces pore space size it is possible that these conditions would be favorable for the formation of new preferential paths at other locations. Studies that show that flow fingers are reused have implications for wet slab avalanches in that only a portion of the total volume of the snowpack is wetted and this allows the upper snowpack to retain slab-like characteristics.

Also, flow fingers allow water to move deeper into the snowpack and pool at certain layers. If water percolates through the snowpack and wets a weak layer, the layer's strength initially decreases (McClung and Schaerer, 1993). Yet, as it becomes saturated it is also more difficult for fractures to propagate in the weak layer, thereby

increasing the layer's strength. Accurately forecasting wet slab avalanches based on an increased load or loss of strength is currently not possible because of limited quantified studies (Conway and Raymond, 1993). However, evaluating the snowpack for areas where water can accumulate may aid in the process of avalanche forecasting (Kattelmann, 1987). Stability is regained once the snowpack refreezes or basal drainage out of the snowpack is equal to the input amount of melt or rain (McClung and Schaerer, 1993). Thus, before the snowpack becomes saturated preferential flow plays an important role in wet slab formation.

Snowpack Stratigraphy

While vertical movement of water within a snowpack depends upon flow fingers, lateral movement of water is also a critical factor in wet slab avalanches (Kattelmann, 1984; Conway, 2004). Like vertical movement, horizontal movement is dependent on snowpack stratigraphy and composition. An impermeable layer within the snowpack causes water to accumulate, move laterally within the snowpack, and create a loss of friction (McClung and Schaerer, 1993). Two separate processes explain how certain layer transitions impede vertical water movement in the snowpack: the capillary boundary effect and a hydraulic conductivity boundary.

The capillary boundary effect in a snowpack was adapted from the concept of liquid flow in porous media (Morel-Seytoux, 1969). Wankiewicz (1979) devised the FINA (Flow Impeding, Neutral, or Accelerating) model that describes water flow in a layered snowpack. Depending on the stratigraphic horizon, water will either be impeded,

accelerated across the horizon, or the horizon will have no effect on vertical flow. The FINA model involves a change in the infiltration rate of water within a snowpack due to a textural difference between two layers (Colbeck, 1979). A layer of fine grains has smaller pore spaces than that of coarse grains. When this fine-grain layer overlies a coarse-grain layer, the layer has a higher capillary attraction relative to the coarse-grain layer below. The smaller pore spaces in the upper fine-grain layer have a higher capillary attraction and act like a sponge, keeping water within the lower part of the top layer. Essentially, the water is held more tightly in suction in the upper layer due to capillary pressure differences between the two layers (Fig. 5). Once this pressure difference is relieved by saturation, and the permeability of the lower layer increases, then water can begin to flow vertically once again (Colbeck, 1973a; Wankiewicz, 1979). For instance, if a fine-grain layer overlies air, then the pressure in the pore spaces of the fine-grain layer must equal the air pressure in order for water to begin moving through the interface (Colbeck 1973a). Waldner et al. (2004) showed the effect of stratigraphy on water movement in an artificial snowpack. They showed that a microstructural difference of fine grained snow types over coarse grained types created a capillary boundary. They found that capillary boundaries changed water percolation, and suggested that capillary boundaries may be more pronounced in natural snowpacks with varying grain size, shape, and metamorphism rates.

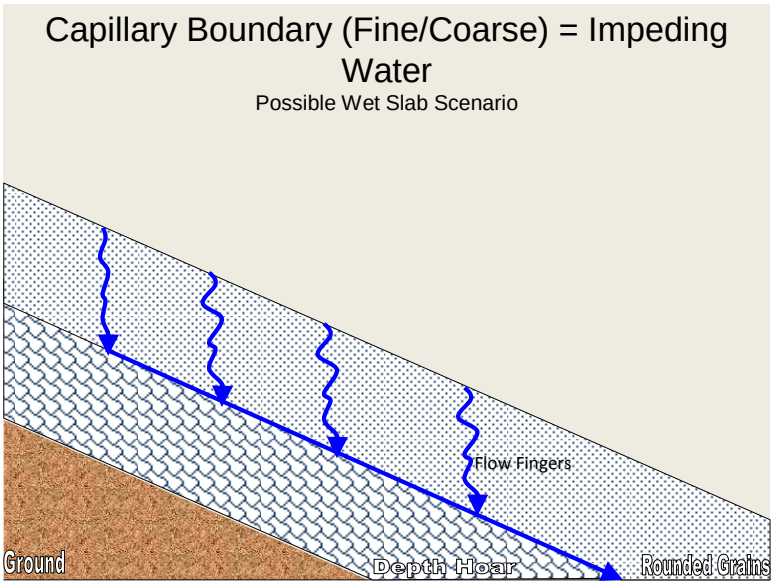

Figure 5: The capillary boundary effect is created when fine grains overlie coarse grains. The smaller pore spaces in the upper fine-grain layer have a higher capillary attraction and act like a sponge, keeping water within the lower part of the top layer (the dark blue layer). When capillary pressures of the pore spaces of both layers become equal (achieved through saturating the top layer), then water begins to move into the lower layer of coarse grains.

A hydraulic conductivity boundary also impedes vertical water movement in the snowpack. This type of layer transition impedes vertical water movement due to a difference in hydraulic conductivity between adjacent layers (Fig. 6). Hydraulic conductivity is the ability of a porous medium to transmit liquid water (Hornberger et al., 1998). More porous media will conduct water more readily than less porous media. A layer of rounded grains over an ice layer is an example of a hydraulic conductivity boundary. The ice layer, in the form of buried melt-freeze crusts, rain crusts, wind crusts, or the refreezing of liquid water above a layer interface, does not conduct water as readily as a layer of rounded grains, for instance, because of the limited pore space in the ice layer relative to the layer of rounded grains. Thus, as water moves vertically through a layer of

rounded grains and reaches the ice layer, flow becomes impeded and water begins to move laterally. This type of layer varies spatially and temporally and has potential to disintegrate rather quickly thus only storing water in the snowpack over a short period (Gerdel, 1954). This interaction plays a role in slope stability as water can affect the bonding of a specific layer with an underlying ice layer.

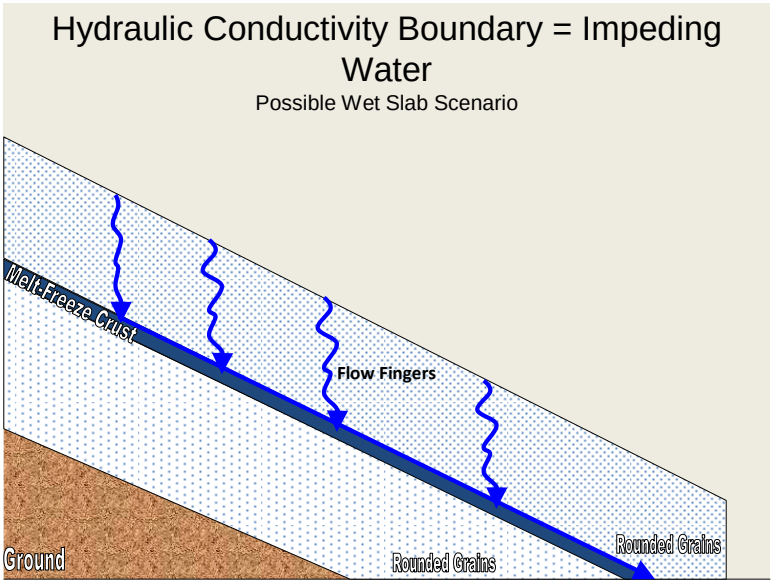

Figure 6: Schematic of a hydraulic conductivity boundary. An ice layer, in this case a melt-freeze crust, serves to impede vertical water movement because it has a lower hydraulic conductivity than the rounded grains above.

The structure consisting of coarse over fine grains is largely considered to have a small effect on vertical movement of water through snow. As water moves from coarser grains with a higher hydraulic conductivity to smaller grains with a lower hydraulic conductivity, water flow will slow down, but is rarely impeded at this type of interface (Hornberger et al, 1998). Field studies on natural snowcovers suggest that microstructural differences within layers may serve to impede water flow (Wankiewicz, 1979; Jordan,

1995). This seems to be the case only in natural snow covers as most laboratory experiments found that coarse-grain over fine-grain layers rarely impedes water flow (Jordan, 1995; Waldner et al., 2004). Thus, microstructural differences may play a role in snow stability.

As the slope increases the thickness of this saturated layer increases lower on the slope because of gravitational water accumulating from upslope and horizontal flow (Colbeck, 1973a). Thus water may drain faster lower on the slope because capillary pressure differences are equaled more quickly, but it also introduces water at a faster rate leading to a more rapid transition from the pendular to the funicular regime and loading. This has particular implications in snow stability because a weakening of bonds along such an interface lower on the slope may lead to fracture of a slab that propagates up the slope. Kattelmann (1984) suggested that any textural difference could serve as a barrier to vertical water flow and act as a potential sliding layer. Thus, there is a need to determine which microstructural differences of layer transitions impede vertical water flow in a natural snowpack.

When water moves throughout a weak layer, bond destruction may occur followed by a collapse which initiates a wet slab avalanche. The crystal composition of such a weak layer varies (e.g. depth hoar, faceted grains), and tends to persist throughout the winter (Reardon and Lundy, 2004). This layer is structurally sound enough to bear the weight of the snow above, yet once free water is introduced and structural disintegration occurs this weak layer may fail (Reardon and Lundy, 2004). This

illustrates the possible importance of snow stratigraphy as a factor in wet slab avalanche formation.

Snow Microstructure and the SnowMicroPenetrometer

Observable layer interfaces in the form of fine-grain layers over coarse-grain layers or ice layers act as impediments to vertical water flow within the snowpack, and these textural differences can exist within seemingly homogenous layers (Kattelmann, 1984). Changes in the microstructure not depicted by the bulk properties of the layer may impede water flow (Jordan, 1995). Thus utilizing a tool that measures snow microstructure is beneficial in identifying potential transitions that impede water. The SnowMicroPenetrometer (SMP) is a motorized, high resolution penetrometer that can accurately measure snow hardness and structural element length (Fig. 7). The SMP was developed to improve the accuracy in detecting thin layers that may not be discovered using other penetrometers, such as the Rammsonde. The SMP has a 5 mm tip with an angle of 60° connected to a force transducer housed inside a cone at the bottom of a rod. This rod is driven by a constant speed motor, and moves through a box that contains the electronics of the instrument (Fig. 7). The SMP measures force as it ruptures each individual structural element independent of penetration velocity and produces a signal of that force (Schneebeli et al., 1999; Johnson and Schneebeli, 1999) (Fig. 8).

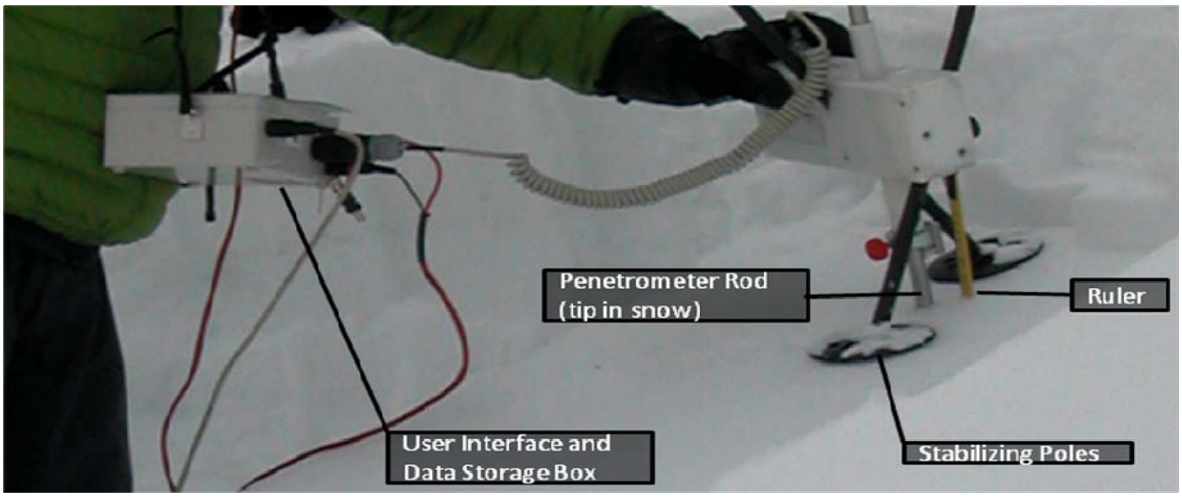

Figure 7: A close-up view of the SMP (SnowMicroPenetrometer). In this image, the penetrating rod is in the snow and the electronics box is being stabilized by the operator's hand. The black poles with powder baskets are used to stabilize the penetrometer as it moves through the snow. The box on the left is the user interface and is where the raw data is collected and temporarily stored.

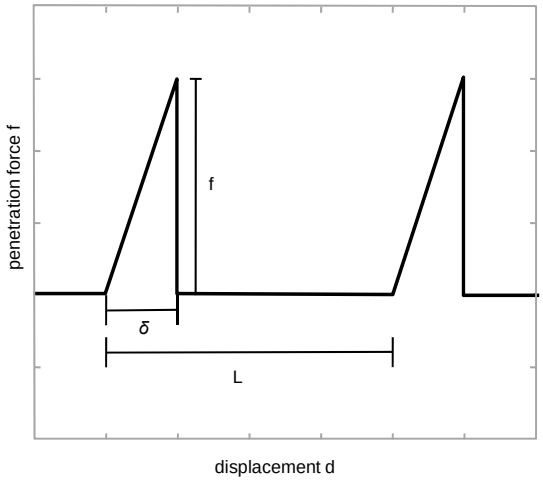

Figure 8: Schematic of SMP signal illustrating structural element length (L), deflection at rupture (δ), and the rupture force (f) (Reproduced from Marshall 2008).

Snow penetration theory was developed to allow the user to estimate microstructural parameters from the signal (Johnson and Schneebeli, 1999). Most studies utilizing the SMP have focused on hardness parameters (Schneebeli et al., 1999;

Birkeland et al., 2004; Lutz et al., 2007). Structural element length (*L*) may be a useful parameter when investigating water flow and the relationship with microstructure. Slight textural differences that are not revealed in bulk properties of snowpit layers may be more evident by examining structural element length. Structural element length can be considered using the element as a cube (Johnson and Schneebeli, 1999; Marshall, 2008), and depends upon the number of ruptures over a given distance (mm).

The use of the SMP in wet snow applications is limited. Techel et al. (2008) utilized the SMP to measure hardness of different layers at varying liquid water contents. By investigating a layer of faceted grains, they found that hardness on a microstructural level decreases as liquid water increases. Trautman et al. (2006) also utilized the SMP in determining hardness of surficial layers during a diurnal melt-freeze cycle and compared these measurements with shear strength measurements. Their results indicate that microstructural hardness as measured with the SMP explains 57% to 71% of the variation in shear strength data. Thus, using the SMP and examining structural element length in addition to hardness on a microstructural scale may allow for identification of layer transitions at slight textural differences that are not evident via standard snowpit measurements, and aid in predicting water movement in the snowpack.

CHAPTER 3

METHODOLOGY

Study Sites

The primary study sites for this research are located in both southwest and northwest Montana, USA. The Bridger Range, Gallatin Range, and Madison Range are in southwest Montana, and the Lewis Range, in Glacier National Park, is in northwest Montana (Fig. 9). The Bridger Range runs from about 5 km northeast of Bozeman to 45 km towards the northwest. It is a relatively narrow mountain range (10 km). Data were collected along the northern and southern boundaries of the Bridger Bowl Ski Area, 24 km north of Bozeman, Montana where elevation ranges from 1900 m to 2200 m (45.83° N, 110.93° W) (Fig. 10). The Bridger Range exhibits a combination of both intermountain and continental snow climates (Mock and Birkeland, 2000).

The Gallatin Range study sites (45.61° N, 110.93° W) are located 15 km southeast of Bozeman in the northern part of the mountain range with elevations ranging from 1704 m to 2200 m. Data were collected around the Mt. Ellis area, accessed via Bear Canyon Road (Fig. 10). This area of the range is similar to the Bridger Range in snow climates due to its proximity.

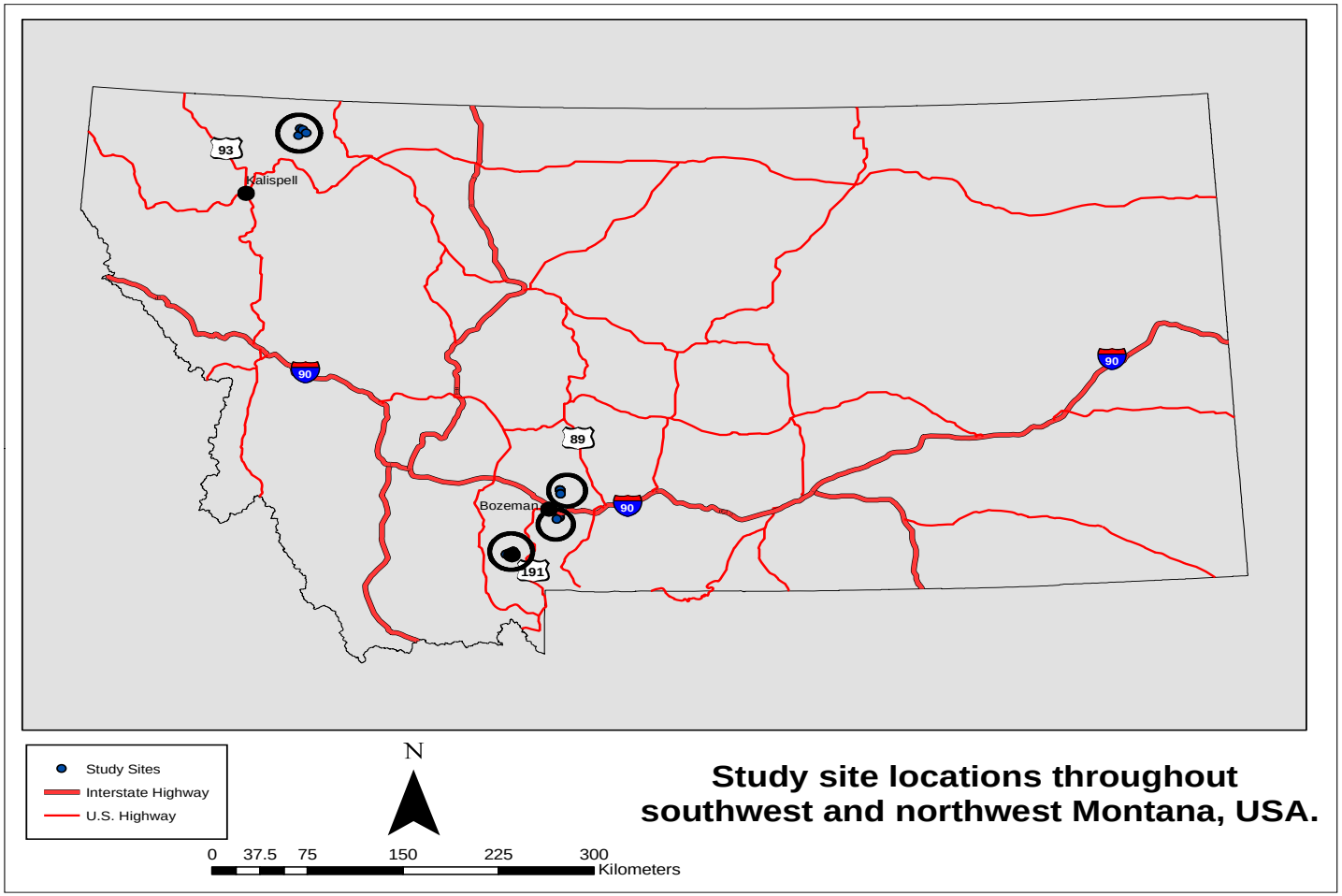

Figure 9: Map of study sites throughout Montana circled in black. There are three study sites in southwest Montana and one in northwest Montana.

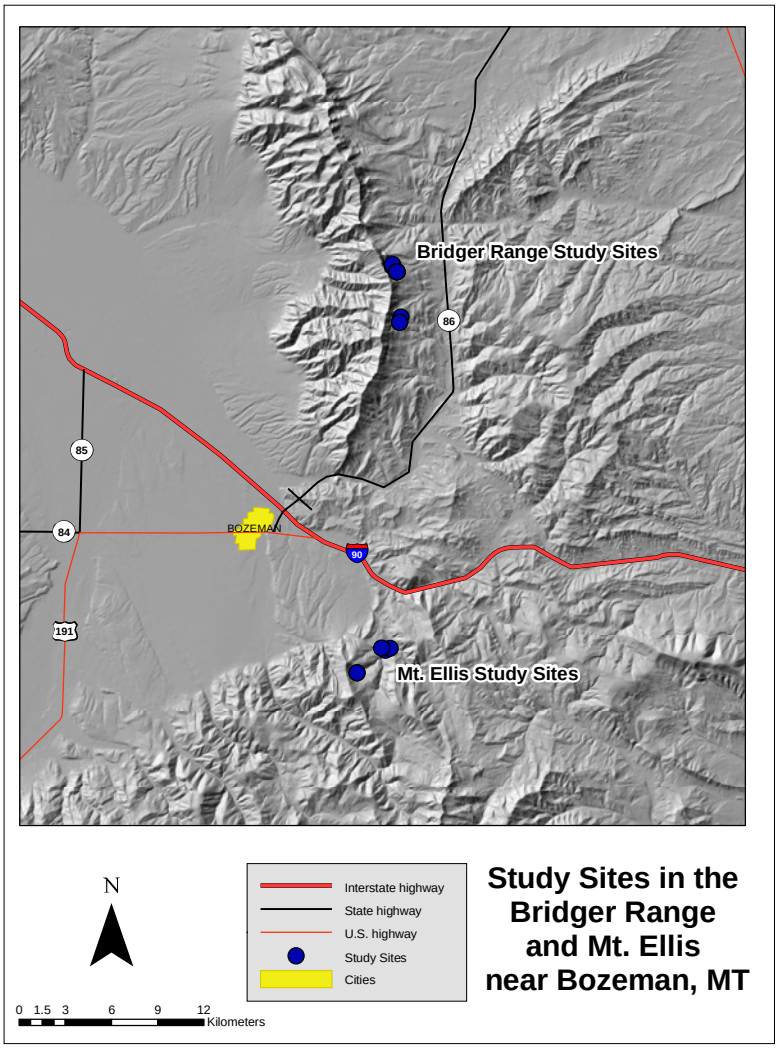

Figure 10: Map depicting study sites in the Bridger Range and Mt. Ellis, northern Gallatin Range, MT.

The Madison Range is 56 km south of Bozeman, Montana. Data were collected near the boundary of Moonlight Basin Ski Area (45.29° N, 111.45° W) and in the Beehive Basin area (45.32° N, 111.39° W) (Fig. 11). Access to the Beehive Basin area was granted through a landowner. The elevation of the study sites in this area ranged

from 2560 m to 2780 m, and this site exhibits a combination of intermountain and continental snow climates as well (Mock and Birkeland, 2000).

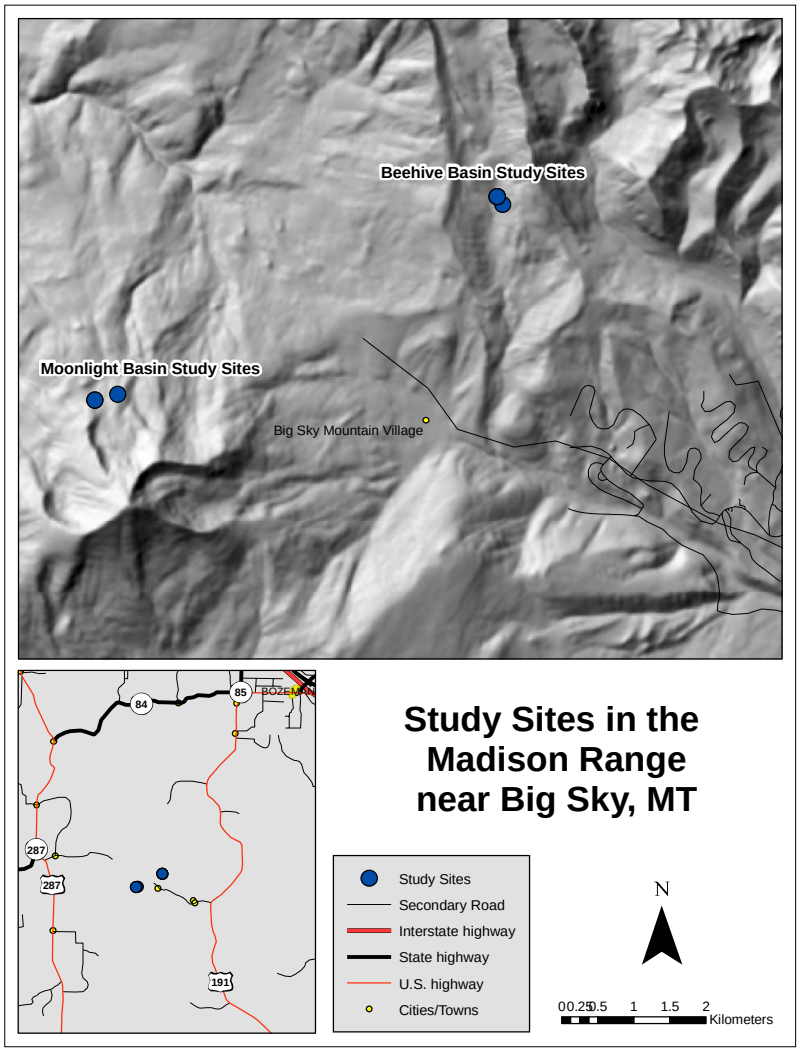

Figure 11: Map depicting study area in Madison Range, MT.

The study sites in Glacier National Park are adjacent to the Going-to-the-Sun Road (GTSR), a two-lane, 80-km roadway traversing through Glacier that is closed each winter because of avalanche hazards, inclement weather, and heavy snowfall (Reardon

and Lundy, 2004) (Fig. 12). Elevations of the study plots ranged from 1280 m to 1820 m and were accessed via the GTSR (45.70° N, 113.80° W). The northern Rocky Mountains within Glacier National Park exhibit an intermountain snow climate (Mock and Birkeland, 2000). During the annual spring opening of the road, avalanches pose a large and unpredictable threat to road workers and park personnel.

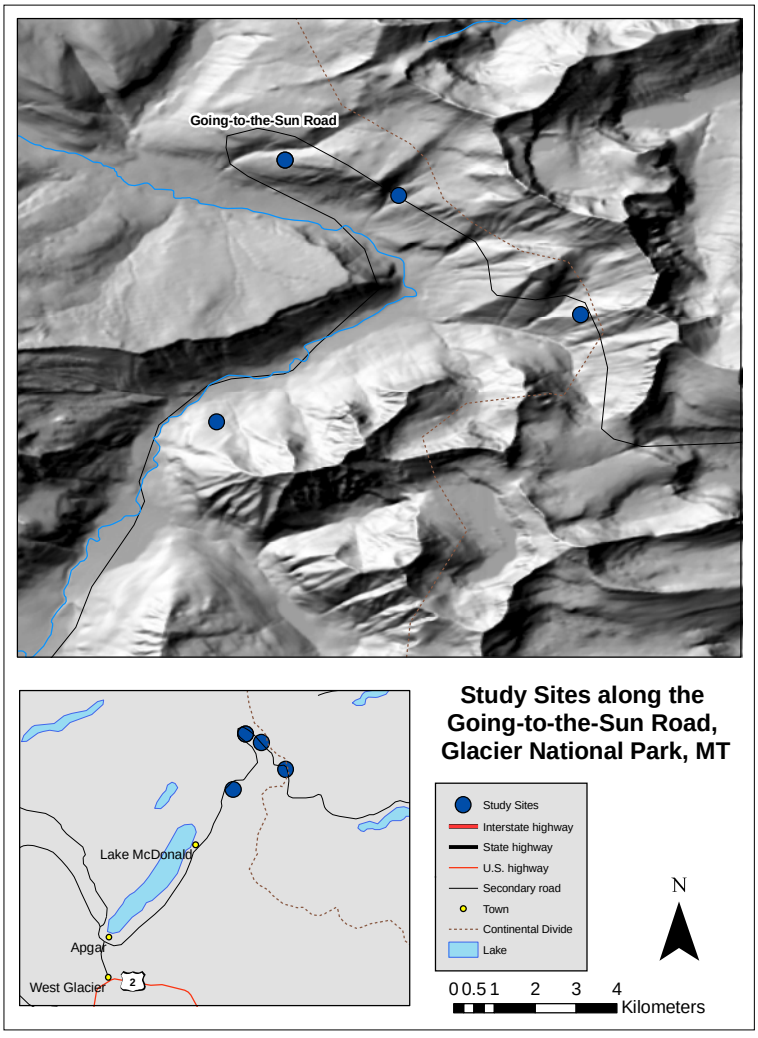

Figure 12: Study area in Glacier National Park, northwestern MT.

The experiments in southwest Montana were performed during the months from January through March, 2008 and in northwest Montana from April through May, 2008. These snow climates and associated snow stratigraphy patterns provided an opportunity to utilize different snowpacks with numerous stratigraphic layers and perform water movement experiments in each.

Field Data Collection

Seligman (1936) first documented the use of dye tracer in snow, and it has been used extensively in numerous other experiments to determine preferential flow paths in a snowpack (Woo et al., 1982; Heywood, 1988; Jordan, 1995; Schneebeli, 1995; Waldner et al., 2004; Trautman, 2007). Because timing of meltwater percolation in the snowpack may be critical for wet slab production, water was added to a dry snowpack during the winter and spring. This simulated rain or meltwater production within the snowpack. I utilized red food coloring and mixed it with water to observe water flow. I applied the colored water with a spray bottle to simulate rain or meltwater production within the snowpack. The spray bottle was a hand-pump pressurized 1 L bottle that allowed for a more uniform flow to the snow surface than a standard hand spray bottle. Dye was applied over a 25 cm x 25 cm square area using a plastic frame for guidance (Fig. 13).

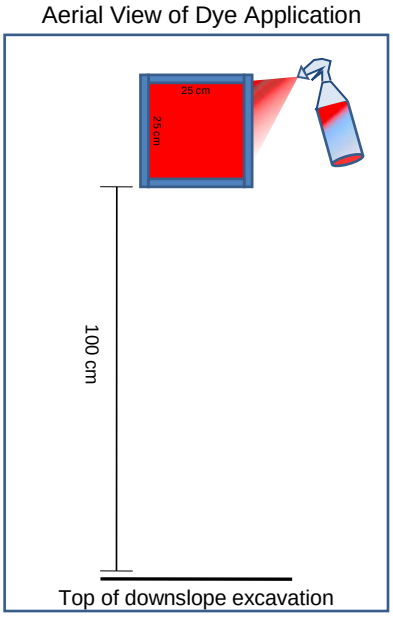

Figure 13: Schematic from an aerial perspective illustrating the application of red-dyed water to the snow surface and the excavation distance relative to the dyed plot.

To test relative uniformity over a 25 cm x 25 cm surface, I sprayed water into ice cube trays of that dimension, then siphoned and measured the amount in each "cube" using a small 200 cc syringe. This ensured a uniform application over the 25 cm x 25 cm plot. Application uniformity is important as flow fingers will form preferentially in an area if there is a depression such as that caused by uneven water application or melting (Williams et al., 1999). I applied water at an approximate rate of 18-20 cm/hr each time. Singh (1997) utilized a rain simulator that applied water 0.02 to 20 cm/hr. Jordan (1995) states that ~18 cm/hr is the optimal rate of irrigation for a 25 cm diameter circular spray area, but her experiments were actually at a much lower rate because of nozzle freezing.

Utilizing dye tracer allowed me to observe flow fingers and determine where water came in contact with layer transitions that impeded water, and to later measure the snow grain size, snow density, layer hand hardness, snow temperature, and snow grain type associated with those boundaries. I utilized a methodology similar to Jordan (1995) who investigated capillary barriers and flow regimes by applying water to a dry snowpack on the plot scale. I excavated a 1 m long side wall and a 1.5 m long vertical wall (depth determined by vertical movement of dyed water) on the downslope side of a snowpit on each slope (Fig. 14). I then worked across the slope excavating the side and increasing the trans-slope distance of the vertical downslope wall as needed to accommodate all of the plots for that session. Each pit was spaced apart enough so that dye from the previous pit did not interfere with the new experimental pit, and I completed one vertical pit profile at one end of the slope to locate layer transitions after applying water (Fig. 14 (b)). The number of pits varied each session due to vertical movement of water within the snowpack.

I cooled the water added to each plot to slightly above 0º C, ranging from 0.1º C to 0.8º C, so as to minimize the amount of meltwater produced by the actual snow grains. By minimizing the amount of meltwater produced I was able to accurately measure the amount of free water in the snowpack. Preliminary experiments conducted in the Montana State University College of Engineering Cold Laboratory showed that sifted snow with density ranging from 300-355 kg/m^2 requires ~60-100 ml of applied water to begin to form preferential flow paths. Thus, with less dense snow in a field situation, I began with water applications of 50 cm^3. For instance, if I applied up to 250 ml of dyed

water and the results were identical to 50 ml then I would increase the amount to 1000 ml to determine if more water had a different effect. If it did, then I would add less water each subsequent application until the results were the same as when I applied 250 ml. This allowed for a more efficient use of water, dye, and time.

I sampled on slopes between 27 º and 34º to ensure relative uniformity of water flow between each sampling day, and measured the following: 1) density (kg/m^3) at every layer using a 250 cm^3 stainless steel cutter and a small cylindrical cutter for thin (1-4 cm thick) layers, 2) temperatures (°C) every 5 cm from the surface to the vertical location of water within the snowpack (linearly extrapolating temperatures for transitions that impeded water if they existed between these measurements), 3) grain type (according to Colbeck et al. (1990), 4) grain size (mm) of each layer using a 30x field microscope, 5) air temperature (°C), 6) applied water temperature (°C), 7) the existence of uniform flow or the number of flow fingers at each slope parallel cut layer 8) the vertical location (cm) of existing layer transitions that impeded water flow within the profile, and 9) downslope distance (cm) water traveled up to 1 m from water application. This downslope distance allowed for adequate downslope movement of water. I measured parameters 1-3 and 5 in a snowpit immediately adjacent to the area of initial water application using standards outlined in Greene et al. (2004).

(a)

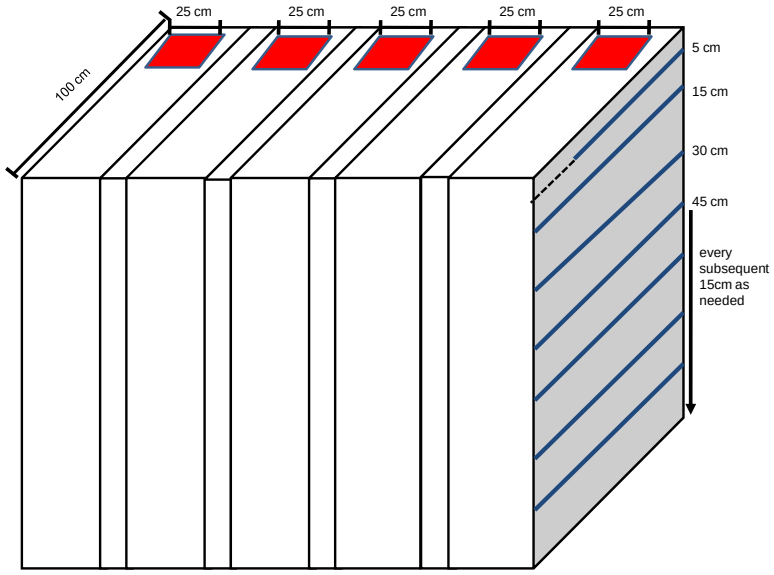

(b)

Figure 14: Photograph (a) and schematic (not to scale) (b) illustrating the dimensions and placement of dye on the snowpack. From left to right (b), dye was applied starting with equivalent of 0.08 mm of water (50 ml) and ending at the last plot with 1.6 cm of applied water. Slope parallel cuts were made from the snow surface at 5 cm, 15 cm, 30 cm, and every subsequent 15 cm as necessary to trace the dyed water.

I applied the dye tracer to each plot beginning with 50 cm^3 over a 2-5 minute period ensuring uniform application. The largest application of 1000 cm^3 over a 5 minute period equates to ~19 cm/h, and this is near the optimal irrigation rate of 18 cm/h for a plot of this size (Jordan, 1995). Ten minutes after all of the water was applied, I made a slope parallel cut 5 cm down from the snow surface using a standard snow saw. This allowed me to determine the existence or absence of laterally moving water and preferential flow fingers throughout each plot. The 10 minute lag time and 5 cm cut allowed for flow finger formation based on findings in other lab experiments that finger fronts travel with a velocity between 0.1 and 1 cm/s (Waldner et al., 2004). I then made a horizontal cut at 15 cm to identify water movement deeper in the snowpack, and continued every 15 cm until dye tracer was not observed (Fig. 14 and 15). I replicated this process on the other plots with increments of 50 cm^3 of water up to the equivalent of 1.6 cm of water added to a dry winter snowpack on the 25 cm x 25 cm plot.

Figure 15: After applying dye, I marked the slope parallel cuts that are conducted 10 minutes after dye application. Photo by Karl Birkeland.

Each sampling day consisted of five test columns on 2-3 different slopes (for a variety of snow structure) depending on meteorological conditions and snow structure. The task of initially simulating meltwater by adding water requires a "winter-like" dry snowpack. Thus, the experiments were conducted on a snowpack that does not contain free water throughout the entire snowpack.

I utilized the SMP to characterize layer transitions that impeded vertical water flow. By utilizing the SMP, I was able to identify existing differences in grain element size and hardness of the interfaces between layers that impeded water flow and compare them to interfaces that did not impede vertical water flow. Because of the high resolution nature of this instrument, I was able to identify grain size differences microscopic observations could not detect. I completed four to10 SMP measurements, for replication

purposes and in conjunction with other experiments using the SMP during field campaigns, on each slope upslope of the area where dyed water was applied (Fig. 16). This allowed for measurements on a non-disturbed and non-wetted section of the site.

Figure 16: Karl Birkeland of the U.S. Forest Service National Avalanche Center completing SMP measurements upslope of the dyed area.

Data Analysis

Preferential Flow

Statistical analysis focused on the variables that likely lead to flow finger formation within the snowpack. The statistical software package *R* (version 2.7.1) (2008) was used to calculate results throughout this study. I used a simple linear regression analysis to determine the existence of a correlation between the amount of water needed

to form flow fingers and each of the snowpack variables investigated (snow grain size, layer density, layer temperature, and layer hand hardness). I then examined the relationship between the number of flow fingers, if present, at each application amount and these variables. Since snow grain type is a categorical variable, I examined the frequency and proportion of grain type measured against the amount of water needed to create flow fingers (Devore and Peck, 2005).

Layer Transitions that Impeded Vertical Water Flow

Statistical analysis focused on the variables that likely lead to layer transitions that impede water within the snowpack. I classified a transition that did not impede water as any observable transition between two layers where water moved through that boundary and did not pool or move laterally. I collected data on 42 layer transitions that impeded water and 32 non-impeding transitions. First, these snowpack variables were investigated for the layer above and layer below both transitions that impeded water and transitions that did not impede water. I first determined the normality of snow grain size, snow density, snow hand hardness, and snow temperature of transitions that impeded water and layers transitions that did not impede vertical water flow.

Since the distribution of the data are largely non-normal, a two sided nonparametric median test or the Mann-Whitney U Test (Devore and Peck, 2005) was conducted to determine significance of snow grain size, snow density, hand hardness, and snow temperature between the layer above and the layer below transitions that impeded water and transitions that did not impede water. The calculated difference between the layer above and layer below water impeding transitions and the layer above and layer

below non-impeding transitions were used to determine statistical significance between the two types of transitions.

I examined the frequency and proportion of each grain type as both a layer above and layer below layer in transitions that impeded water and transitions that did not impede water. I completed a Chi squared test of homogeneity to test for homogeneity of proportions for each crystal type (Devore and Peck, 2005). Then I partitioned the data based on crystal type and examined the frequency of the layer above and the layer below, and performed a one-sample Mann-Whitney U test for snow grain size, snow density, hand hardness, and snow temperature of transitions that impeded water. For instance, I examined all transitions that impeded water and transitions that did not impeded water where new snow was present as either the layer above or the layer below (or both), and calculated the frequency and proportion of each crystal type when new snow is present. I also completed a Chi squared test of homogeneity to determine homogeneity of proportions. The partitioning of data based on grain type allowed for a more detailed characterization of individual crystal types in layer transitions that impeded vertical water flow.

The data generated from SMP measurements were used to investigate transitions that impeded water on a microstructural scale. Using Interactive Data Language (IDL) data analysis software, the raw SMP signal was examined to determine the extent of signal error (or noise) and given a qualitative ranking on a scale of 1 to 3 (1=clean signal). Various thresholds of signal error were used to allow for the cleanest signal with the most confidence (Lutz, 2008). Once the signal was deemed appropriate for use, I

determined the vertical location of each layer transition that impeded water and delineated it on the manual snow profiles for use in a programming script to identify the boundary within the SMP profile. Programming scripts devised by Lutz (2008) were used to smooth the signal in a seven-point weighted 10 mm Moving Statistical window procedure and produce penetration resistance (Newtons), mean number of ruptures per mm , and structural element length (L). This smoothing allowed for easier detection and automation of layer transitions. Ranks were then calculated for the mean number of ruptures and structural element length (Marshall, 2008). SnowMicroPenetrometer measurements were taken during eight sampling sessions where transitions that impeded vertical water movement existed. The transitions were ranked based on step change and rate of change. The step change is the absolute value difference in structural element length, and the rate of change is the slope value of element length between the layer above and the layer below (Fig. 17). Utilizing these metrics allowed for a direct comparison between transitions that impeded water and those transitions that did not.

Descriptive statistics were calculated including the median and interquartile range of step change, rate of change, and percent increase. This allowed for both quantitative and qualitative analysis of water impeding transitions and non-impeding transitions within each profile and for the entire dataset. I then completed a Mann-Whitney U Test of the difference of step change value, rate of change, and percent increase of structural element length between transitions that impeded water and transitions that did not.

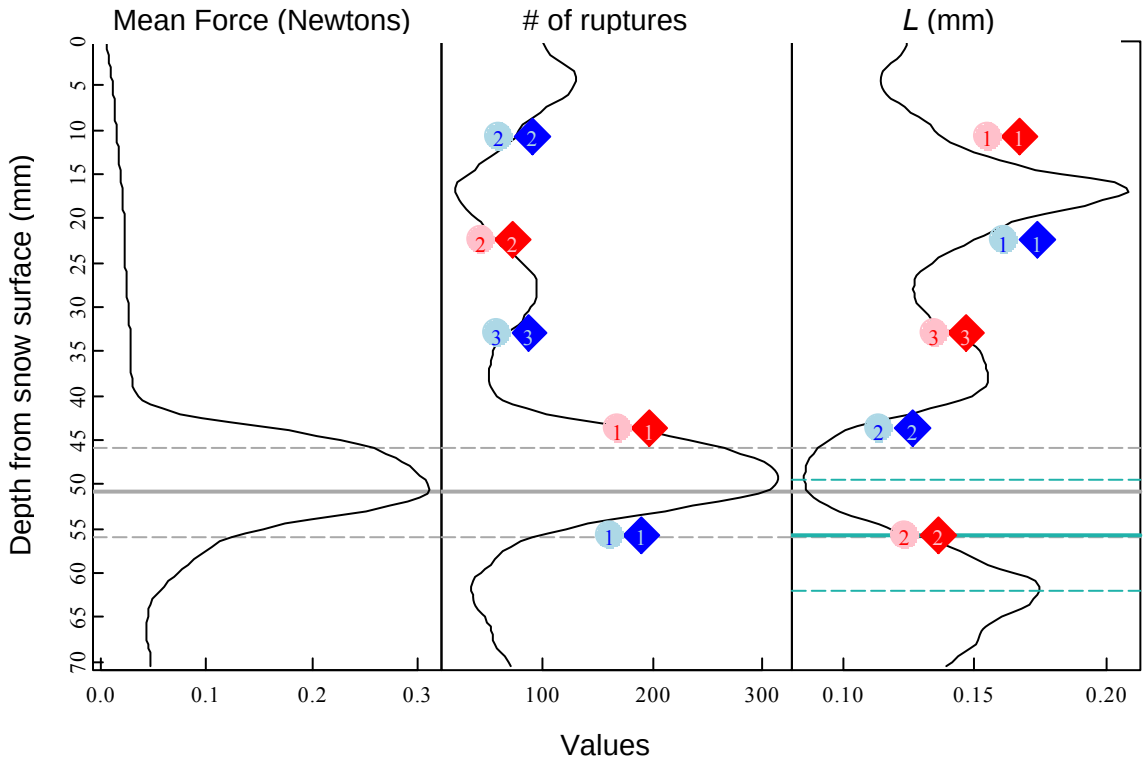

Figure 17: SMP profile displaying mean rupture Force, mean number of ruptures, and structural element length (L). The numbered circles indicate the rank of the step change, and the numbered diamonds the rank of slope for the top 5 ranked transition for each profile. Blue indicates a decrease in value and red a positive change in the value. The gray solid lines indicate the location of a transition that impeded water based on the manual profile, and the gray dashed lines provide a 5 mm scale on either side. The teal lines represent the actual transition location where the values were measured in the SMP profile.

CHAPTER 4

RESULTS AND DISCUSSION

Water Application

The 1.5 L bottle sprayer used to apply dyed water to the snow surface had a relatively uniform spray pattern (Table 1). The ice-cube tray test was analyzed using a Chi squared test of uniformity ($\chi^2 = 544$, p-value = 0.2951), and showed that by using the ice cube tray test method the bottle sprayer produced a uniform application of dyed water ($\alpha = 0.05$). While every "cube" in the tray did not receive equal amounts (μ=16.0, σ=3.4), the overall application proved to be uniform. The ice cube trays are also not a smooth medium like a snow surface. The ridges in between each cube may have played a role in determining the amount of water that accumulated in each cube. The bottom left and right corners of the entire matrix received the least amount of water. Thus, during field application a concentrated effort (steady application) was made to ensure uniformity over the entire plot of applied water.

Table 1: The amount of water (cm3) siphoned out of each "cube" in 2 ice cube trays placed side-by-side. This test was completed to determine uniformity of the pressurized hand sprayer.

Tray 1		Tray 2	
14.5	19.25	17.5	14
6.5	21	19	18
18	17.5	15.5	18.5
17	15.5	14	17
17.5	16.5	14	17
17.5	17.75	17	17.5
16	17.25	20.5	16
6.5	10	11	6.5

Layer Transitions that Impeded Vertical Water Flow

Data were collected on 41 transitions that impeded water and 32 transitions that did not impede water. Twenty-four transitions that impeded water contained new snow grains or fragmented and precipitation particles as either the layer above the transition, the layer below the transition, or both. While five transitions containing new snow grains or fragmented and precipitation particles did not impede water. Ten transitions that impeded water contained rounded grains as either the layer above the transition, the layer below the transition, or both, while 12 transitions containing rounded grains did not impede water. Nine transitions that impeded water contained faceted crystals as either the layer above the transition, the layer below the transition, or both, while 10 transitions containing faceted crystals did not impede water. Five transitions that impeded water contained wet grains as either the layer above the transition, the layer below the transition, or both, while 11 transitions that contained wet grains did not. Fifteen transitions contained a crust as either the layer above the transition, the layer below the transition, or both, while 20 transitions that contained a crust did not impede water.

Snow Grain Size

In layer transitions that impeded water, the grain size of the layer above was significantly smaller ($p < 0.05$) than the layer below, while no significant difference was found between layers in transitions that did not impede water (Table 2). Most of the grain sizes of each layer had a non-normal distribution based on a Shapiro-Wilks test of normality (Table 2). All tests of normality throughout this analysis were performed at α

= 0.05, and distributions with p-values less than 0.05 were considered non-normal. $Q_{.25}$ and $Q_{.75}$ represent the 25th and 75th quartile, respectively, in all results. While the ranges of grain size for both layers of transitions that impeded water overlapped, the median value was 0.75 for the layers above and a median value of 1.00 for the layers below (Table 2, Fig. 18). This suggests that transitions that impeded water consisted of smaller grains over larger grains, and layer transitions that did not impede water had equal grain sizes between the two layers. This result is consistent with Wankiewicz's FINA model of water flow through the snowpack (1979).

Table 2: Descriptive statistics and p-values for the Shapiro-Wilks (SW) test of normality and the nonparametric Mann-Whitney U Test (MW) for grain size (mm) of layers above and layers below transitions that impeded water (Impeding) and transitions that did not impede water (Not Impeding). $Q_{.25}$ and $Q_{.75}$ represent the 25th and 75th quartile, respectively.

Layer	***n***	**median**	**$Q_{.25}$**	**$Q_{.75}$**	**p-value (SW test for normality)**	**p-value (MW U Test)**
Layer Above Impeding	39	0.75	0.44	1.00	0.0007	0.0496
Layer Below Impeding	39	1.00	0.50	3.00	0.0023	
Layer Above Not Impeding	23	0.88	0.63	2.50	0.0160	0.4536
Layer Below Not Impeding	23	0.75	0.50	1.75	0.3138	

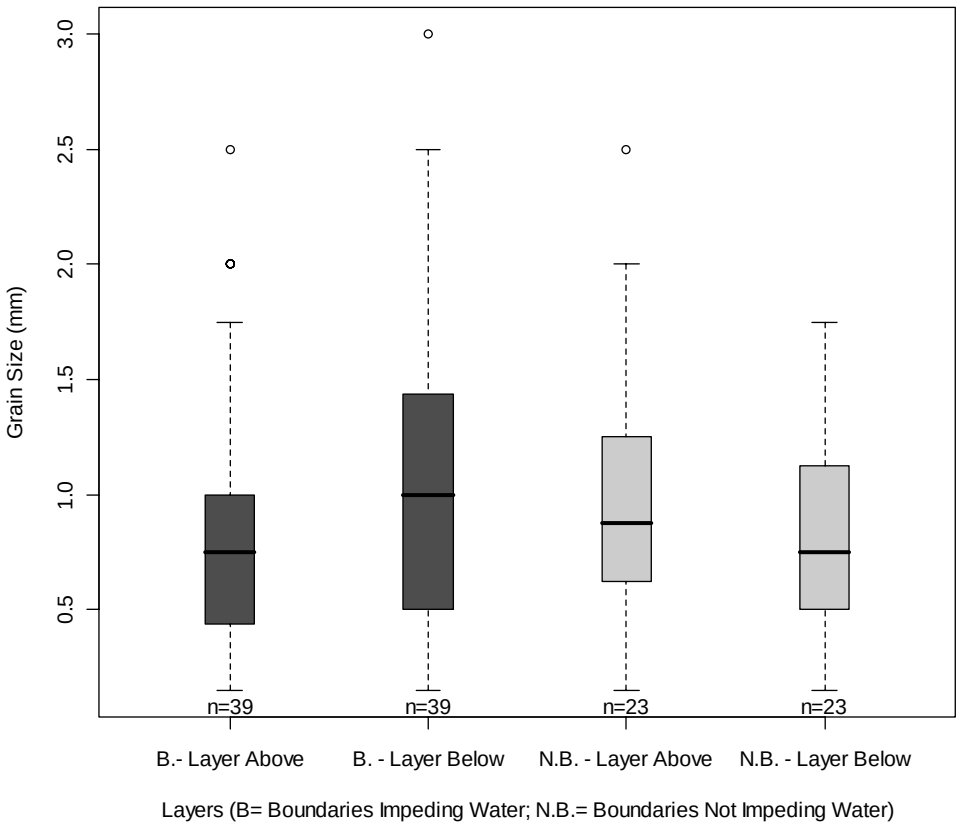

Figure 18: Box plot of grain size (mm) of layers above and layers below transitions that impeded water and transitions that did not impede water. Thick black lines indicate median, boxes interquartile range, whiskers extend to the 0.05 and 0.95 quantiles, and the circles indicate outliers.

These results are consistent with a theoretical framework (Colbeck, 1974, 1979) and experiments (Jordan, 1995; Waldner et al., 2004) that show fine-grain snow crystals over coarse-grain snow crystals impede the vertical movement of water in a snowpack, and coarse-grain over fine-grain structures do not have an impeding effect on the vertical movement of water (Wankiewicz, 1979). For this dataset the statistical results show that for transitions that impeded water the top layer consisted of smaller grains. However,

samples with equal grain size between layers above and below could be attributed to a very fine textural difference that was not captured in the bulk properties during measurement. For instance, during one field day a transition impeding water existed ~3 cm from the snow surface (Fig. 19). Measurements revealed the same grain size, but visual inspection with a 30x microscope showed rimed stellars over unrimed stellars. Slight textural difference with no obvious visual difference in grain size can move water many meters downslope.

(a)

(b)

Figure 19: Red dyed water moving along: (a) capillary barrier of rimed stellars over unrimed stellars ~3cm from the snow surface, and (b) moving near the snow surface within newly fallen dendrites.

Grain size differences (grain size of layer above minus grain size of layer below) were compared between transitions that impeded water and transitions that did not. If transitions that impeded water had smaller grained layers above than layers below and

transitions that did not impede water were comprised of the opposite structure or one of same sized grains, then a significant difference between the two would show the difference between layers in transitions that impeded water as always being negative. However, these results indicate that the median grain size difference between transitions that impeded water and transitions that did not was not significantly different (p-value > 0.05) (Table 3).

Table 3: Descriptive statistics and p-values for the Shapiro-Wilks (SW) test of normality and the nonparametric Mann-Whitney U Test (MW) of the grain size (mm) difference of layers above and layers below transitions that impeded water (Impeding) and transitions that did not impede water (Not Impeding). $Q_{.25}$ and $Q_{.75}$ represent the 25th and 75th quartiles, respectively.

Transition	***n***	**median**	**$Q_{.25}$**	**$Q_{.75}$**	**p-value (SW test for normality)**	**p-value (MW U Test)**
Impeding	36	0.00	-0.50	0.06	0.0260	0.0722
Not Impeding	23	0.13	-0.31	0.44	0.1876	

Grain-size differences at layer transitions which did not impede water extend to negative values. This is notable as one would expect transitions with negative differences to impede water (Fig. 20). However, the median grain size was 0.13 mm indicating that generally there were larger grains over smaller grains at most transitions that impeded water. The most negative grain-size difference was -1.25 mm, which reflects small grains over large grains. The negative outliers may result from an inability to detect small grain size differences with a 30x hand microscope in freshly fallen snow. In addition, when the layers are particularly thin (<3 cm) and of the same type of crystal, it was often difficult to distinguish grain size with adequate resolution. This problem may explain the existence of positive outliers in the samples of transitions that impeded water (Fig. 20). For example, a grain size difference of 1.6 mm suggests larger grains over

smaller grains which unexpectedly impede water. In this particular sample, small faceted grains (0.3-0.5 mm) were under larger newly fallen dendrites (2.0 mm). One reason this transition was identified as a transition that impeded water may be attributed to error in identifying new snow crystals in this 7 cm thick layer. Identifying new dendrites is sometimes difficult due to the multiple axes and overlapping crystal structures. Thus the size of the crystals may have been inflated.

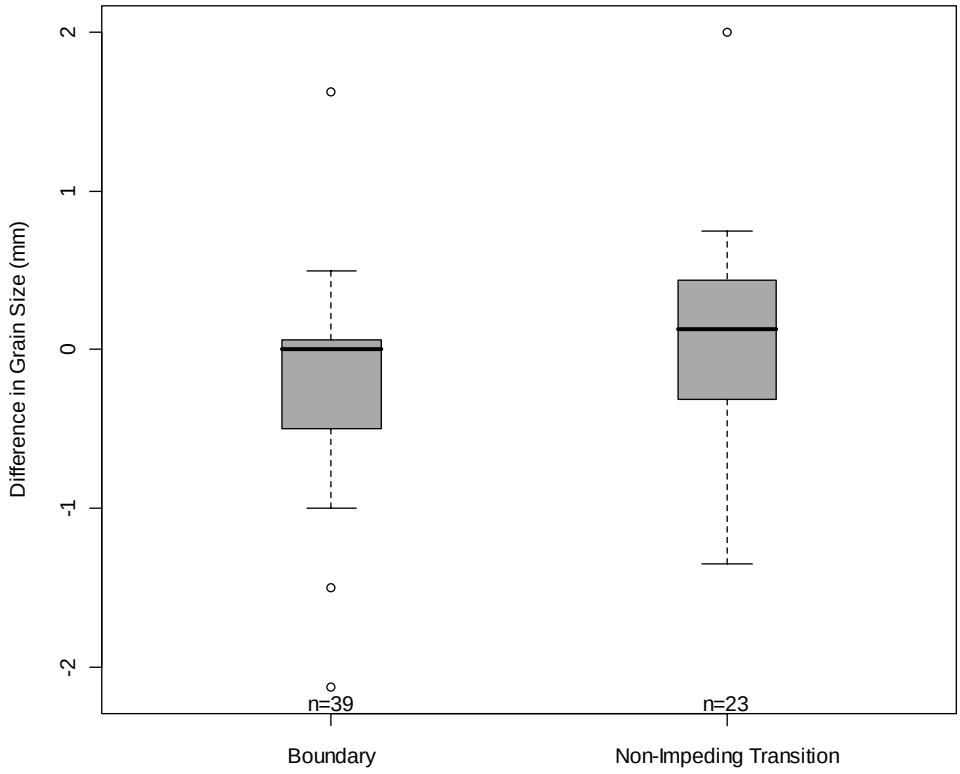

Figure 20: Box plot of grain size (mm) difference (layer above minus layer below) between transitions that impeded water (boundary) and transitions that did not impede water. Thick black lines indicate median, boxes interquartile range, whiskers extend to the 0.05 and 0.95 quantiles, and the circles indicate outliers.

While grain size difference in some transitions that impede water is obvious (such as rounded grains over depth hoar) (Hartman and Borgeson, 2008), these results illustrate that it is not apparent in all transitions. Such boundaries where grain size of the layer

above and the layer below is visually observed as the same have often been referred to as merely slight textural differences (Kattelmann, 1984). My results showed these differences moved water downslope for meters (Fig. 17). This has implications for slope stability throughout the winter and spring. During mid-winter rain-on-snow events, water is added to a dry snowpack that may consist of newly fallen snow. Thus, monitoring the upper snowpack for slight differences in grain size may be useful for avalanche forecasters when determining water movement and resulting avalanches. Knowing whether water remains near the snow surface and results in wet loose avalanches or if it percolates deeper in the snowpack and moves along a transition at a weak layer is important for forecasting. In spring, the grain size difference may be more noticeable and easier to identify as the snowpack becomes more homogenous, and water-impeding layers exist at obvious grain size transitions.

Layer Density

Like grain size, layer densities also were non-normally distributed (Table 4). So, a non-parametric statistical test was used. The layer above a transition that impeded water was significantly less dense than the layer below the transition ($p < 0.05$). Densities did not vary between layers above and below transitions that did not impede water ($p > 0.05$). This suggests that the layer above transitions that impeded water have a lower median density than the layers below. Conversely, for transitions that did not impede water layers above have similar density to layers below.

Table 4: Descriptive statistics and p-values for the Shapiro-Wilks (SW) test of normality and the nonparametric Mann-Whitney U Test (MW) for density (kg/m^3) of layers above and layers below transitions that impeded water (Impeding) and transitions that did not impede water (Not Impeding). $Q_{.25}$ and $Q_{.75}$ represent the 25^{th} and 75^{th} quartile, respectively.

Layer	*n*	median	$Q_{.25}$	$Q_{.75}$	p-value (SW test of normality)	p-value (MW U Test)
Layer Above Impeding	36	137	80	254	0.0002	0.0033
Layer Below Impeding	36	196	112	298	0.0036	
Layer Above Not Impeding	22	273	159	380	0.1394	0.5628
Layer Below Not Impeding	22	272	172	398	0.0500	

This result is interesting because capillary boundaries have been reported to typically consist of denser layers above less dense layers (Wankiewicz, 1979). In my dataset, only six of the 36 transitions included a dense ice lens above a less dense layer (a hydraulic conductivity boundary). This observation suggests that transitions caused by hydraulic conductivity (more dense over less dense) should be distinguished from capillary boundaries (less dense over more dense). However, the ranges of density of layers above and layers below overlapped to a great extent (Fig. 21). Thus, while the median densities differed significantly, I cannot conclude that transitions that impede water always consist of less dense layers over more dense layers. Illangasekare et al. (1990) found in Arctic snowpacks that less dense depth hoar layers under more dense ice crusts impede vertical water movement. In my dataset, depth hoar was not investigated, but large faceted grains were investigated. In each case this layer was a less dense layer below a transition that impeded water (capillary boundary). The results I found are similar to those found by Jordan (1995) where transitions that impede water can exist at interfaces where the layer above can be either more or less dense than the layer beneath. Caution must be used, however, as density may be a weak indicator of transitions that

impede water as can be evidenced by observations of water being impeded above depth hoar, which is more dense yet more porous than layers above (Brown, 2008). Also, and perhaps more importantly, field methods for measuring density are often inexact as measuring thin layers is quite difficult. The standard tools used were quite large relative to layer size and perhaps inadequate for measuring very thin layers.

Because layer transitions that impeded water flow formed at seemingly indistinguishable layer interfaces within new snow, density measurements in these layers were either equal or very near equal. The significance that layers above were less dense than layers below can possibly be attributed to slight density differences that are lost in the bulk properties when measuring density with a 250 cm^3 cutter. My results differ from the common theory that transitions that impede vertical water flow must consist of a large density difference between the layers above and layers below. My results are similar to studies that showed water moving downslope for tens of meters along a slight textural difference (Kattelmann, 1987; Heywood, 1988). Because my data consisted of a large range of densities and snow grain types they illustrate the diversity of layer transitions that can impede vertical water movement in the snowpack.

No significant difference in density existed between layers above and layers below transitions that did not impede water flow (Fig. 21). The common hypothesis in literature is that the layer above should be less dense and more porous while the layer below would be the opposite (Wankiewicz, 1979). This would allow uninhibited water flow across the transition from a more porous to a less porous layer. However, my results are not consistent with this concept. My data show that there was a wide range of

overlapping density values in transitions that did not impede water perhaps due to slight textural differences. This is perhaps more easily seen when comparing the density differences (layer above minus layer below) of transitions that impeded water and transitions that did not impede water.

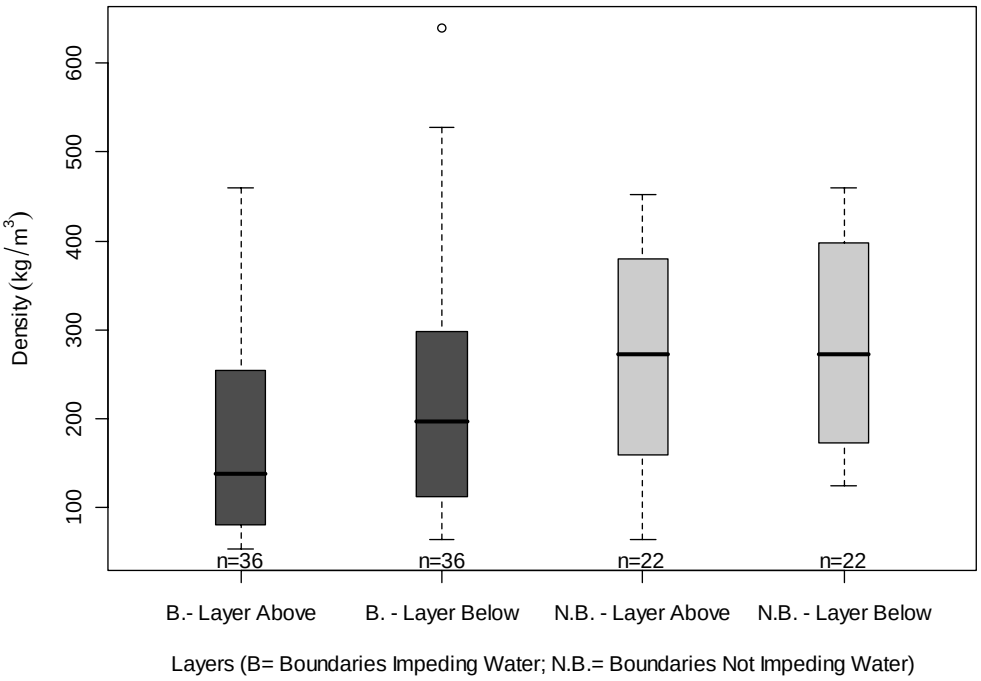

Figure 21: Box plot of density (kg/m^3) of layers above and layers below transitions that impeded water and transitions that did not impede water. Thick black lines indicate median, boxes interquartile range, whiskers extend to the 0.05 and 0.95 quantiles, and the circles indicate outliers.

Density differences (layer above minus layer below) did not significantly differ between transitions that impeded water and transitions that did not (Table 5). However, 75% of the time transitions that impeded water exhibited a density difference of less than zero between the layer above the transition and the layer below (Fig. 22). The small absolute differences illustrate that these transitions may exist at slight density differences and also when the layer above the boundary is actually less dense than the layer below.

Density differences can be subtle in transitions that impede water. The distribution of density differences of transitions that did not impede water was larger than those that did. This dataset shows that it may be difficult to characterize water-impeding transitions based on density values alone. The layer above the transitions that impeded water was both more and less dense than the layer below and similar to transitions that did not impede water flow.

Table 5: Descriptive statistics and p-values for the Shapiro-Wilks (SW) test of normality and the nonparametric Mann-Whitney U Test (MW) of the density (kg/m^3) difference between the layers above and layers below transitions that impeded water and transitions that did not impede water. $Q_{.25}$ and $Q_{.75}$ represent the 25^{th} and 75^{th} quartile, respectively.

Layer	***n***	**median**	**$Q_{.25}$**	**$Q_{.75}$**	**p-value (SW test for normality)**	**p-value (MW U Test)**
Impeding	36	0	-80	0	<0.0001	0.2778
Not Impeding	21	0	-73	68	0.5200	

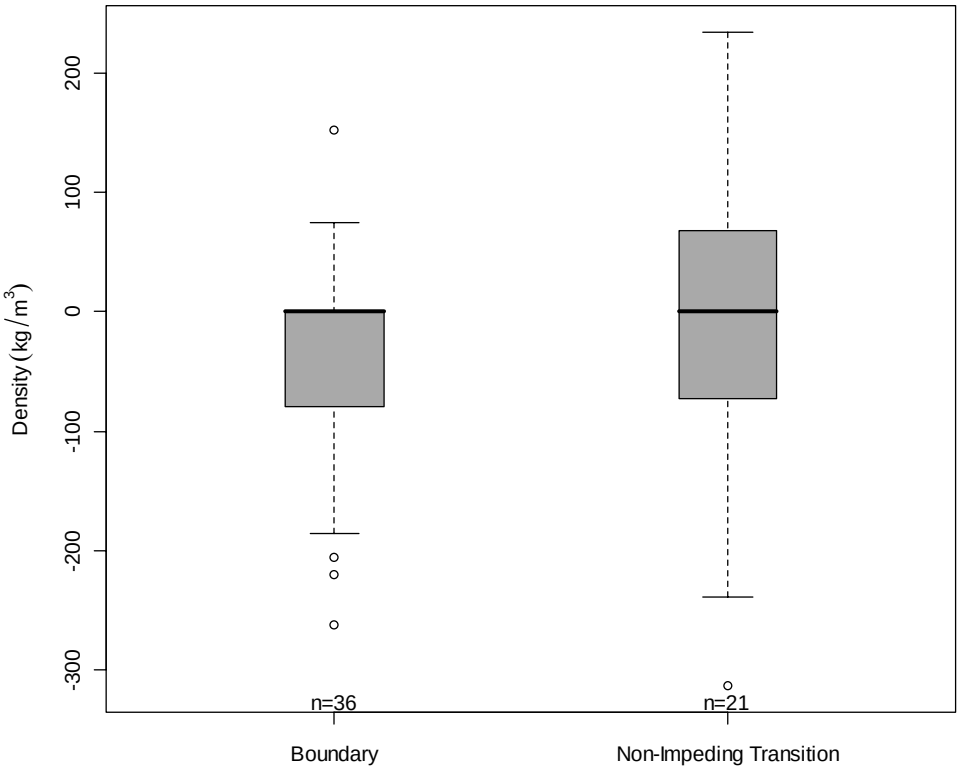

Figure 22: Box plot of density (kg/m^3) difference (layer above minus layer below) of layers above and layers below transitions that impeded water (boundary) and transitions that did not impede water. Thick black lines indicate median, boxes interquartile range, whiskers extend to the 0.05 and 0.95 quantiles, and the circles indicate outliers.

Layer Hand Hardness

Field hand hardness measurements were taken according to Greene et al. (2004), and these measurements were converted to numeric values for analysis (Table 6).

Throughout this section hand hardness is referred to using the term hardness.

Table 6: Field measurement hand hardness scores converted to numeric values for ease of analysis.

Hand Test	F	F+	4F-	4F	4F+	1F-	1F	1F+	P-	P	P+	K-	K	K+	I
Score	1	1.34	1.67	2	2.34	2.67	3	3.34	3.67	4	4.34	4.67	5	5.34	5.67

Most of the layer hardness scores had a non-normal distribution based on a Shapiro-Wilks test of normality (Table 7). In addition, the data were categorical so non-parametric techniques were used for analysis. Hardness did not significantly vary between the layer above and the layer below transitions that impeded water ($p > 0.05$). There was also no significant difference between the layer above and the layer below transitions that did not impede water flow ($p > 0.05$).

Table 7: Descriptive statistics and p-values for the Shapiro-Wilks (SW) test of normality and the nonparametric Mann-Whitney U Test (MW) for hand hardness (R) of the layers above and layers below transitions that impeded water (Impeding) and transitions that did not impede water (Not Impeding). $Q_{.25}$ and $Q_{.75}$ represent the 25th and 75th quartile, respectively.

Layer	*n*	median	$Q_{.25}$	$Q_{.75}$	p-value (SW test of normality)	p-value (MW U Test)
Layer Above Impeding	41	1.33	1.00	2.67	<0.0001	0.2015
Layer Below Impeding	41	2.00	1.33	3.00	0.0022	
Layer Above Not Impeding	32	3.00	2.00	2.84	0.0155	0.6057
Layer Below Not Impeding	32	3.00	2.00	3.67	0.0163	

The middle 50% of both the layer above and below transitions that impede water were very similar illustrating the overlap of hardness between both layers (Fig. 23). The lower median hardness of the layer above these transitions compared to the layer below can be attributed to the 24 cases where water impeding boundaries formed near the snow surface within new snow or broken particles. The hardness of the layer above in these samples was less or equal to the hardness of the layer below. However, this dataset also consisted of transitions that impeded water where hard wind slab layers existed over softer faceted grains (Fig. 24). Thus, based on this dataset, hardness values have a

considerable range for both the layer above and the layer below and neither layer is significantly more or less hard than the other.

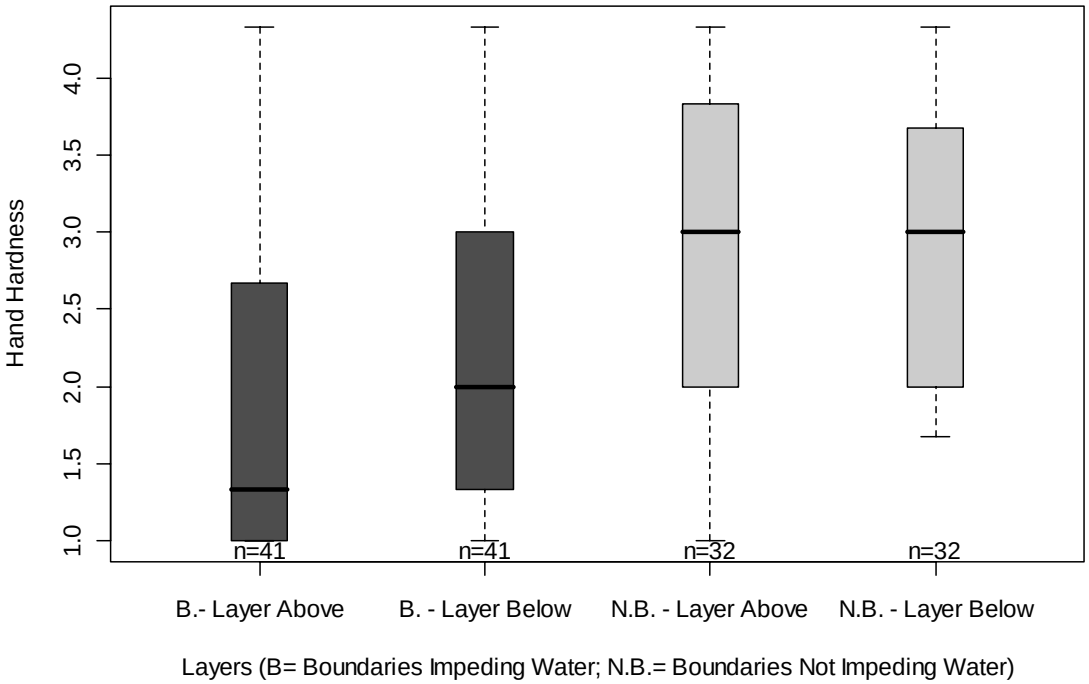

Figure 23: Box plot of hand hardness of layers above and layers below transitions that impeded water and transitions that did not impede water. Thick black lines indicate median, boxes interquartile range, whiskers extend to the 0.05 and 0.95 quantiles, and the circles indicate outliers.

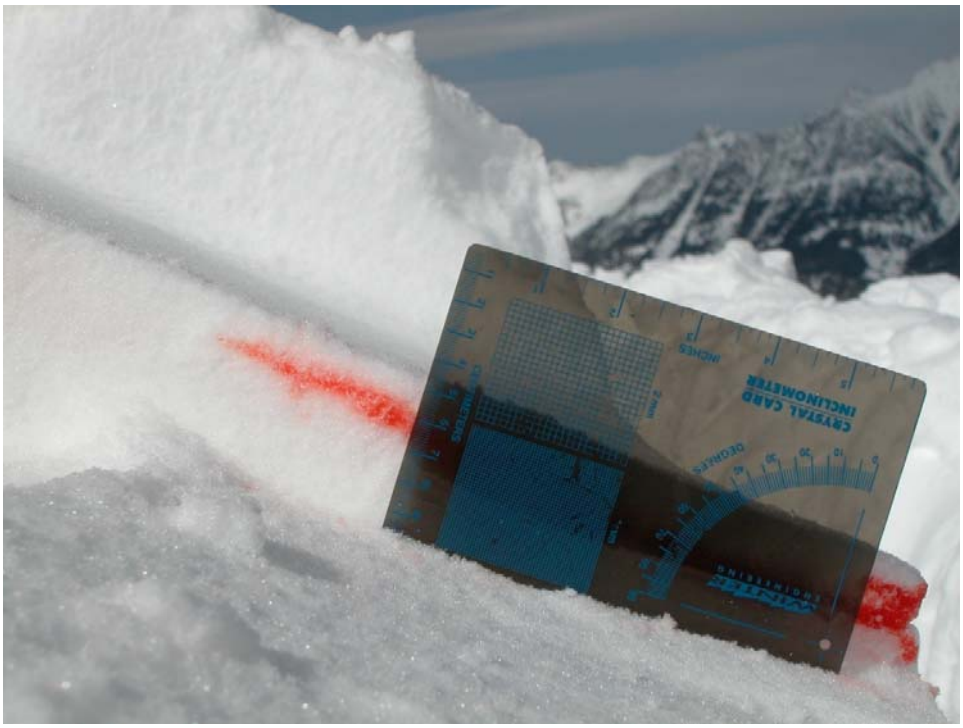

Figure 24: Transition that impeded water shown by red dyed water at interface of 1 finger hard buried wind slab over a 4 finger hard layer of mixed faceted grains.

No significant difference in hardness existed between layers above and layers below transitions that did not impede water (Table 7). An interesting result is that both the layer above and the layer below transitions that did not impede water were harder than either layer of transitions that impeded water. While it cannot be assumed from these results that transitions that impede water occur more often in softer snow, it is notable that the layer below transitions that did not impede water had the smallest range of hardness. This suggests that transitions with very soft layers (softer than 4 finger hardness) as the layer below are more likely to impede water. This is consistent with observations and studies that show soft depth hoar layers as a failure layer in wet slab avalanches (Hartman and Borgeson, 2008). Hartman and Borgeson (2008) found that

penetrometer readings showed a decrease in hardness over time as water reached a transition between a stiff (hard), skier compacted layer over a brittle depth hoar layer.

Hardness differences (layer above minus layer below) for transitions that impeded water were not significantly different from transitions that did not impede water ($p > 0.05$) (Table 8). The range of hardness is larger for layers that did not impede water than for transitions that impeded water (Fig. 25). The outliers on the low end of transitions that impeded water indicate cases where a small amount of soft new snow fell over a hard melt-freeze crust. Whereas the outliers on the positive end are the cases of a hard wind crust over softer faceted grains. It is clear that for transitions that impeded water both the layer above and the layer below can be either softer or harder than the other and for transitions that did not impede water most of the differences seem to be fairly spread out indicating no clear pattern of hardness for either. Also, thin layers are harder to detect using a hand hardness scale and some of the actual hardness in these layers may have been lost in bulk properties measurements. Thus, using hand hardness to characterize potential transitions that may impede water may be a technique which is too coarse to identify transitions that impede water flow.

Table 8: Descriptive statistics and p-values for the Shapiro-Wilks (SW) test of normality and the nonparametric Mann-Whitney U Test (MW) of the hand hardness (R) difference between the layers above and layers below transitions that impeded water and transitions that did not impede water. $Q_{.25}$ and $Q_{.75}$ represent the 25th and 75th quartile, respectively.

Layer	***n***	**median**	**$Q_{.25}$**	**$Q_{.75}$**	**p-value (SW test for normality)**	**p-value (MW U Test)**
Impeding	41	-0.33	-1.00	0.00	0.2789	0.7634
Not Impeding	32	-0.33	-1.67	1.17	0.0817	

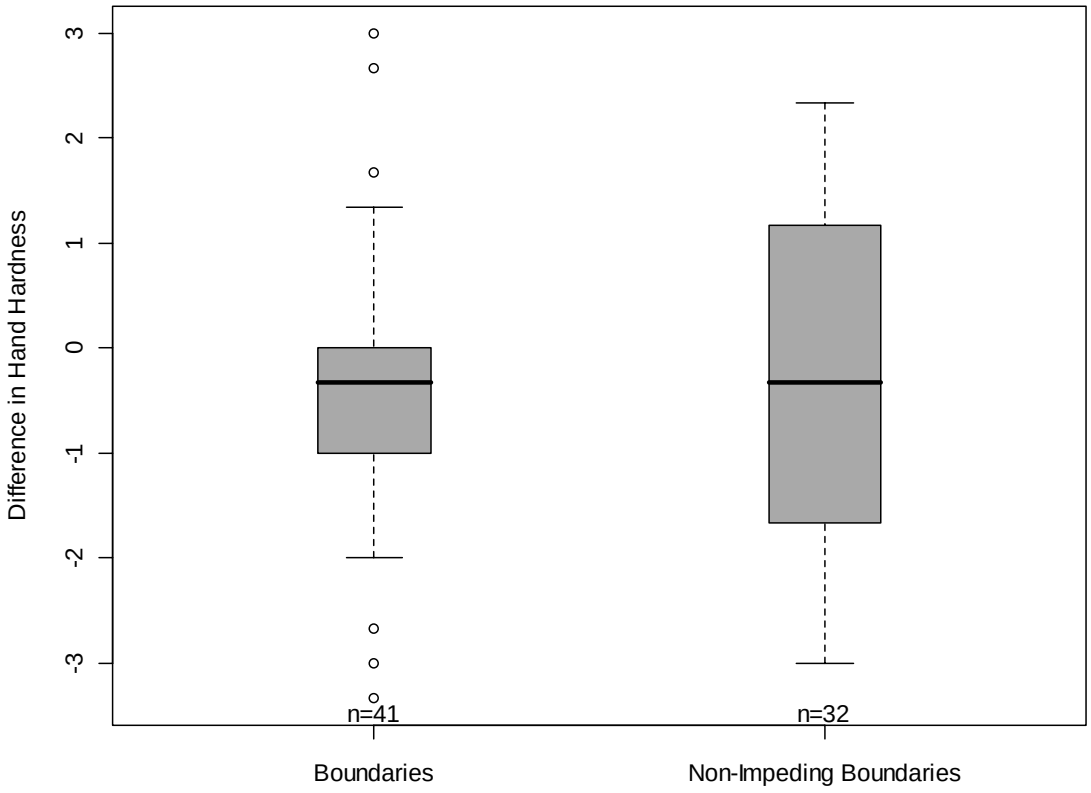

Figure 25: Box plot of hardness difference (layer above minus layer below) of layers above and layers below transitions that impeded water (boundary) and transitions that did not impede water. Thick black lines indicate median, boxes interquartile range, whiskers extend to the 0.05 and 0.95 quantiles, and the circles indicate outliers.

Snow Temperature

Measured snow temperature results illustrate that both transitions that impede water and those that do not impede water can occur in a wide range of snow temperatures, and there is no significant difference between the two ($p > 0.05$) (Table 9). However, transitions that impeded water were generally colder (median = -2.8 °C) than those that did not (median = -1.2 °C) (Fig. 26). Kattelmann (1987) stated that the cold content of snow is not capable of freezing much water as it ponds at a capillary boundary or hydraulic conductivity boundary except in extremely cold and very dense snowpacks. The median temperatures of transitions that impeded water were lower, yet the cases in my sample never reached below -12° C and those samples were typically not very dense. Thus, the ponding of water at lower temperatures is most likely not due to freezing. These results illustrate that both transitions that impede water and those that do not can occur in a wide range of snow temperatures and that temperature is not likely to be a useful metric in charactering transitions that impede water movement.

Table 9: Descriptive statistics and p-values for the Shapiro-Wilks (SW) test of normality and the nonparametric Mann-Whitney U Test (MW) of temperature (°C) between transitions that impeded water and transitions that did not impede water. $Q_{.25}$ and $Q_{.75}$ represent the 25th and 75th quartile, respectively.

Layer	***n***	**median**	**$Q_{.25}$**	**$Q_{.75}$**	**p-value (SW test for normality)**	**p-value (MW U Test)**
Impeding	41	-2.8	-6.8	-0.8	0.0019	0.0683
Not Impeding	32	-1.2	-5.1	0	0.0001	

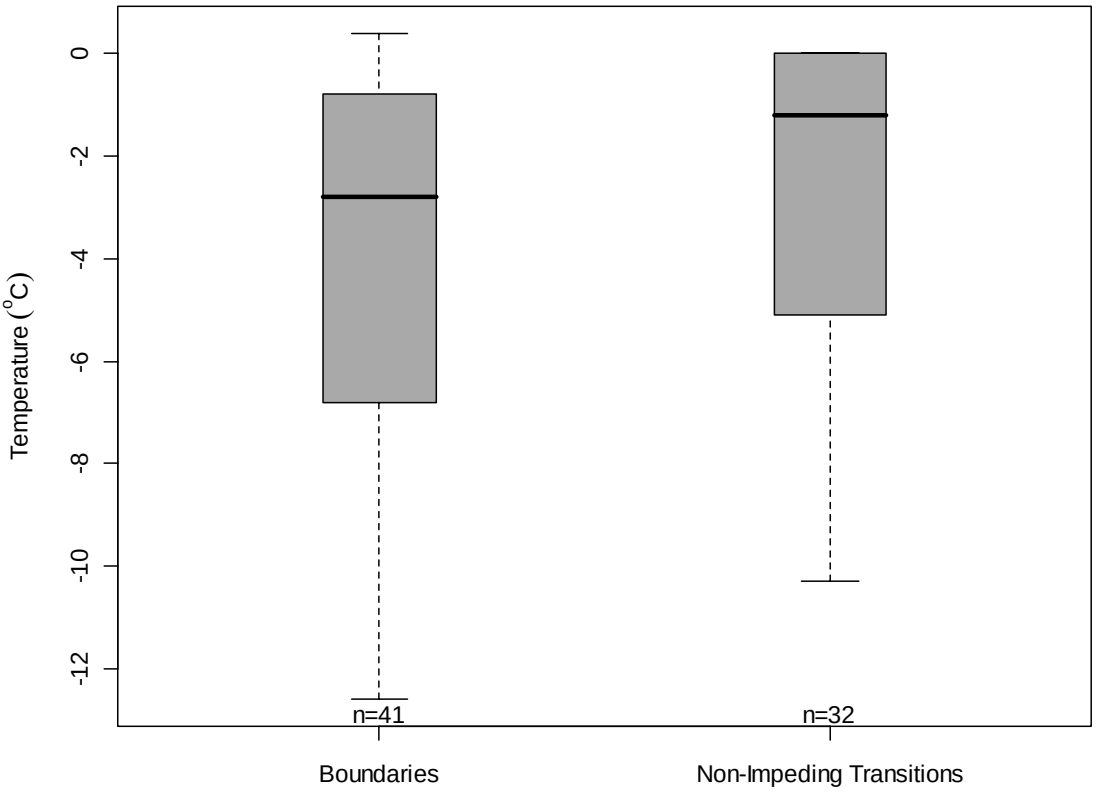

Figure 26: Box plot of snow temperature transitions that impeded water (Boundaries) and transitions that did not impede water. Thick black lines indicate median, boxes interquartile range, whiskers extend to the 0.05 and 0.95 quantiles, and the circles indicate outliers.

Snow Crystal Type

Since the nature of a capillary boundary or hydraulic conductivity boundary varies depending on the grain type, the data was partitioned based on grain type. The data were separated into five categories based on whether that particular grain type was present either above or below the layer transition: new snow crystals (crystal type 1), rounded grains (crystal type 3), faceted crystals (crystal type 4), wet grains (crystal type 6), and crusts (crystal type 9). All of the crystal types except decomposing and fragmented precipitation particles (crystal type 2) observed in these experiments can be

classified into these categories. For the analysis, decomposing precipitation particles were included with new snow crystals because they are both recently deposited crystals. Some interfaces are used for more than one category; for example, faceted grains overlying a crust are used for both the faceted grains category and the crusts category. Statistical analyses were then conducted on snow grain size, density, and hand hardness on these partitioned data.

Of the transitions that impeded water observed in this study, new snow particles were the most common layer above the boundary (29%) and fragmented precipitation particles were the most common layer below the boundary (26%) (Fig. 27). Conversely, these two types of crystals were also the least common layers in interfaces that did not impede water (6% and 6%, respectively, for top layers and 0% and 3%, respectively, for bottom layers). Wet grains and rounded grains were not prevalent as either a layer above or a layer below in layer transitions that impeded water (Appendix A). Chi squared tests of homogeneity showed that there was no significance that any grain type was more likely to be the layer above or the layer below than any other grain type (p-value <0.05).

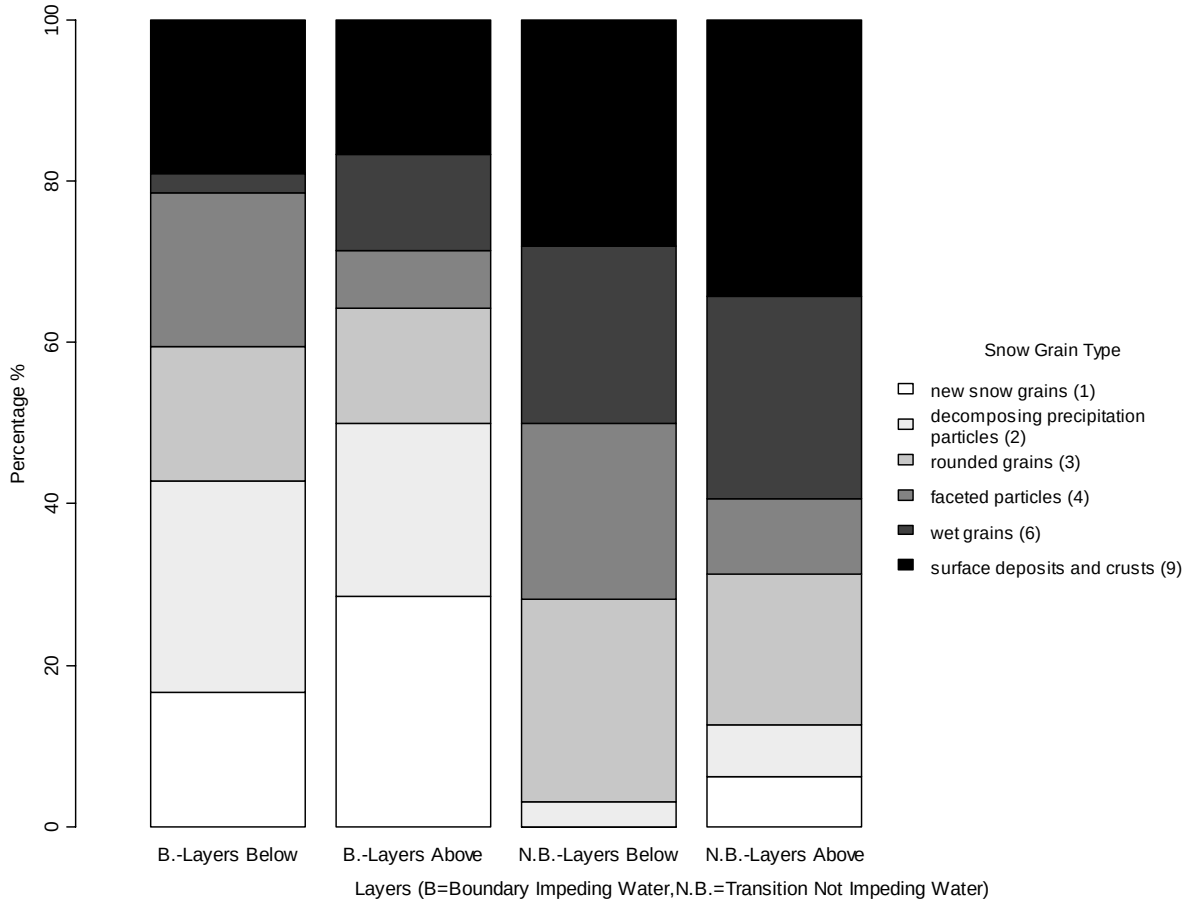

Figure 27: Relative proportions of crystal types comprising the layers above and below transitions that impeded water and transitions that did not impede water of all samples.

New and Decomposing Fragmented Precipitation Particles: Of 29 interfaces involving new snow and fragmented particles, 24 of those interfaces impeded water while five of them did not (Appendix A). In general, the crystals above the transitions that impeded water were precipitation particles (54%), decomposing and fragmented precipitation particles (35%), and other grains consisting of melt-freeze crusts and wind crusts (11%). The crystals below the boundary consisted of precipitation particles (27%), decomposing fragmented precipitation particles (54%), and other grains (19%) including large rounded grains, small faceted particles, and melt-freeze crusts (Fig. 28). The crystal types below and above each interface differed with the exception of five cases. Only seven of the 24 interfaces (29%) involved grain types other than new or precipitation particles while 17 of 24 (71%) had only new snow. The interfaces involving melt-freeze crusts consisted of a few centimeters ($\leq$ 5 cm) of new snow over the crust. Though crystal type generally varied, densities typically did not; 14 of 24 (58%) interfaces with complete density measurements had the same – or nearly the same – measured density above and below the water-impeding boundary, yet statistical tests showed a significant difference in median density between the layers above and below transitions that impeded water ($p > 0.05$) (Table 10). This may be attributed to the low density new snow layers above a very dense crust evident in a hydraulic conductivity boundary. It must be noted that density measurements were coarse due to subtle properties lost in the bulk measurement of density. Changes in hardness and crystal size were also subtle. Hand hardness was either the same, or the upper layer was softer than the lower layer except for four cases, yet the median values were not significantly different (α=0.05) (p-

value=0.12). Further, with the exception of five cases the upper layer had smaller grained crystals than the layer below the interface. However, the difference in median grain size for the entire sample is not significantly different ($p > 0.05$). Essentially, transitions that impede water in new snow can be created from extremely subtle changes in the crystal type. Those changes can often be identified through careful investigation of crystal types with a 30x hand microscope. However, there is no pattern for the crystal types involved in these boundaries. For example, the data show that sometimes a transition that impedes water can consist of columns over plates, while other times it can consist of plates over columns.

I observed only five cases where interfaces within new snow did not impede vertical water movement, so strong conclusions cannot be made. In these cases, only one case consisted of decomposing particles below small faceted grains. This is interesting because a subtle change in crystals within new snow always acted as a water-impeding boundary in this study. It is possible that I missed some of these subtle interfaces. However, this emphasizes that any change in crystal type with new snow layers may be capable of acting as a transition that impedes water flow.

Table 10: Sample size, median, and p-value of Mann-Whitney U test for grain size (E) (mm), density (ρ) (kg/m^3), and hand hardness (R) for transitions that impeded water involving new snow and fragmented precipitation particles (symbols from Colbeck , 1990).

	Layer Above		**Layer Below**		**p-value (MW U Test)**
	n	**median**	***n***	**median**	
E	23	0.75	23	1.00	0.32
ρ	23	112	23	129	0.02
R	24	1.00	24	1.50	0.12

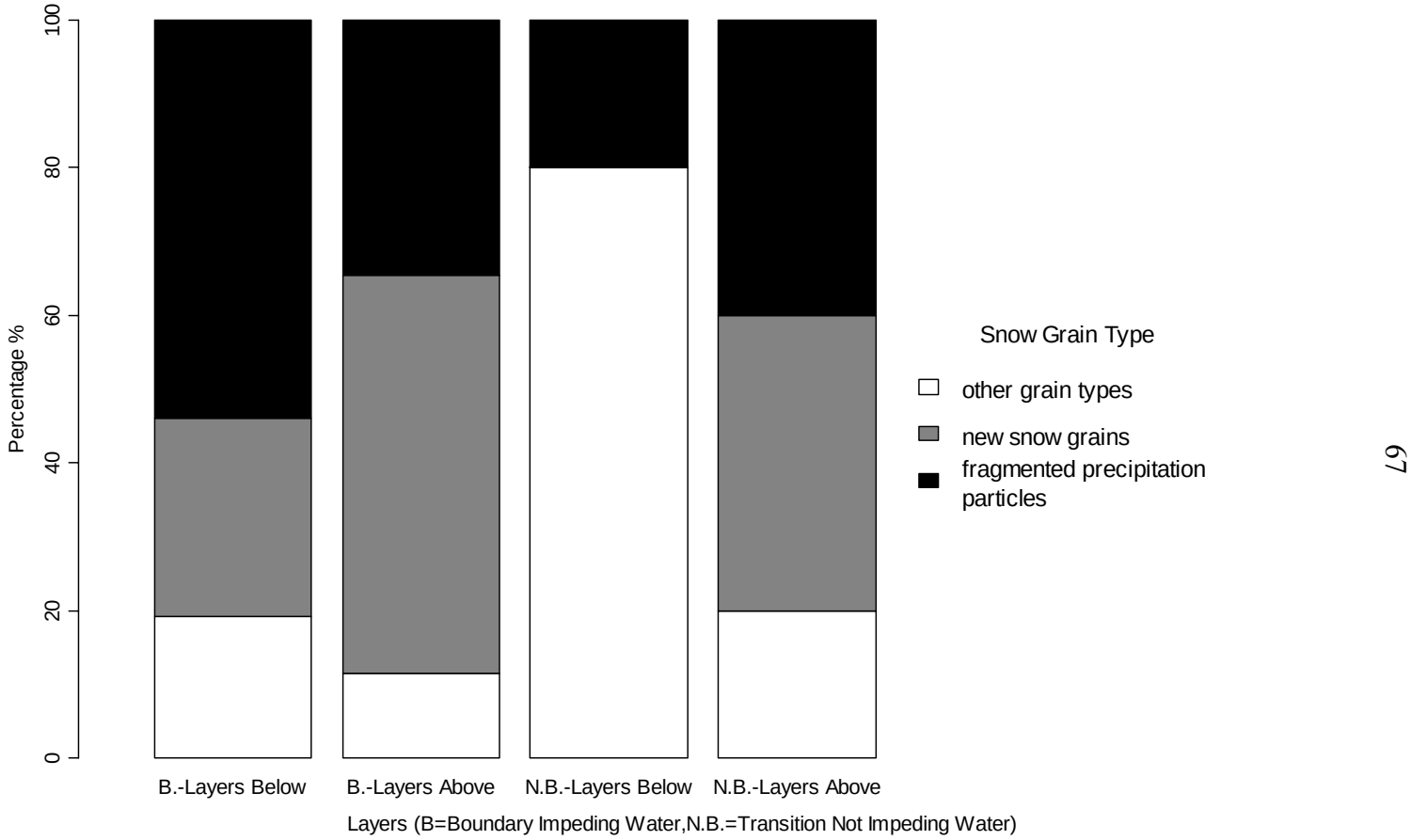

Figure 28: Bar chart displaying the proportions of crystal types in all layers above and below transitions that impeded water and transitions that did not impede water involving new snow and fragmented precipitation particles.

Melt-freeze and Wind Crusts: Crusts, especially melt-freeze crusts, are commonly assumed to act as a barrier to water flow. Often, crusts could easily be identified when dyed water pooled above or below (Table 11; Fig. 29). Note that these two types of crusts represent hydraulic conductivity or capillary boundaries. A melt-freeze crust is an example of a hydraulic conductivity boundary due to the change in hydraulic conductivity between the melt-freeze crust and the adjacent layer. A wind crust is an example of a capillary boundary because it contains fine grains relative to the layer below. This work showed that where crusts were present as either the layer above or the layer below the transition, melt-freeze crusts indeed were prevalent (53%) as the bottom layer, yet also comprised the upper layer of capillary barriers (20%) as well (Fig. 30). Of 35 interfaces involving crusts, 15 of those interfaces (43%) acted as transitions that impeded water while 20 (57%) did not (Appendix A). The crystals above the boundaries were composed of melt-freeze (27%) and wind crusts (27%) and other grains (53%) including stellar dendrites, rounded particles, faceted grains, and wet grains. The layers below were comprised of crusts (53%) and precipitation particles, rounded grains, and faceted grains (together comprise 47%). Nine of the 15 interfaces had a layer above the transitions that was harder *and* denser than the layer below. Yet, statistical analyses showed no significant difference for hardness between the layers above and below the interface ($p > 0.05$) or for density ($p > 0.05$) (Table 11). Also, in nine of the 15 (60%) cases the layers above were comprised of crystals of smaller or equal sized grains than the layers below, but statistical tests again showed no significant difference ($p > 0.05$).

Thus, it can be concluded based on this dataset that crusts can be both above and below boundaries that impede water. Melt-freeze crusts were the most common of the crust layers present, but buried wind crusts were also present in the experiments. Interestingly, of the interfaces with buried wind crusts, this type of crust always served as the layer above the water-impeding boundary.

Twenty layer transitions were observed that contained a crust layer in which water moved directly through without being impeded. In these cases, crusts also existed as both the layer above (55%) and the layer below (45%) the boundary adjacent to varying crystal types (Fig. 28). The most prominent crystal type (aside from crusts) in this category as a layer above is wet grains (20%); rounded grains serve as the most common type layer below the transition (25%). Differences in layer density, hardness, and grain size also vary. Thus, it is difficult to identify any strong patterns that predict whether the crust will impede water, and, if so, whether it tends to be the layer above or the layer below the impeding boundary.

Table 11: Sample size, median, and p-value of Mann-Whitney U test for grain size (E) (mm), density (ρ) (kg/m3), and hand hardness (R) for transitions that impeded water involving crusts (symbols from Colbeck, 1999).

	Layer Above		**Layer Below**		**p-value (MW U Test)**
	n	**median**	**n**	**median**	
E	15	0.75	13	0.75	0.19
ρ	13	239	11	240	0.29
R	14	2.34	14	2.84	0.65

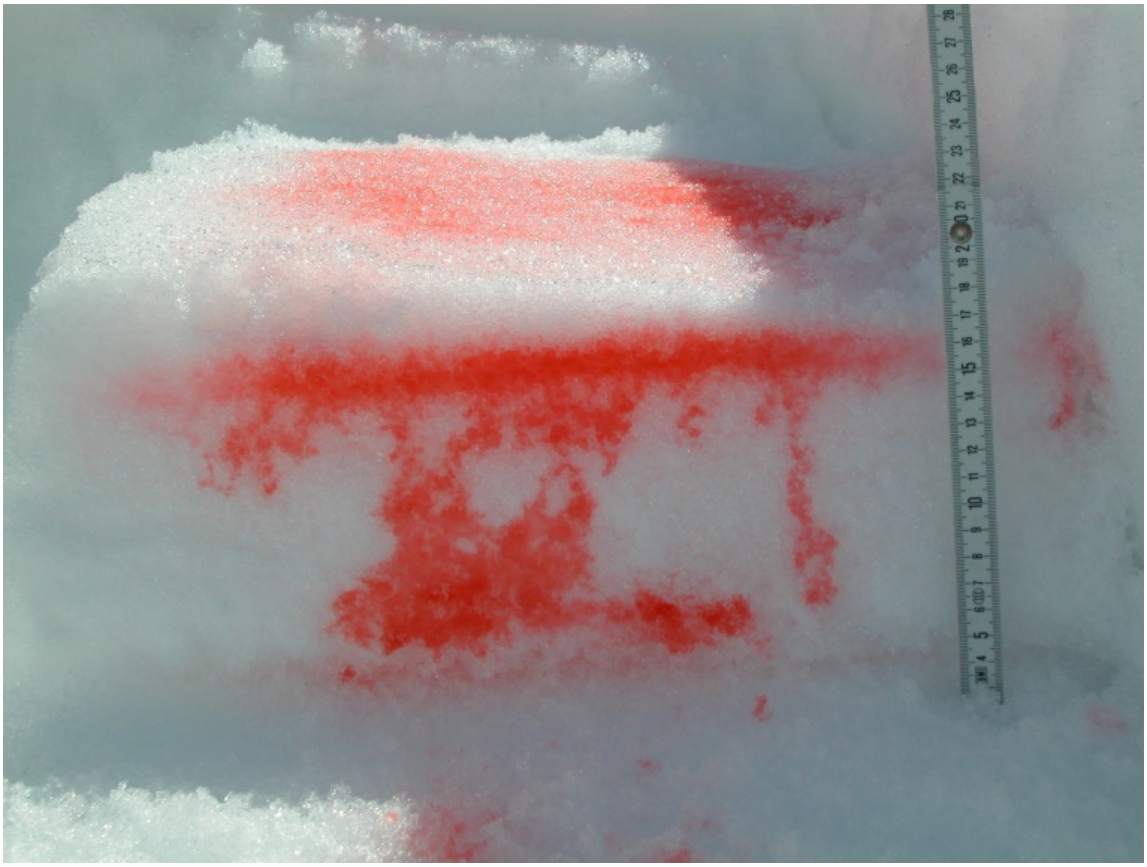

Figure 29: Water pooling above a buried melt-freeze crust in a previously wetted snowpack before moving vertically through many flow fingers established during meltwater percolation.

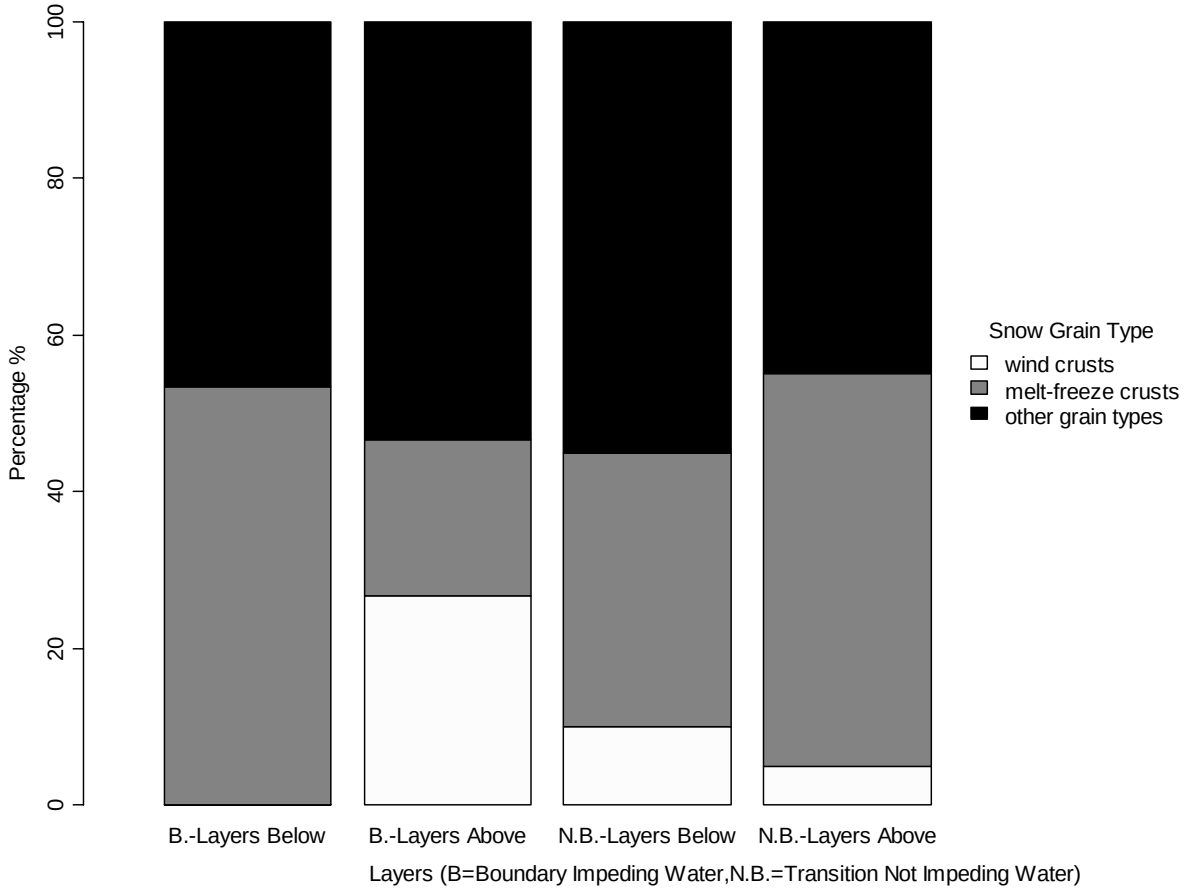

Figure 30: Bar chart displaying the relative proportions of crystal types associated with transitions involving all types of crusts that impeded water and transitions that did not.

Faceted Crystals: Of 19 interfaces involving faceted crystals, nine (47%) of those interfaces impeded vertical water flow while 10 (53%) of them did not (Appendix A). The crystals above the transitions that impeded water were small faceted grains and mixed-form faceted grains (33%) and other crystal types (67%) including columns, highly broken particles, small rounded grains, large rounded grains, and wind crusts. Those below the transition were solid faceted grains, small faceted grains, and mixed-form faceted grains (89%), or melt-freeze crusts (11%) (Fig. 31). All of the crystal types differed between the layer above and the layer below in each transition, and only two contained one type of facet over another (Appendix A). Eight of the nine (89%) transitions that impeded water had faceted crystals as the layer below, while one had a melt-freeze crust as the layer below. Three of the layer transitions involved a crust as a layer above or below the impeding boundary. Reardon and Lundy (2004) describe this "funny business" layer (a mix of faceted grains and a crust) as the failure layer in a large wet slab avalanche cycle in the spring of 2003 in Glacier National Park.

When faceted grains were present, they comprised the layer below in all but one of the transitions that impeded water. This may be due to the "coarseness" (less suction) of faceted grains compared to the overlying layer. This is an example of a capillary boundary. The impedance of water may be attributed to characteristics of transitions that impede water, but statistical results show no significant difference between the layers above and below transitions that impeded water for density ($p > 0.05$), hardness ($p > 0.05$), or grain size ($p > 0.05$) (Table 12). Thus, classifying water-impeding boundaries involving faceted grains based on these variables is difficult.

Table 12: Sample size, median, and p-value of Mann-Whitney U test for grain size (E) (mm), density (ρ) (kg/m^3), and hand hardness (R) for transitions involving faceted grains that impeded water (symbols from Colbeck, 1999).

	Layer Above		Layer Below		p-value
	n	**median**	**n**	**median**	**(MW U Test)**
E	9	0.50	9	0.50	0.77
ρ	9	164	8	228	0.35
R	9	2.00	9	2.00	0.90

Not every transition involving faceted grains impeded water. Results show 10 interfaces with faceted grains that did not impede vertical water flow. Of these interfaces, the layer above the transition consisted of faceted grains (30%) and stellar dendrites, fragmented particles, rounded grains, and melt-freeze crusts (together comprising 70%). While the layer below the transition consisted of faceted grains (70%) and other crystal types including fragmented particles, and melt-freeze crusts (30%) (Fig. 31). Faceted grains were almost as evident as the layer below transitions that did not impede water as they were in transitions that impeded water. Further, the adjacent crystal types to these faceted grains in both impeding and non-impeding boundaries were nearly identical making it difficult to predict what may or may not impede water. Therefore, careful examination during periods of water flow through interfaces involving faceted grains is the best means of identifying transitions that may impede vertical water flow.

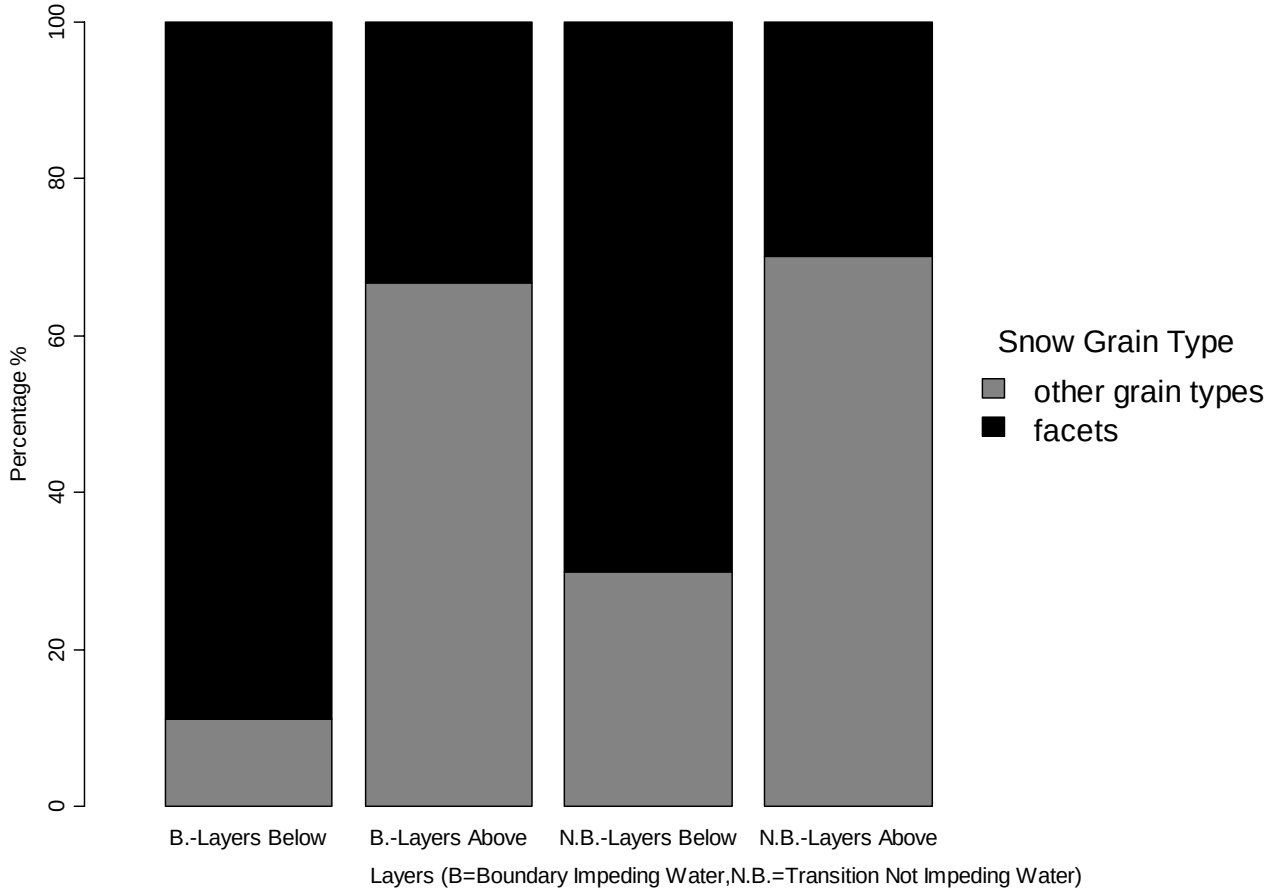

Figure 31: Bar chart displaying the relative proportions of crystal types associated with transitions involving all types of faceted grains that impeded water and transitions that did not.

Rounded Grains: Data were collected on 22 transitions that contained rounded grains. Of these 22 transitions, 10 (42%) impeded vertical water flow (Appendix A). The layers above transitions that impeded water flow consisted of rounded grains (40%) and other grains (60%) that consisted of highly broken particles, wet grains, and melt-freeze crusts, while rounded grains (40%) and other grains including faceted grains, and melt-freeze crusts (60%) comprised the layer below transitions that impeded water (Fig. 32). There seem to be no clear patterns in the crystal/grain type composition of either the layer above or the layer below transitions that impeded water that contain rounded grains. However, the densities of the layers above are significantly less than the layers below transitions that impeded water ($p > 0.05$) (Table 13).

Hydraulic conductivity boundaries (such as rounded grains over a melt-freeze crust) and the small sample size of both layers may partially explain this result. Such a small sample provides a limited range of density values thus skewing the data towards the lower end in this dataset. It may also be partially explained by sampling error. While every precaution was taken to sample consistently for thin layers, exact values for layers at the transitions may have been lost due in the bulk property measurement methods for density. Hardness for transitions involving rounded grains for the layers above was not significantly different than layers below transitions that impeded water ($p > 0.05$). Hardness values for three of the six transitions that impeded water showed softer layers as the layer above. For grain size, half the transitions had layers above that were larger than the layer below and there was no significant difference ($p > 0.05$).

Table 13: Sample size, median, and p-value of Mann-Whitney U test for grain size (E) (mm), density (ρ) (kg/m^3), and hand hardness (R) for capillary barriers involving rounded grains (symbols from Colbeck, 1999).

	Layer Above		**Layer Below**		**p-value**
	n	**median**	**n**	**median**	**(MW U Test)**
E	10	0.63	8	0.75	0.40
ρ	9	244	8	334	0.03
R	9	2.33	9	3	0.90

There were 12 layer transitions that contained rounded crystals as either the layer above or below transitions that did not impede water (Appendix A). Of these transitions, rounded grains (50%), crusts (42%) and new snow (8 %) comprise the layer above, while the layer below consists of rounded grains (66%), crusts (17%), and faceted grains (17%) (Fig. 32). These 12 transitions exhibit no clear patterns in grain size, density, or hardness. Thus it is difficult to compare these transitions to those that impeded water.

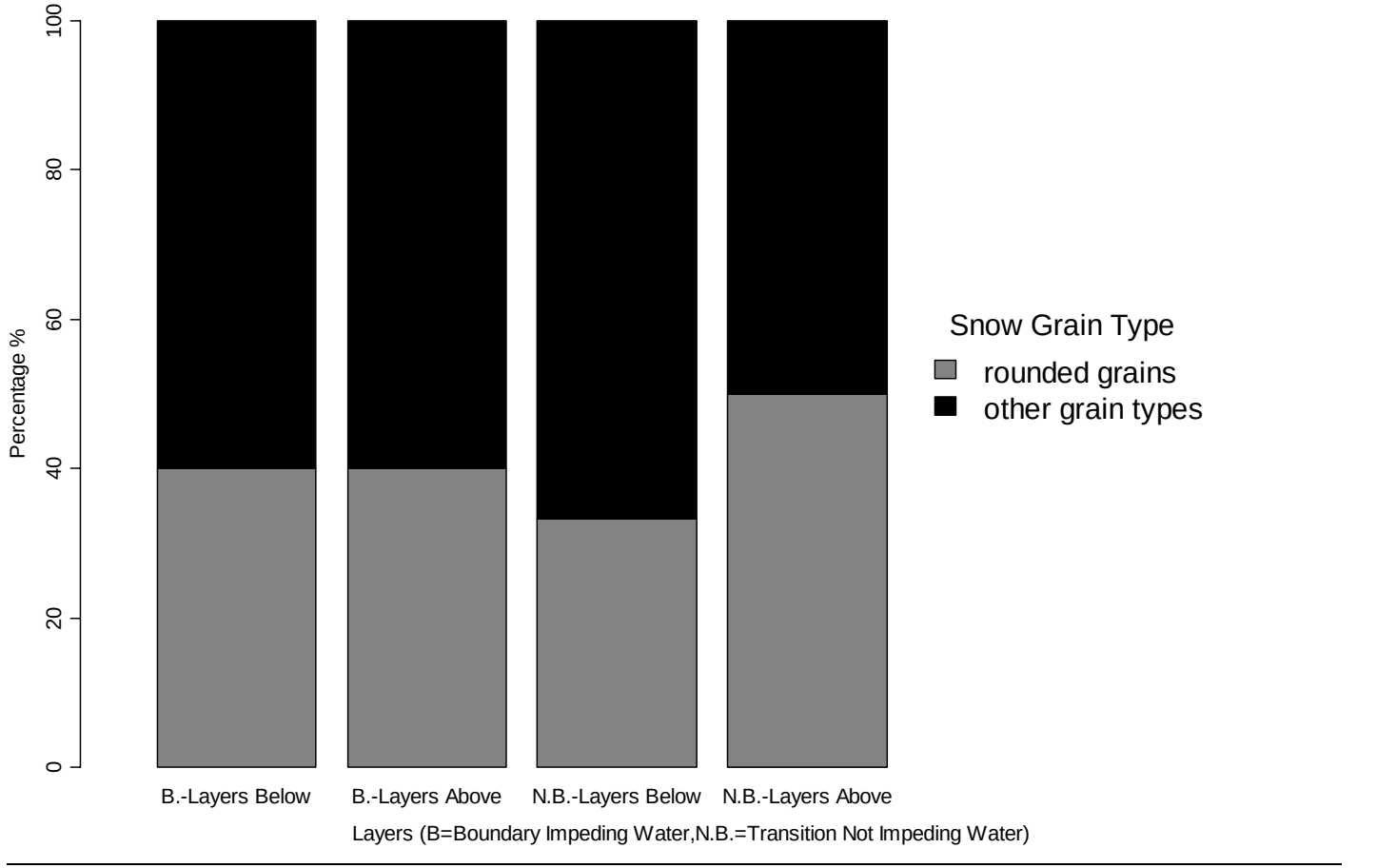

Figure 32: Bar chart displaying the relative proportions of crystal types associated with transitions involving all types of rounded grains that impeded water and transitions that did not.

Wet Grains: Wet grains proved challenging to analyze because of the small sample size (n=16) and the nature of an already wet snowpack (Appendix A). The snowpack in this dataset was trending or already at a relatively wet and homogenous snowpack thus making it difficult to determine the effect of applied water. For the purpose of this study wet grains, were grains that contained any amount of free water visible with a 30x field microscope. Of transitions that contained wet grains five impeded water and 11 did not impede the vertical flow of water. The layer above boundaries that impeded water always consisted of wet grains (100%), while the layer below consisted of wet grains (20%), rounded grains (20%), and crusts (60%) (Fig. 33). Statistical tests were performed on density, hand hardness, and grain size for all types of transitions involving wet grains, but due to the small sample size results were omitted because of lack of confidence in significance values.

There were 11 layer transitions involving wet grains that did not impede vertical water flow (Fig. 33) (Appendix A). There were no clear patterns in density, hardness, and grain size for these transitions. There were numerous melt-freeze crusts as either the layer above or the layer below the water impeding boundary. This result illustrates that crusts, while typically thought of as barriers to water flow, do not always serve this purpose. This is consistent with observations made by Conway and Benedict (1994).

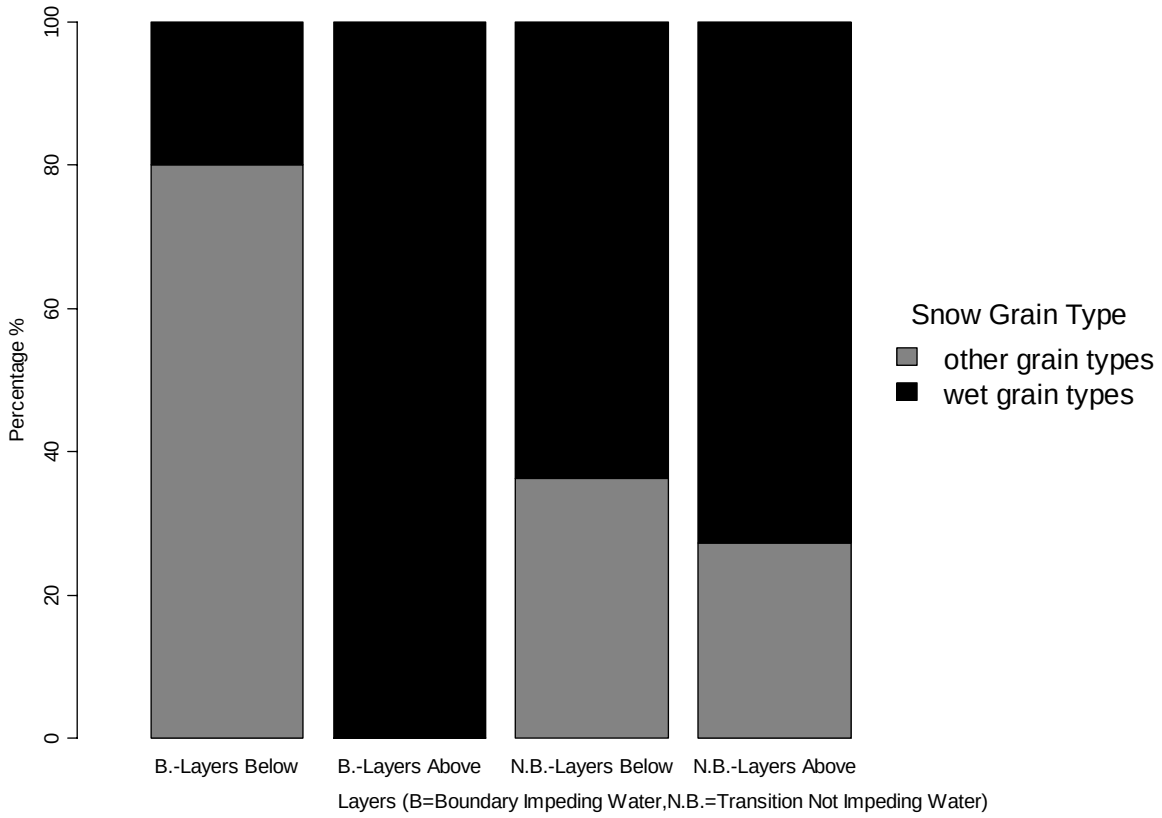

Figure 33: Bar chart displaying the relative proportions of crystal types associated with transitions involving all types of wet grains that impeded water and transitions that did not.

Snow Crystal Type and Stratigraphy Summary: The relationships between the snow crystal types play a role in determining whether a layer transition impedes water or not. These results illustrate the complexity of capillary boundary and hydraulic conductivity boundary formation. Though I investigated 51 transitions that impeded water, it was not possible to measure significant patterns in snow crystal type alone in those layers. For new snow these transitions were exceedingly subtle, but 83% of the time they still served to allow downhill water transport for at least 1 m of slope distance, a finding consistent with past work (Kattelmann, 1987). These findings suggest that rain or meltwater on new snow is likely to move water downslope and laterally along quite subtle textural changes within that new snow.

Crusts existed either as the layer above or as the layer below transitions that impeded water. I also observed the same conditions in transitions that did not impede water suggesting that the presence of crusts does not always imply that it will impede water. Also, water not only flows along the top of crusts but also below the crusts. While both wind and melt-freeze crusts formed the layer above transitions that impede water, I observed only melt-freeze crusts below the transitions that impeded water.

In only one out of nine cases were faceted grains found above a transition that impeded water. In all other cases where faceted grains were associated with these water-impeding boundaries, they were below the transition. Because faceted grains typically form porous, loosely compacted layers, I did expect other adjacent layers to hold the water better. This emphasizes the importance of carefully monitoring faceted layers when free water starts moving through the snowpack. Water flowing along strong

capillary boundaries or hydraulic conductivity boundaries may weaken bonds at grain boundaries (McClung and Schaerer 1993).

Microstructure and SMP Results

Capillary boundaries were identified in the SMP signal based on manual snow profiles and every boundary either corresponded with, or came within 0.5 mm of, a positive structural element length change of the SMP signal (Appendices B and C). Therefore, since every capillary boundary existed at a transition from smaller element lengths to larger lengths the following results compare capillary boundaries with other layer transitions that only have a positive change in structural element length. Thus, I investigated transitions from a smaller to a larger structural element length.

I collected structural element length (L) SMP measurements because capillary boundaries are typically characterized by fine grains over coarse grains. Thus, structural element length helped to parameterize slight textural differences that might act as capillary boundaries where grain size differences between the two layers is nearly indistinguishable. A sudden drop in the SMP signal indicates a rupture in a structure and when a structural element comes into contact with the penetrometer it will rupture over the given penetration distance (Johnson and Schneebeli, 1999). Structural element length can be considered using the element as a cube, and depends upon the number of ruptures over a given distance (mm). Using the SMP to determine structural element length of adjacent layers allowed me to detect a difference in very subtle layers. Structural element length can be translated to infer grain size. Thus, having a smaller structural element

length over a larger one denotes a transition that can impede water. The following results are a comparison of all capillary boundaries and transitions that did not impede water investigated, and a detailed focus on one individual sample profile for a comparison of transitions within one day of profiles.

The small sample size of capillary boundaries (n=32) relative to the transitions that did not impede water (n=221) is a function of the presence of one to three barriers per profile compared to numerous other identifiable transitions within each profile that did not impede water.

The step change, rate of change, and percent increase are all measurements of structural element length (see Chapter 3). The step change, rate of change, percent increase, and the rank of rates of structural element length were significantly different between capillary boundaries and transitions that did not impede water for the entire dataset from all eight sessions (Table 14). Step change was significantly larger in transitions that impeded water than those that did not impede water ($p<0.05$). The step change interquartile range for capillary boundaries contained much more spread than that of transitions and the median was significantly larger (Fig. 34). This suggests that the change in the actual value of structural element length is greater in transitions that are capillary boundaries. There does not, however, appear to be a minimum threshold value of change in structural element length for a transition to be a capillary boundary as the ranges of both types of transitions overlap. For transitions that did not impede water, 95% of the samples were less than 75% of those that did impede water indicating that capillary boundaries can exist at even microstructurally subtle changes, but generally

have larger step changes than transitions that do not impede water. This result was not apparent through standard snowpit measurements of grains size for the entire dataset. Manual observations for capillary boundaries showed a variety of grain size transitions including small over large grains, equal grain size, and even large over small grains, thus illustrating that the SMP may provide a much more robust technique for identifying capillary boundaries as an absolute change in structural element length when standard measurements do not capture such changes. However, it must be noted that for all SMP analyses, capillary boundaries have a much smaller sample size than transitions that did not impede water and the middle 50% may perhaps be smaller with a larger dataset (Table 14). These results indicate transitions with larger changes in structural element length tend to be capillary boundaries and smaller changes tend not to impede vertical water flow. This can be extended to grain size reasonably well to illustrate the fine over coarse grain regime (Wankiewicz, 1979; Colbeck, 1974).

Table 14: Descriptive statistics and p-values for the nonparametric Mann-Whitney U Test of step change, rate of change, and percent increase of structural element length (L) between capillary boundaries and transitions that did not impede water (T.N.I.W).

Metric	Transition	*n*	median	$Q_{.25}$	$Q_{.75}$	p-value (M-W U Test)
Step Change	**Capillary Boundary**	32	0.159	0.105	0.469	<0.0001
	T.N.I.W.	221	0.012	0.003	0.039	
Rate of Change	**Capillary Boundary**	32	0.013	0.010	0.039	<0.0001
	T.N.I.W.	221	0.003	0.001	0.006	
Percent Increase	**Capillary Boundary**	32	1.214	1.140	1.496	<0.0001
	T.N.I.W.	221	1.014	1.003	1.040	
Rank of Step Change	**Capillary Boundary**	32	1	1	2	<0.0001
	T.N.I.W.	221	7	3	13	

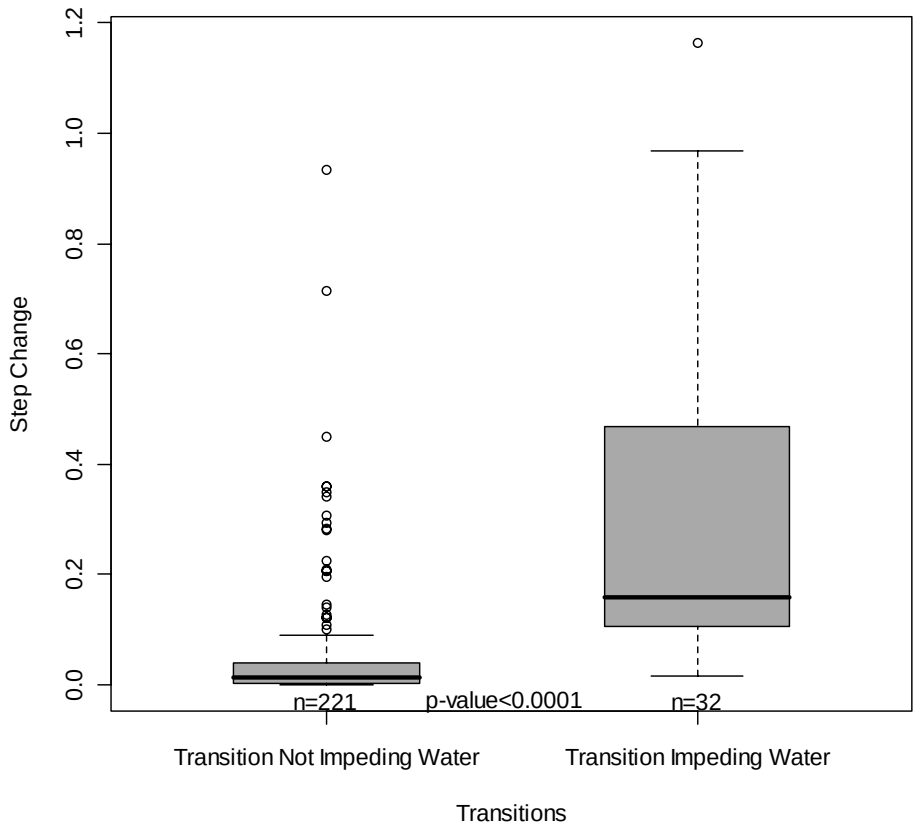

Figure 34: Box plot of step change of capillary boundaries and transitions that did not impede water. Thick black lines indicate median, boxes interquartile range, whiskers extend to the 0.05 and 0.95 quantiles, and the circles indicate outliers.

Similar to the step change value, the rate of change was significantly larger in capillary boundaries than transitions that did not impede water ($p<0.05$) (Fig. 35). This suggests that there is a steeper change in structural element length in capillary boundaries than other transitions. The steeper the change in structural element length implies a more rapid shift from smaller to larger grains on a microstructural scale and indicates that the rate of change between layers above and layers below a transition also dictate whether or not the transition will impede vertical water flow. Once again, there appears to be no

minimum threshold of rate of change, however, 50% of the capillary boundaries had rates of change that exceed 95% of the transitions that did not impede water. This is interesting because it suggests that capillary boundaries can exist at very small rates of change between layers.

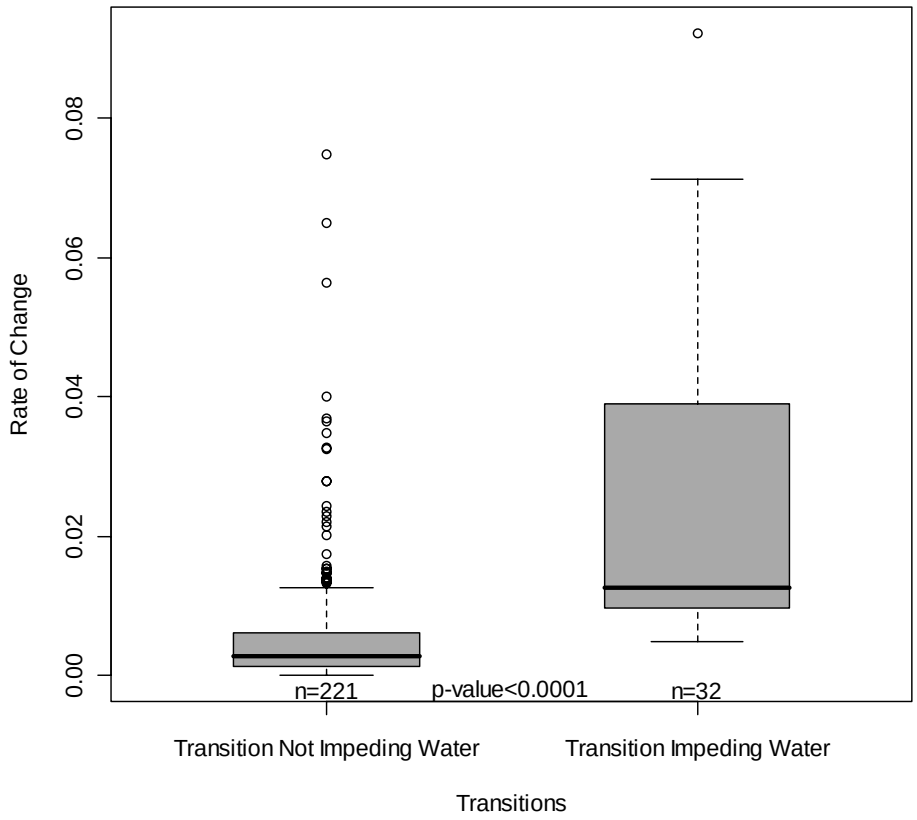

Figure 35: Box plot of rate of change of capillary boundaries and transitions that did not impede water. Thick black lines indicate median, boxes interquartile range, whiskers extend to the 0.05 and 0.95 quantiles, and the circles indicate outliers.

The percent increase is the ratio between the maximum value of structural element length and to the minimum value for that transition. The percent increase in transitions that were capillary boundaries was significantly larger than transitions that did

not impede water ($p<0.05$) (Fig. 36). This metric is similar to the step change, but as a percentage it provides an interesting perspective. The percent values are relatively small for both transitions and this subtle actual value for increase in element length is notable. For instance, a median ratio increase of 1.2 for capillary boundaries (which translates to a 20% increase) in grain size translates to a transition from 1 mm fine grains to 1.2 mm grain size. This subtle increase of just 0.2 mm between the layer above and the layer below roughly coincides with the manually measured grain size difference of median grain size (0.25 mm difference) (Table 1). Yet when the paired differences of manual grain size measurements were calculated the median was zero mm suggesting no difference (Table 2). Thus it appears that the SMP is sensitive enough to detect some of the subtle textural changes I had difficulty identifying with standard methods. There appears to be no minimum threshold of percent increase. For my dataset, a minimum percent increase is not required for a transition to impede water.

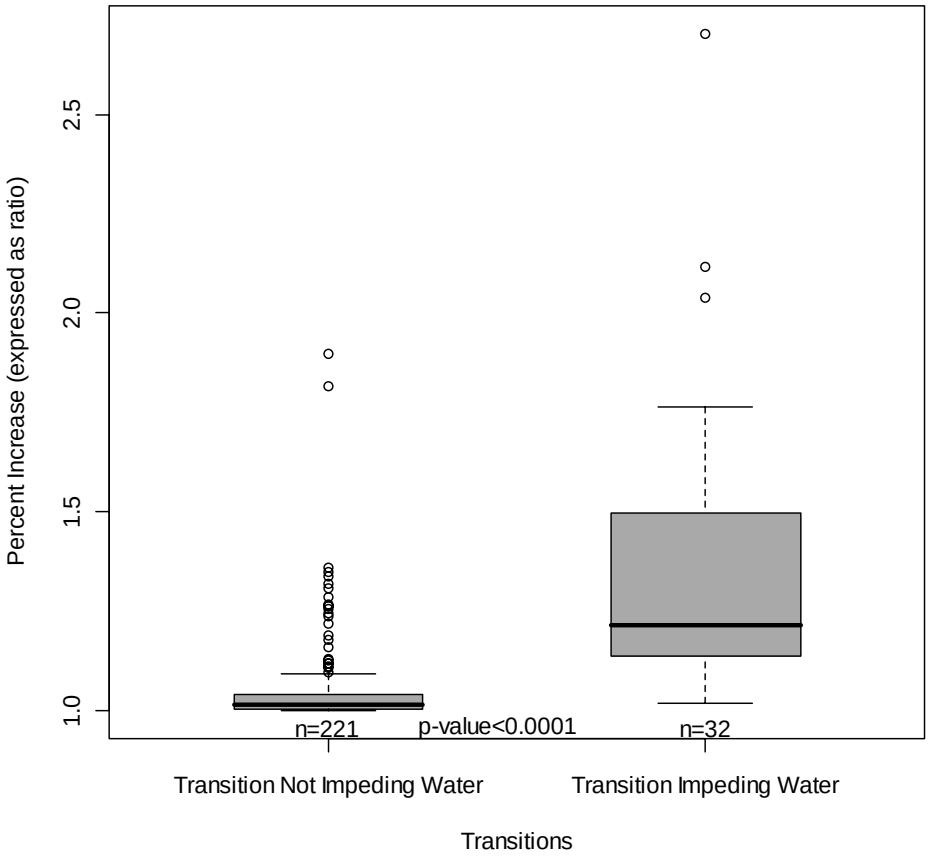

Figure 36: Box plot of percent increase (expressed as ratio) of capillary boundaries and transitions that did not impede water. Thick black lines indicate median, boxes interquartile range, whiskers extend to the 0.05 and 0.95 quantiles, and the circles indicate outliers.

All transitions were ranked based on the absolute change in structural element length between the layer above and the layer below for each profile. These ranks were compared between transitions that were capillary boundaries and transitions that did not impede water (e.g. the largest change in structural element length between any two measureable layers received the rank of 1. Thus a rank of one is higher than a rank of five). For each profile, capillary boundaries had a significantly higher rank than transitions that did not impede water (Table 14). This is interesting because the central

value for capillary boundaries was also the highest rank or the largest change. Of the ranks of step change for capillary boundaries, 95 % existed as either a rank of 1 or 2 (Fig. 37). This illustrates that on a microstructural scale for a given snowpack with capillary boundaries those transitions usually have the highest rank of absolute change.

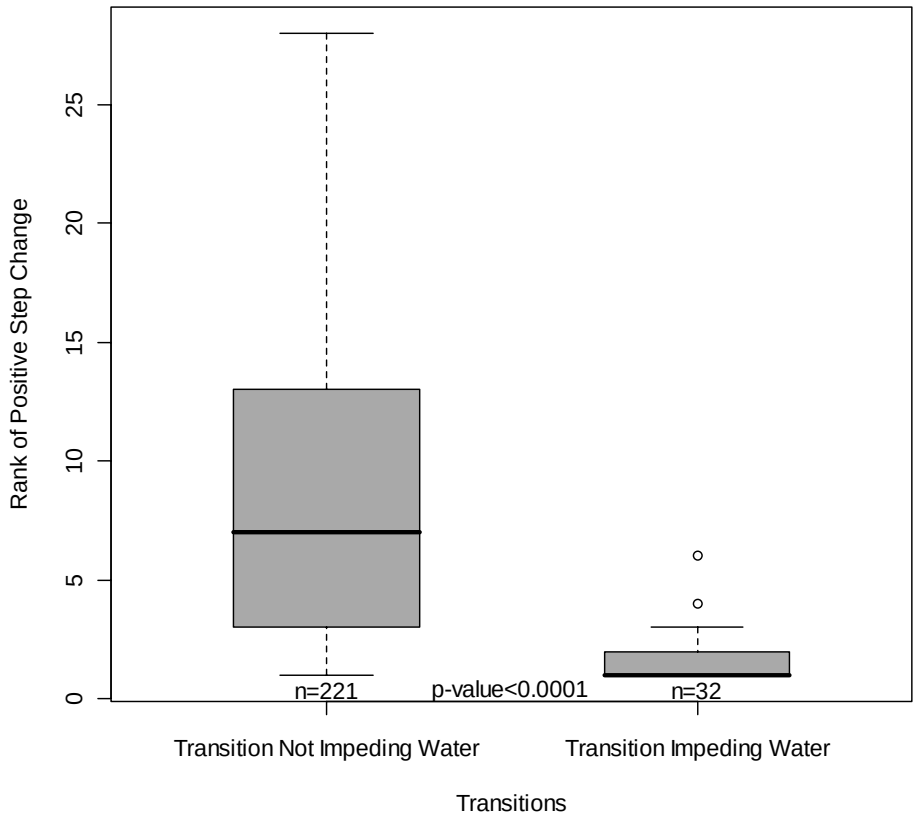

Figure 37: Box plot of rank of positive step change of capillary boundaries and transitions that did not impede water. Thick black lines indicate median, boxes interquartile range, whiskers extend to the 0.05 and 0.95 quantiles, and the circles indicate outliers.

SMP Case Study: The SMP results from the first session (5 February 2008) utilizing the SMP provided 10 useful profiles with one capillary boundary and numerous other positive layer transitions that did not impede vertical water flow (Fig. 38). The

absolute ranks of the entire dataset were compared and the results from 5 February 2008 are provided for an example of the relationship between SMP signal and the parameters investigated (step change, rate of change, percent increase). The manual profile shows only two layers as water failed to percolate beyond the transition between these layers (Fig. 39). The capillary boundary (labeled as a solid teal line) for this profile from Day 1 was 53.5 mm, and had the largest absolute change and rate of change from minimum to maximum value of structural element length. It is also interesting to note that the largest value of mean hardness (F) and the largest number of mean ruptures (N) occurred just before the slope increases and structural element length increases as well. This suggests that the layer above the capillary barrier was the hardest layer in this specific profile.

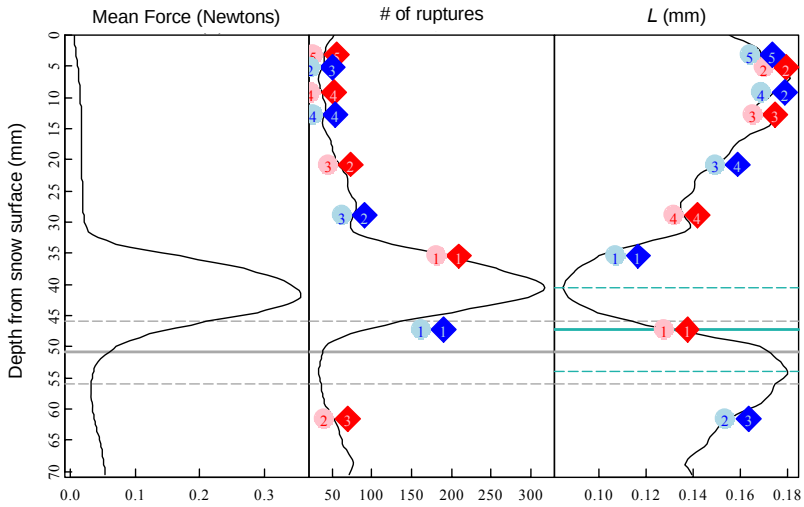

Figure 38: One (of 10) SMP profile for 5 February 2008 displaying mean rupture force, mean number of ruptures, and structural element length (L). The numbered circles indicate the rank of the step change, and the numbered diamonds the rank of slope for the transitions for each profile (1=largest change). Blue indicates a decrease in value and red a positive change in the value. The gray solid lines indicate the location of peak hardness near the capillary barrier based on the manual profile, and the gray dashed lines provide a 5 mm scale on either side. The solid teal line represents the manual delineation of capillary barriers and the dashed teal lines a 5mm scale on both sides.

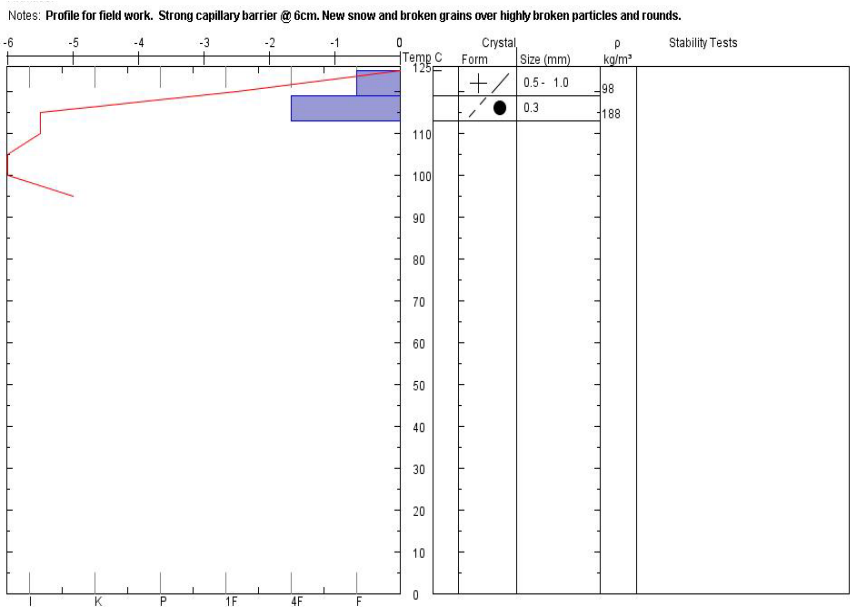

Figure 39: Manual profile from 5, February, 2008. The profile shows only two layers because water failed to percolate beyond the transition between these two layers.

Step change, rate of change, percent increase, and rank of step change were all significantly larger for capillary boundaries than for transitions that did not impede water (Table 15). The step change, rate of change, and percent increase all correspond to patterns evident throughout the entire dataset (Fig. 40, 41, and 42). The rank of step change for 5 February 2008 is interesting because nine out of 10 capillary boundaries were ranked as the largest absolute change relative to the other transitions in that profile; one had a rank of two (Fig. 43). Thus, this day is representative of the overall dataset and shows a significantly larger increase from fine grains to coarse grains in capillary boundaries.

Table 15: Day 1 descriptive statistics and p-values for the nonparametric Mann-Whitney U Test of step change, rate of change, and percent increase of structural element length (L) between capillary boundaries and transitions that did not impede water (T.N.I.W).

Metric	Transition	*n*	median	$Q_{.25}$	$Q_{.75}$	p-value (M-W U Test)
Step Change	**Capillary Boundary**	10	0.600	0.410	0.890	<0.0001
	T.N.I.W.	36	0.049	0.013	0.143	
Rate of Change	**Capillary Boundary**	10	0.059	0.041	0.070	<0.0001
	T.N.I.W.	36	0.015	0.007	0.028	
Percent Increase	**Capillary Boundary**	10	1.622	1.354	1.766	<0.0001
	T.N.I.W.	36	1.031	1.011	1.117	
Rank of Step Change	**Capillary Boundary**	10	1	1	1	<0.0001
	T.N.I.W.	36	3	2	4	

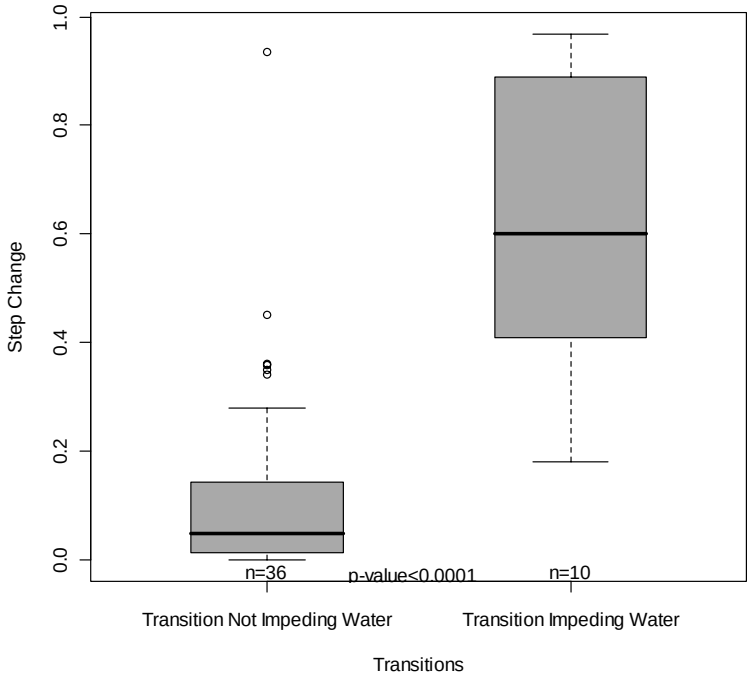

Figure 40: Box plot of positive step change of capillary boundaries and transitions that did not impede water for Day 1. Thick black lines indicate median, boxes interquartile range, whiskers extend to the 0.05 and 0.95 quantiles, and the circles indicate outliers.

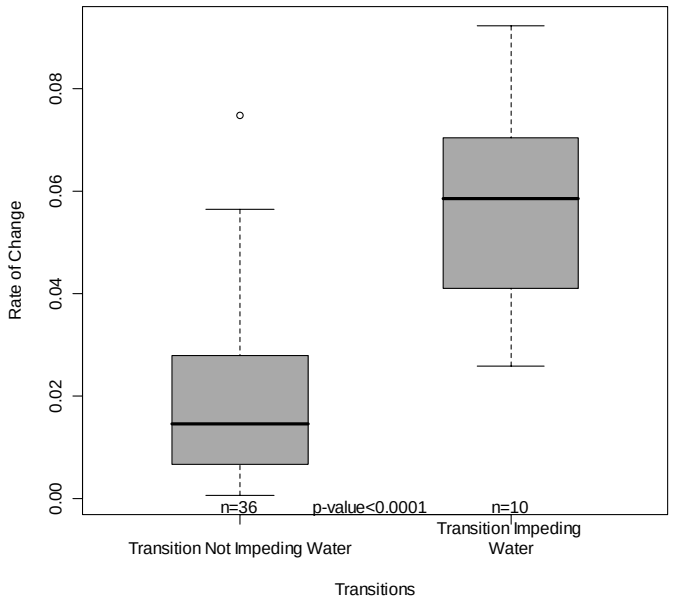

Figure 41: Box plot of rate of change of capillary boundaries and transitions that did not impede water for Day 1. Thick black lines indicate median, boxes interquartile range, whiskers extend to the 0.05 and 0.95 quantiles, and the circles indicate outliers.

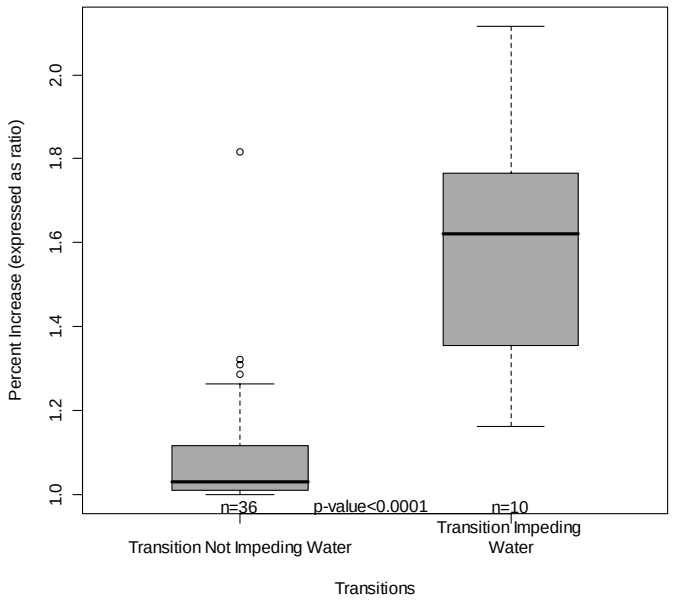

Figure 42: Box plot percent increase (expressed as ratio) of capillary boundaries and transitions that did not impede water for Day 1. Thick black lines indicate median, boxes interquartile range, whiskers extend to the 0.05 and 0.95 quantiles, and the circles indicate outliers.

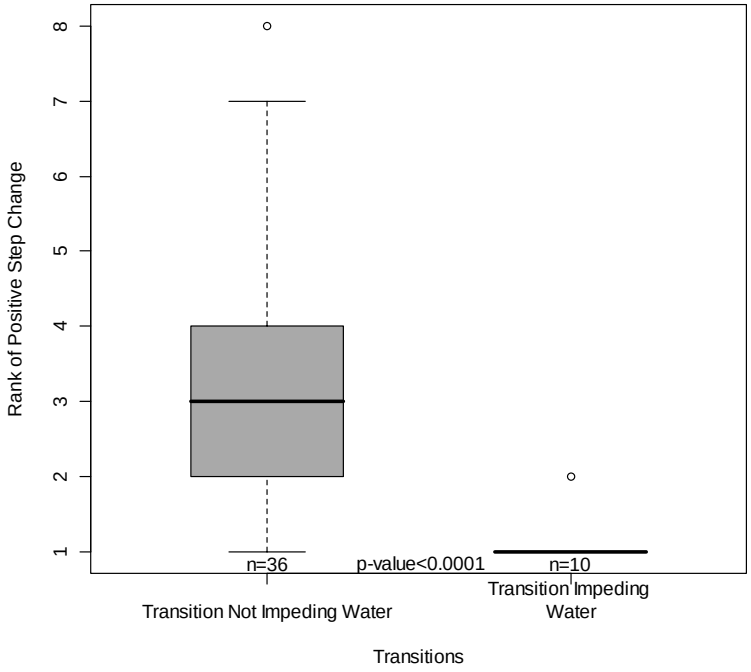

Figure 43: Box plot of rank of positive step change for capillary boundaries and transitions that did not impede water for Day 1. Thick black lines indicate median, boxes interquartile range, whiskers extend to the 0.05 and 0.95 quantiles, and the circles indicate outliers.

The results from SMP measurements indicate that microstructural analysis of the snowpack greatly aids in characterizing capillary boundaries. The results generated from standard snowpit measurements show some patterns, but it could not be concluded that there was a significant difference in grain size between the layer above and the layer below a capillary boundary. The SMP, however, provides evidence to conclude that capillary boundaries in this dataset existed at larger absolute changes, percent increases of step change, and rates of change in structural element length than transitions that did not impede water. The SMP also shows that capillary boundaries are ranked as having larger transitions than transitions that did not impede water. This is interesting because

manual profiles did not indicate a significant change in grain size between the layer above and the layer below the capillary boundary. The use of the SMP to detect subtle transitions and aid in characterizing capillary boundaries is useful. Techel et al. (2008) utilized the SMP to investigate hardness in a wet snow application, and also found the instrument a useful tool with which to characterize wet snow processes. While perhaps not a forecasting tool itself, these results are encouraging. Thus, careful attention must be given to subtle transitions which are difficult to observe with standard pit-description procedures that can potentially impede vertical water flow particularly if a weak layer is present.

Preferential Flow

Increasing amounts of water were added to a dry snowpack to determine critical amounts needed to form flow fingers in varying stratigraphic layers. Snow grain size, density, and snow temperature were analyzed against amounts of water applied. I experienced occasional freezing of the nozzle and pump of the water applicator, and this changed the application rate slightly. However, this interruption may have affected water application rates during only five experiment days.

My results show no significant relationship between the amount of water applied and the formation of flow fingers. Flow fingers formed almost every time water was applied to dry snow (Fig. 44). The only cases where matrix flow occurred during experimentation after water application was in previously wetted snow. In most cases water seemed to be held by capillary pressure at the surface for a short amount of time before enough water was added for a gravity flow regime to occur. Preferential flow occurred almost instantaneously after water started moving vertically. If water was continually added, then matrix flow would follow this flow finger front. This was contrary to my hypothesis that there is a threshold amount of water needed to transition from matrix flow to flow fingers in the snowpack. I discovered that when water was added to a dry, inclined, and stratified snowcover preferential flow occurred as soon as gravity flow became the dominant process. Water moved rapidly in the absence of water-impeding boundaries with rates of 1 to 6 m/hr, a result consistent with other studies (Kattelmann, 1987; Waldner et al., 2004). Thus, I performed a qualitative analysis on the

amount of water needed to transition from water being held in capillarity to the formation of flow fingers. These observations are consistent with measurements of wave front speed observed by Kattelmann (1987) who described that a small amount of water was frozen at the surface and a fluctuating amount was stored in capillaries for minutes to weeks.

Figure 44: Flow fingers ~30 cm from the snow surface after the top 30 cm was removed to determine the existence of preferential flow. Flow fingers almost always formed when water was added to a dry snowpack except for already wetted snow where preferential flow had previously been established.

Because flow fingers formed in nearly every case, there was no relationship between the amount of water applied and density, snow grain size, and temperature. There was also no clear relationship between amounts of water and the number of flow fingers formed. The existence of transitions that impeded water and subsequent accumulation of water at layer interfaces particularly near the surface also made it

difficult to quantify the amount of water that moved through flow fingers in various grain types. However, there is an interesting qualitative comparison between the amount of water needed to transition from water stored or refrozen near the surface to the formation flow fingers (Fig. 45). This comparison is consistent with the observation that flow fingers almost always form when water is added to a dry snowpack. For new snow particles only 0.08 cm of water was needed 45% of the time to form flow fingers. The other 55% of the time water application ranged up to 0.5 cm of water needed for this transition. This is interesting because 48% of all occurrences needed very little water to begin vertical movement of water in the form of flow fingers. In contrast, 0.08 cm (the smallest amount of water applied) were required only 33% of the time for fragmented precipitation particles. These fragmented particles typically required more water (0.8 – 1.6 cm) than new snow particles for flow finger formation. When water moved through crusts it required amounts of water ranging from 0.08 cm to 1.6 cm in nearly equal proportions. These results appear to depend upon where the crust was located. The crusts on the surface (e.g. wind crusts or sun crusts) required more water to penetrate, thus it was difficult to distinguish between a capillary boundary, hydraulic conductivity boundary, or water refreezing at the surface. There appears to be no clear pattern in rounded, faceted, or wet grains.

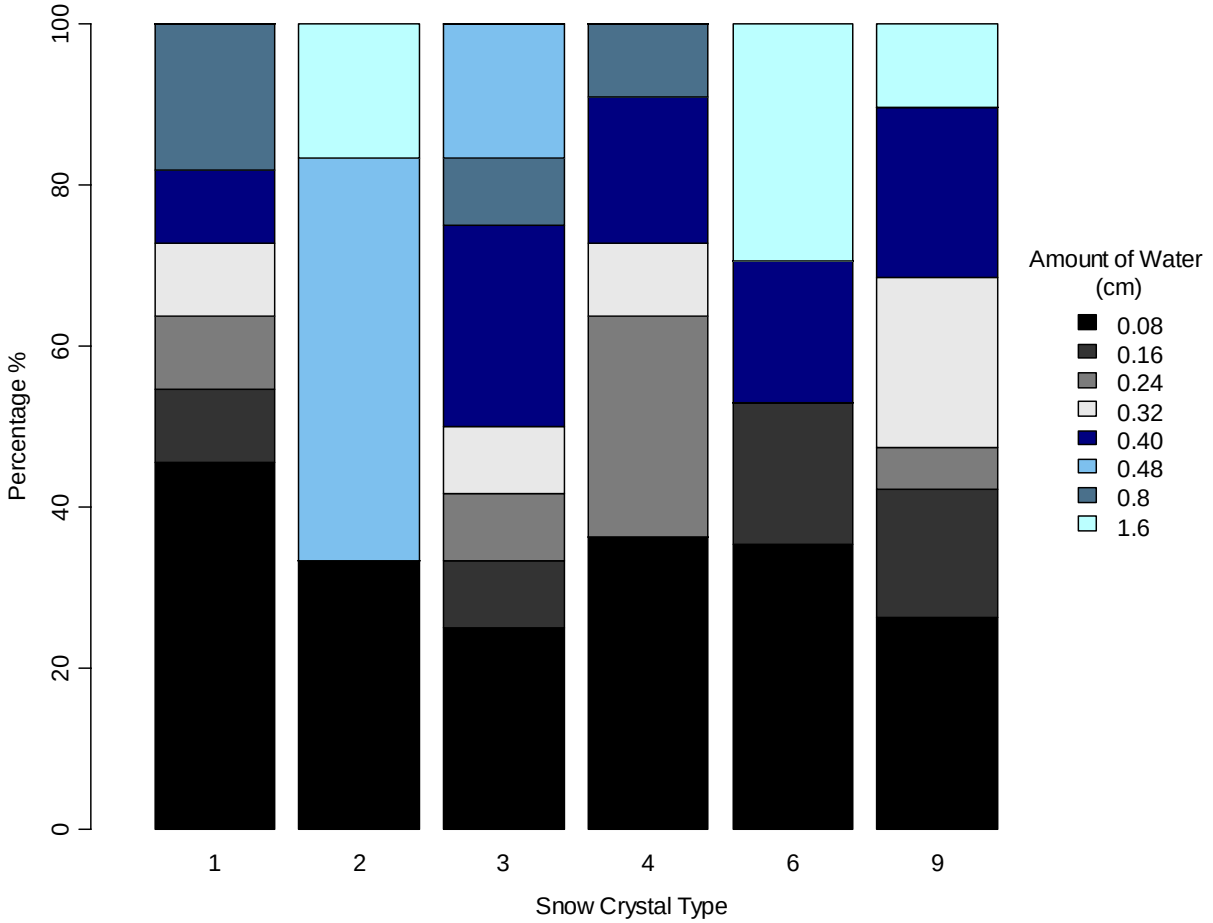

Figure 45: The amount of water added to the snowpack that required the transition from water being held at the surface to flow finger formation in various snow grain/crystal types.

When liquid water was applied to dry, new snow it was held in the upper few centimeters of the snowpack and remained there until it either refroze or was released at a small rate as snow grains metamorphosed in the presence of water. These observations are consistent with studies investigating the retention of water in new snow (Kattelmann, 1987). This has implications in wet loose snow avalanches. As new snow is warmed by increasing air temperatures following a warm front or a rain-on-new-snow event, the amount of melt or rain is important. If enough water is retained in the surface snow then wet loose snow avalanching is possible (Conway, 2004), yet if enough free water is introduced into the snowpack, then flow fingers may form, and route water deeper in the snowpack to potential water-impeding transitions. At this stage it may accumulate, and if a weak layer is present, then a wet slab avalanche may be possible.

The routing of free water deeper in the snowpack through flow fingers still has implications as previously hypothesized. While a critical amount of water necessary to form flow fingers was not quantifiable and preferential flow was exceptionally variable, flow fingers are nevertheless important in moving water to and along layer transitions that impede vertical water flow. These results indicate that flow fingers form with very small amounts of free water, and can deliver water quickly to layer transitions that impede water lower in the snowpack.

Wet Slab Avalanche Case Studies

Some recent wet slab avalanches demonstrate the importance of this work in explaining these cycles. In this section I explore the relationship of water movement in the snow to wet slab avalanches using two wet slab avalanche cycles in Big Sky Ski Resort, Montana, and the Little Cottonwood Canyon, Utah. Because wet slab avalanches are relatively rare it is difficult to assemble a large complete database with both meteorological and detailed snowpack variables. Part of my research focused on compiling wet slab avalanches across western North America, but over a period of two winter and spring seasons (2006-2007 and 2007-2008) data were collected on only three wet slab avalanche cycles. Although it is difficult to perform a quantitative analysis on such a small dataset, a study into the structure of the snowpack that contributed to these case studies was completed.

Big Sky Ski Resort is located approximately 55 km south of Bozeman, Montana in the Madison Range. The wet slab avalanche cycle at Big Sky Ski Resort occurred on 2 May 2007, at approximately 1230 hours in Black Rock Gully in The Bowl. It occurred during the first major warming event of the spring after the ski area had closed to the public for the season. Subsequent fracture profiles were not conducted until 4 May 2007 (Fig. 46). However, a storm had moved through in the intervening days and temperatures decreased thus causing liquid water in the snowpack at the crown to freeze. The bed surface consisted of cup shaped depth hoar and large faceted grains ranging from 2-4 mm. The slide started from high on the slope above a small cliff band as what appeared

to have been a wet loose avalanche, which then triggered a wet slab avalanche below the cliffs. There were three slab releases all located in separate but very shallow gullies along the north aspect of The Bowl (Fig. 47). It is interesting to note the failure layer consisted of coarse-grain depth hoar under a fine-grain buried rain crust that persisted from late December, 2006. It is likely that this layer impeded water flow and that the bonding within the layer of faceted grains/depth hoar was affected by the lateral movement of water at this interface.

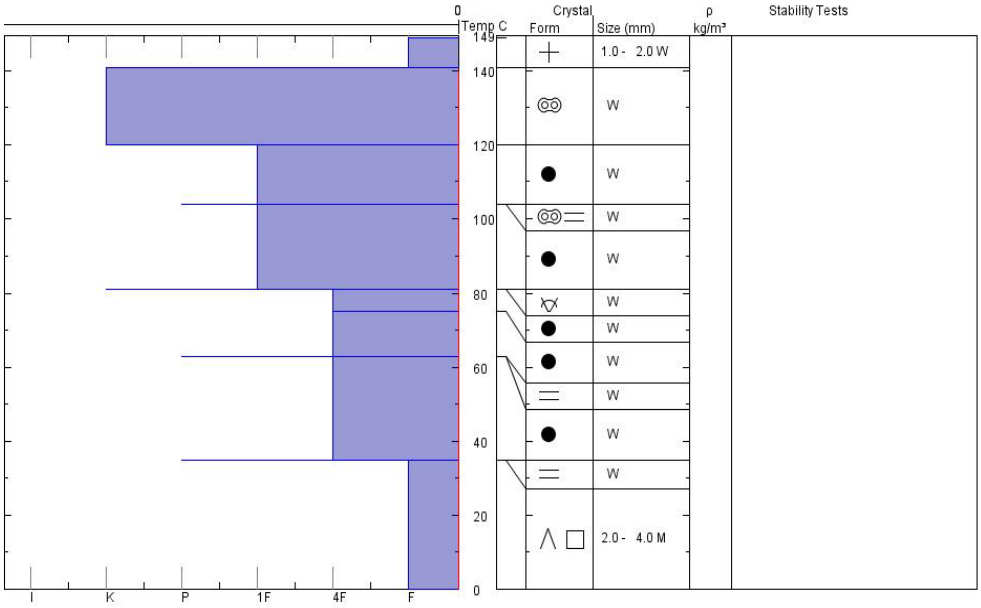

Figure 46: Crown profile of wet slab avalanche at Big Sky Ski Resort that occurred in Black Rock Gully on 2 March 2007. The failure layer is a mix of depth hoar and large-grained faceted crystals under a thin ice crust. There were three separate slabs all within shallow gullies on the north face of The Bowl. General rating for all three slab releases: WS-N-R3.5-D3-O.

Figure 47: Wet slab avalanche in The Bowl at Big Sky Ski Resort. Three separate slab releases exist and were apparently triggered by a wet loose avalanche from the cliffs above. The debris is approximately 1.5-2 m deep and approximately 200 m wide. The crown to stauchwall measures ~50-60 m. Photo by Scott Savage, Big Sky Snow Safety.

A wet slab cycle occurred between 12-17 March 2007 in the Little Cottonwood Canyon of the Wasatch Range, Utah, approximately 40 km southeast of Salt Lake City. Data from seven individual avalanches were collected. All avalanche times were estimated to the quarter hour. They occurred between 1500 hours and 1800 hours. Crown profiles were not conducted on every observed crown, but the snow structure was nearly the same throughout the range on these days (Naisbitt, 2007). The failure layer consisted of a buried melt-freeze crust with wet old faceted grains above and a moist slab of 1 mm rounded polycrystals above the faceted grains (Fig. 48). It is interesting to note that the slab was merely damp and the faceted grains were noted as being wet. This

structure illustrates how water may move preferentially through the slab allowing the upper part of the snowpack to retain slab-like characteristics by keeping it mostly dry or only slightly moist. The faceted grains were wet which seems to indicate that water was transported to a capillary boundary at the interface of the damp, smaller polycrystals over the wetter, larger faceted grains. As water moved within the bottom of the layer of the smaller grains, it melted bonds within the larger, weaker faceted grains resulting in a wet slab avalanche. The avalanches in this cycle occurred naturally and were also skier triggered (Fig. 49).

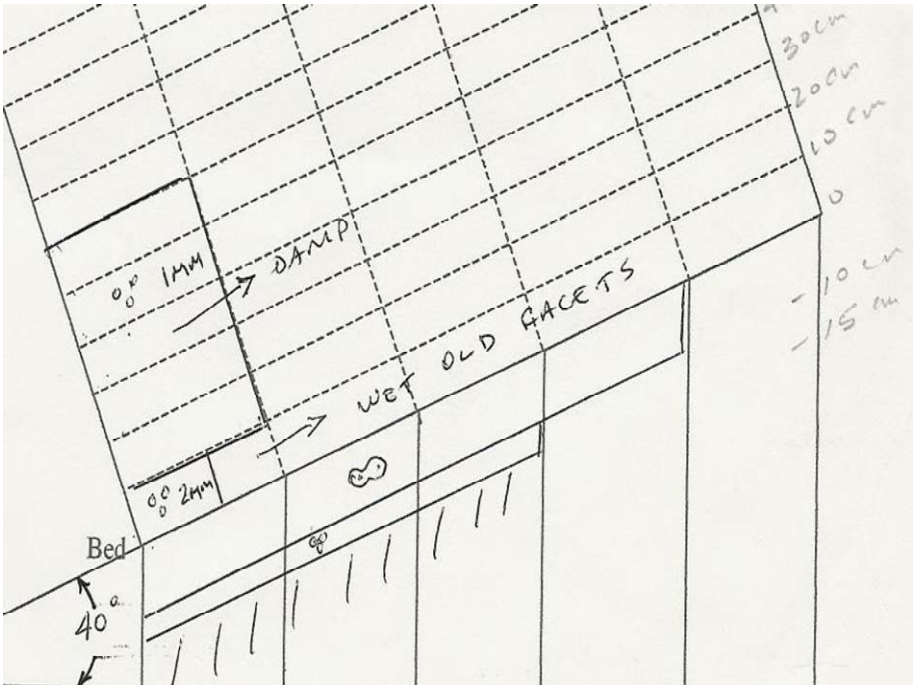

Figure 48: Profile of bottom portion of snowpack of Flagstaff avalanche in the Little Cottonwood Canyon, Utah. This profile was from the second observed avalanche during the cycle and occurred on 12 March 2007 Profile schematic provided by UDOT.

Figure 49: In Little Cottonwood Canyon, Utah, two separate slab releases in Flagstaff Face East and West slide paths that occurred on 13 March 2007. The first slide was triggered by a skier and the second slide released sympathetically after the first one.

CHAPTER 5

SUMMARY AND CONCLUSIONS

Water flow through the snowpack has many implications in slope stability. Water moves preferentially through the snowpack through vertical flow channels called flow fingers. This allows water to move vertically to transitions that can potentially impede water where it then can accumulate and spread laterally. While much work has focused on water movement in the snow, there are few studies that have investigated free water when it is first introduced to a dry snowpack, and the resulting interaction with layer transitions that impede water flow. The focus on wet slab avalanches in this work fostered a methodology that allowed for relative ease of identification of certain snowpack variables, especially grain size, that affect water movement and may contribute to wet slab avalanches. By applying water to a dry snowpack, I was able to examine interactions that occur during rain-on-snow events and during snowmelt cycles. I measured grain size, layer density, layer hardness, snow temperature, and grain type to determine the role they have in water movement in a snowpack. I focused specifically on layer transitions that impeded water flow and compared the variables of these transitions to layers that did not impede water flow. Experiments showed that very subtle layer transitions impeded vertical water flow and the stratigraphic parameters observed through manual snow profiles were the same within the layers above and below these transitions. Thus, I utilized the SnowMicroPenetrometer (SMP) to characterize specific transitions that impeded water (e.g. capillary boundaries) for eight sampling plots. This allowed for

a detailed investigation of capillary boundaries on a microstructural scale. I also found preferential flow within the snowpack, in the form of flow fingers, to be highly variable, and I provided a qualitative analysis of this variability. This analysis showed that there was no relationship between snow grain size, density, hardness, temperature and grain type and the amount of water needed to form flow fingers.

Transitions that Impeded Vertical Water Flow

At the beginning of this experiment I expected to find that vertical water movement in the snowpack was impeded at various layer transitions. I found two types of transitions to impede vertical water flow within the snowpack – hydraulic conductivity boundaries and capillary boundaries. Hydraulic conductivity boundaries manifested themselves in the form of a buried melt-freeze, rain, or sun crust where water was impeded above these crusts. In contrast, capillary boundaries, the most prevalent transition that impeded water in this study, consisted of fine grains over coarse grains, where water was impeded along the bottom of the layer above the transition.

The first objective of this study was to answer the following question: Do snow grain size, layer density, layer hardness, snow temperature, and snow grain type affect vertical water movement in a snowpack, and, if so, what are the characteristics of layer transitions that impede vertical water movement (including capillary boundaries and hydraulic conductivity boundaries)? In layer transitions that impeded water, the grain size of the layer above was significantly smaller than the layer below. No significant difference in grain size existed between layers above and layers below transitions that did

not impede water. The median grain size difference (grain size of layer above minus grain size of layer below) between transitions that impeded water and transitions that did not was not significantly different. Grain size differences in some transitions that impeded water flow were visually obvious, but they were not apparent in all transitions that impeded water flow. Results show these differences can cause water to move downslope for up to 2 m. This has implications for slope stability throughout the winter and spring. Thus, monitoring the snowpack for slight differences in grain size may be useful for avalanche forecasters when forecasting for water movement and resulting avalanches. Whether water remains near the snow surface and results in wet loose avalanches or if it percolates deeper in the snowpack and results in wet slab avalanches, monitoring water flow is important. In spring, versus winter, the grain size difference was more noticeable and easier to identify as the snowpack became more homogenous, and transitions that impeded water existed at obvious grain size transitions.

The layers above transitions that impeded water were significantly less dense than the layers below transitions. This result differed from another study (Illangasekare et al., 1990) but agreed with a study more similar to this project (Jordan, 1995). This result was somewhat surprising because the literature suggests capillary boundaries, the most common type of transition that impeded water in this study, typically consist of denser layers above less dense layers (Waldner, 2004). No significant difference in density existed between layers above and layers below transitions that did not impede water. Also, median density differences (layer above minus layer below) did not significantly differ between transitions that impeded water and transitions that did not. Density,

however, may be a poor indicator of transitions that impede water, particularly those transitions that exist in new snow, due to coarse sampling volumes characteristic of standard density measuring tools.

Hardness did not significantly vary between the layer above and the layer below transitions that impeded water. No significant difference in hardness existed between layers above and layers below transitions that did not impede water. There was no significant difference in hardness differences (layer above minus layer below) between the layer above and the layer below transitions that impeded water and transitions that did not impede water. I found that the layer above and the layer below can be harder or softer than the other, and that the actual hardness of both layers has a wide range from fist hardness to pencil hardness. The dataset consisted of numerous cases of soft, new snow over harder, fragmented snow, but also consisted of cases where hard, wind slab layers existed over layers of softer, faceted grains.

Measured snow temperature results illustrate that both transitions that impede water and those that do not impede water can occur in a wide range of snow temperatures, and there is no significant difference between the two. Temperature is not a useful metric in charactering transitions that impede water movement.

A qualitative analysis of grain type showed that there is no pattern which predicts whether water will be impeded at a transition. Transitions that impede water in new snow can be created from extremely subtle changes in the grain type. Those changes can often be identified when dyed water accumulates at the transition with a 30X hand microscope.

This dataset shows that crusts can be both the layer above or below transitions that impede water. Melt-freeze crusts were the most common of the crust layers present, but buried wind crusts were also present in my experiments. Interestingly, of the interfaces with buried wind crusts, this type of crust always served as the layer above the transition that impeded water. When faceted grains were present, they comprised the layer below in seven of eight transitions that impeded water. This may be due to the larger pore space of faceted grains compared to the overlying layer. Reardon and Lundy (2004) describe the "funny business" layer (a mix of faceted grains and a crust) as the failure layer in a large wet slab avalanche cycle in the spring of 2003 in Glacier National Park. This combination of a crust and faceted grains was similar to a layer in a wet slab cycle that occurred at the Big Sky Ski Area in May, 2007 and Little Cottonwood Canyon, Utah in March, 2007.

Another objective of this study was to answer the following question: Can the SnowMicroPen (SMP) be used to aid in identifying potential capillary boundaries in the snowpack? A sudden drop in the SMP signal indicates a rupture in a structure and when a structural element comes into contact with the penetrometer it will rupture over the given penetration distance (Johnson and Schneebeli, 1999). Structural element length can be considered using the element as a cube, and depends upon the number of ruptures over a given distance (mm). Using the SMP to determine structural element length of adjacent layers allowed me to detect a difference in very subtle layers. Structural element length can be translated to infer grain size. Thus, having a smaller structural element length over a larger one denotes a transition that can impede water.

The SMP provided a means to investigate capillary boundaries that could not be seen through manual field methods (Colbeck 1990). These field methods of capillary boundaries showed a variety of grain size transitions including small over large grains, equal-sized grains, and large over small grains. However, the SMP identified capillary boundaries as an absolute change in structural element length, when standard measurements did not capture such changes. The step change, rate of change, and percent increase are all measurements of structural element length. The step change, rate of change, and percent increase of structural element length were significantly larger in capillary boundaries than in transitions that did not impede water for the entire dataset. When all transitions were ranked according to absolute change for each profile, capillary boundaries consistently ranked in the top two of all transitions evident within each SMP profile, with a median of 1 (being the largest step change). These results indicated transitions with larger changes in structural element length were capillary boundaries and smaller changes were not capillary boundaries. This can be extended to grain size to illustrate the idea that fine over coarse grains results in capillary boundaries (Wankiewicz, 1979; Colbeck, 1974). For this research, results from SMP measurements indicate that microstructural analysis of the snowpack aids in characterizing transitions that impede water flow, but cost and ease of transport might prohibit it from being used in operational settings, such as backcountry and highway avalanche forecasting. Thus, careful monitoring of water movement, perhaps using dye tracer, is needed, instead, to investigate very small grain size differences for practitioners trying to determine if a layer transition might impede water.

Preferential Flow

The final objective of this study was to answer the following question: Do snow grain size, layer density, layer hardness, snow temperature, and snow grain type affect flow finger formation as free water is introduced to a dry and a wet snowpack? Capturing the nature of preferential flow through the methodology used here was very difficult. I hypothesized that flow finger formation required a critical amount of water and may be important in wet slab formation. However, after water was applied to a dry snowpack, water was held in capillarity for 30 seconds to two minutes at the surface and then flow fingers would form once vertical flow movement was initiated. There was no significant relationship between the amount of water necessary to form flow fingers and snow grain size, snow density, hand hardness, snow temperature, or grain type.

Implications for Avalanche Forecasting

Layer transitions that transport water laterally and downslope for long distances occurred with all observed grain types. Knowing where water may be impeded in a snowpack has implications for both wet loose and wet slab avalanches. As demonstrated in this experiment, a strong transition that impeded water often existed within freshly fallen snow. This new snow can serve to change the liquid water regime from pendular to funicular and wet loose avalanches may occur due to increased water content within the top few centimeters of the snowpack.

In the absence of a near surface transition that impedes water, water can form flow fingers and flow to a deeper transition that impedes water (and might include a weak layer). For avalanche forecasters, it would be useful to identify layer transitions of smaller grains over larger grains (these were found to be effective transitions), and where weak layers exist, before a forecasted melt cycle or rain event. As indicated through these results, the transitions need not be large, so careful stratigraphic identification is required.

Future Research

More work is needed to better understand the complexities of the interaction of water flow and snowpack stratigraphy, and the role it plays in wet slab avalanche formation. This experiment was originally designed to examine preferential flow and transitions that impede water flow on a natural, stratified and inclined snowpack. While I applied varying amounts of water in these experiments, each site was constructed as a test plot, not a slope-scale experiment. Thus, a detailed, quantified investigation of many wet slab failure layers is necessary to rule out certain layer transitions as potential failure layers. For instance, carefully monitoring water flow during a forecasted warming event in the spring, or a rain-on-snow event, and detailing the water movement within the snowpack would be useful. This would be especially useful when a facet/crust combination exists near the base of the snowpack. Also, slope-scale experiments utilizing mid-snowpack and basal snowpack lysimeters would be useful in determining water amounts held in water-impeding transitions during such periods or during artificial

application periods. This research illustrates that developing a strong methodology to test preferential flow and how it could possibly contribute to wet slab avalanche formation is necessary for future work.

Therefore, it is a complex problem with no simple answers. This work provides a start for understanding transitions that impede water flow in an inclined snowpack. It does aid practitioners and researchers in identifying the locations where free water within the snowpack may move downslope laterally and where potential failure layers in a wet slab avalanche scenario exist.

REFERENCES CITED

Ambach, W., and Howorka, F., 1965, Avalanche activity and free water content of snow at Obergurgl: International Association of Scientific Hydrology Publication, v. 69, p. 65-72.

Atkins, D., 2005, Personal Communication, Former Avalanche Forecater, Colorado Avalanche Information Center: Boulder, CO, USA.

Baggi, S., and Schweizer, J., 2008, Characteristics of wet snow avalanche activity: 20 years of observations from a high alpine valley (Dischma, Switzerland): Natural Hazards, v. 49 (in press).

Birkeland, K.W., Kronholm, K., Schneebeli, M., and Pielmeier, C., 2004, Changes in the shear strength and micro-penetration hardness of a buried surface-hoar layer: Annals of Glaciology, v. 38, p. 223-228.

Brown, A., 2008, On wet slabs and yellow snow-A practitioners observations, *in* Proceedings, International Snow Science Workshop: Whistler, B.C., Canada, p. 299-305.

Brun, E., and Rey, L., 1986, Field study on snow mechanical properties with special regard to liquid water content, *in* Avalanche Formation, Movement, and Effects (Proceedings of the Davos Symposium): Davos, Switzerland, International Association of Hydrologic Sciences Publication, no. 162, p. 183-193.

Colbeck, S.C., 1972, A theory of water percolation in snow: Journal of Glaciology, v. 11, p. 369-385.

Colbeck, S.C.,1973a, Effects of stratigraphic layers on water flow through snow: U.S.Army Corps of Engineers Cold Regions Research and Engineering Laboratory Research Report 311, 18 p.

Colbeck, S.C., 1973b, Theory of Metamorphism of Wet Snow: U.S.Army Corps of Engineers Cold Regions Research and Engineering Laboratory Special Report, 16 p.

Colbeck, S.C., 1974, Water flow through snow overlying an impermeable boundary: Water Resources Research, v. 10, p. 119-123.

Colbeck, S.C., 1976, Analysis of water flow in dry snow: Water Resources Research, v. 12, p. 523-527.

Colbeck, S.C., 1978, The physical aspects of water flow though snow, *in* Chow, V. T., ed., Advances in Hydroscience: New York, Academic Press, p. 155-206.

Colbeck, S.C., 1979, Water flow through heterogenous snow: Cold Regions Science and Technology, v. 1, p. 37-45.

Colbeck, S.C., 1982, An overview of seasonal snow metamorphism: Reviews of Geophysics, v. 20, p. 45-61.

Colbeck, S.C., Akitaya, E., Armstrong, R., Gubler, H., Lafeuille, J., Lied, K., McClung, D., and Morris, E., 1990, The international classification for seasonal snow on the ground: Hanover, International Association of Scientific Hydrology, 23 p..

Coleou, C., Xu, K., Lesaffre, B., and Brzoska, J.B., 1999, Capillary rise in snow: Hydrological Processes, v. 13, p. 1721-1732.

Conway, H., 2004, Storm Lewis: A rain-on-snow event on the Milford Road, New Zealand, Transit New Zealand Milford Road Avalanche Program, *in* Proceedings, International Snow Science Workshop: Jackson Hole, WY, USA, p. 557-565.

Conway, H., and Benedict, R., 1994, Infiltration of water into snow: Water Resources Research, p. 641-649.

Conway, H., Breyfogle, S., and Wilbour, C., 1988, Observations relating to wet snow stability, *in* Proceedings, International Snow Science Workshop: Whistler, BC, Canada, p. 211-222.

Conway, H., and Raymond, C. F., 1993, Snow stability during rain: Journal of Glaciology, v. 39, p. 635-642.

Denoth, A., 1980, The pendular-funicular transition in snow: Journal of Glaciology, v. 25, p. 93-97.

Denoth, A., 2003, Structural phase changes of the liquid water component in alpine snow: Cold Regions Science and Technology, v. 37, p. 227-232.

Devore, J., and Peck, R., 2005, Statistics - The Exploration and Analysis of Data: Belmont, Brooks/Cole, 766 p.

Gerdel, R.W., 1954, The transmission of water through snow: Transactions of the American Geophysical Union, v. 35, p. 475-485.

Greene, E., Birkeland, K.W., Elder, K., Johnson, G., Landry, C., McCammon, I., Moore, M., Sharaf, D., Sterbenz, C., Tremper, B., and Williams, K., 2004, Snow, Weather, and Avalanches: Observational Guidelines for Avalanche Programs in the United States.: Pagosa Springs, American Avalanche Association, 140 p.

Harrington, R., and Bales, R.C., 1998, Interannual, seasonal, and spatial patterns of meltwater and solute fluxes in a seasonal snowpack: Water Resources Research, v. 34, p. 823-831.

Hartman, H., and Borgeson, L.E., 2008, Wet slab instability at the Arapahoe Basin Ski Area, *in* Proceedings, International Snow Science Workshop: Whistler, BC, Canada, p. 163-169.

Heywood, L., 1988, Rain on snow avalanche events: Some observations, *in* Proceedings, International Snow Science Workshop: Whistler, BC, Canada, p. 125-136.

Hornberger, G.M, Raffensperger, J.P., Wiberg, P.L., and Eshleman K.N., 1998, Elements of Physical Hydrology: Baltimore, The Johns Hopkins University Press, 302 p.

Illangasekare, T.H., Walter, R.J., Meier, M.F., and Pfeffer, W.T., 1990, Modeling of meltwater infiltration in subfreezing snow: Water Resources Research, v. 26, p. 1001-1012.

Johnson, F., 2006, Personal Communication, Ski patrol director, Bridger Bowl Ski Area: Bozeman, MT, USA.

Johnson, J.B., and Schneebeli, M., 1999, Characterizing the microstructural and micromechanical properties of snow: Cold Regions Science and Technology, v. 30, p. 91-100.

Jordan, R., 1995, Effects of capillary discontinuities on water flow and water retention in layered snowcovers: Defence Science Journal, v. 45, p. 79-91.

Kattelmann, R., 1984, Wet slab instability, *in* Proceedings, International Snow Science Workshop: Aspen, CO, p. 102-108.

Kattelmann, R., 1987, Some measurements of water movement and storage in snow, *in* Avalanche Formation, Movement, and Effects (Proceedings of the Davos Symposium): Davos, Switzerland, International Association of Hydrologic Sciences Publication, no. 162, p. 245-253.

Kattelmann, R., and Dozier, J., 1999, Observations of snowpack ripening in the Sierra Nevada, California, USA: Journal of Glaciology, v. 45, p. 409-416.

Lutz, E., 2008, Personal Communication, PhD Candidate, Montana State University: Bozeman, MT, USA.

Lutz, E., Birkeland, K. W., Kronholm, K., Hansen, K., and Aspinall, R., 2007, Surface hoar characteristics derived from a snow micropenetrometer using moving window statistical operations: Cold Regions Science and Technology, v. 47, p. 118-133.

Marsh, P., and Woo, M.K., 1984, Wetting front advance and freezing of meltwater within a snowcover-1. Observations in the Canadian Arctic: Water Resources Research, v. 20, p. 1853-1864.

Marshall, H.P., 2008, Personal Communication via Eric Lutz, Assistant Professor, Center for Geophysical Investigation of the Shallow Subsurface, Boise State University: Boise, ID, USA.

McClung, D., and Schaerer, P., 1993, The Avalanche Handbook: Seattle, The Mountaineers, 272 p.

Morel-Seytoux, H.J., 1969, Introduction to flow of immiscible liquids in porous media, *in* DeWiest, R.J.M., ed., Flow Through Porous Media: New York, p. 456-515.

Naisbitt, A., 2007, Personal Communication, Utah Department of Transportation Avalanche Forecaster: Salt Lake City, UT, USA.

Nieber, J.L., 1996, Modeling finger development and persistence in initially dry porous media: Geoderma, v. 70, p. 207-229.

Pfeffer, W.T., Humphrey, N.F., 1996, Determination of timing and location of water movement and ice-layer formation by temperature measurements in sub-freezing snow: Journal of Glaciology, v. 42, p. 292-304.

R Development Core Team, 2008, R Foundation for Statistical Computing, Vienna, Austria, http://www.R-project.org

Reardon, B.A., and Lundy C., 2004, Forecasting for natural avalanches during spring opening of the Going-to-the-Sun Road, Glacier National Park, USA, *in* Proceedings, International Snow Science Workshop: Jackson, WY, USA, p. 565-581.

Schneebeli, M., 1995, Development and stability of preferential flow paths in a layered snowpack, *in* Biogeochemistry of seasonally snow covered catchments (Proceedings of a Boulder Symposium): Boulder, CO, p. 89-95.

Schneebeli, M., Pielmeier, C., and Johnson, J.B., 1999, Measuring snow microstructure and hardness using a high resolution penetrometer: Cold Regions Science and Technology, v. 30, p. 101-114.

Seligman, G., 1936, Snow Structure and Ski Fields: London, Macmillan, 555 p.

Sililo, T.N., and Tellam, J.H., 2000, Fingering in unsaturated zone flow: a qualitative review with laboratory experiments on heterogenous systems: Ground Water, v. 38, p. 864-871.

Singh, P., Spitzbart, G., Hubl, H., Weinmeister, H.W., 1997, Hydrological response of snowpack under rain-on-snow events: a field study: Journal of Hydrology, v. 202, p. 1-20.

Techel, F., Pielmeier, C., and Schneebeli, M., 2008, The first wetting of snow: Micro-structural hardness measurements using a snow micro penetrometer, *in* Proceedings, International Snow Science Workshop: Whistler, BC, Canada, p. 1019-1026.

Trautman, S.A., Lutz, E., Birkeland, K.W., and Custer, S.G., 2006, Relating wet loose snow avalanching to surficial shear strength, *in* Proceedings, International Snow Science Workshop: Telluride, CO, p. 71-78.

Trautman, S.A., 2007, Wet loose snow avalanching in southwestern Montana, [MSc. Thesis]: Bozeman, Montana State University, 115 p.

Waldner, P.A., Schneebeli, M., Schultze-Zimmerman, U., and Fluhler, H., 2004, Effect of snow structure on water flow and solute transport: Hydrological Processes, v. 18,p. 1271-1290.

Wakahama, G., 1968, The metamorphism of wet snow: International Association of Hydrological Sciences Publication, v. 79, 370-378.

Wankiewicz, A., 1979, A review of water movement in snow, *in* Colbeck, S. C., and Ray, M., eds., Modeling Snow Cover Runoff: Hanover, NH, US Army Cold Regions Research Engineering Laboratory, p. 222-252.

(WWAN), Westwide Avalanche Network, 2006, Accident Report, http://www.avalanche.org/proc-show.php3?OID=7002917

Williams, M.W., Sommerfeld, R., Massman, S., and Rikkers, M., 1999, Correlation lengths of meltwater flow through ripe snowpacks, Colorado Front Range, USA: Hydrological Processes, v. 13, p. 1807-1826.

Woo, M.K., Heron, R., and Marsh, P., 1982, Basal ice in high Arctic snowpacks: Arctic and Alpine Research, v. 14, p. 251-260.

APPENDICES

APPENDIX A

FIELD DATA TABLES

Table 16: Characteristics of Layer Transitions Involving New Snow (1) and Fragmented Precipitation Particles (2)

(ρ=kg/m^3, R=scale (Fist=1, Fist+=1.33, 1F-=1.67, 1F=2.00, etc.), E=mm, T=°C, NA=Not Available)

Interface	CrType abv	CrType below	ρ above	ρ below	R above	R *below*	E *above*	E *below*	T
Impeding 1	1a	1d	72	72	1.00	1.00	2.00	2.00	-7.2
Impeding 2	1a	1d	72	72	1.00	1.00	2.00	3.00	-7.2
Impeding 3	1d	1a	64	64	1.00	1.33	2.50	2.50	-6.8
Impeding 4	1a	1d	80	80	1.00	1.33	1.00	1.00	-12.6
Impeding 5	1a	1c	68	68	1.00	1.00	0.75	0.75	-10.1
Impeding 6	1c	2a	68	100	1.00	2.00	0.75	1.25	-9.8
Impeding 7	1d	2a	138	138	1.00	1.00	1.00	2.50	-0.7
Impeding 8	1d	1d	186	NA	1.00	1.33	0.88	0.88	0.4
Impeding 9	1c	1f	116	112	1.00	1.00	0.38	1.13	0.0
Impeding 10	1d	9e	120	NA	1.33	4.00	1.00	2.00	-4.7
Impeding 11	1d	9e	53	239	1.00	4.33	1.50	2.00	-2.8
Impeding 12	1a	4b	64	144	1.00	2.00	2.00	0.38	-11.3
Impeding 13	9d	2b	144	144	1.33	1.67	0.15	0.15	-1
Impeding 14	2b	2b	72	72	1.00	1.00	0.75	0.75	-4.9
Impeding 15	2a	2b	80	80	1.00	1.67	2.00	1.50	-11
Impeding 16	2b	4b	124	176	2.67	1.33	0.50	0.38	-8.4
Impeding 17	2b	3b	136	176	2.33	3.33	1.50	1.50	-7.9
Impeding 18	2a	2b	108	188	1.33	1.67	0.75	0.25	-3.1
Impeding 19	2b	2b	119	119	1.67	1.67	0.75	0.75	-0.8
Impeding 20	2a	2a	132	228	1.00	1.00	0.75	1.38	-0.3
Impeding 21	9e	2b	186	112	3.67	1.00	0.75	0.50	-0.8
Impeding 22	9d	2b	NA	152	3.00	2.00	0.20	0.38	-6.5
Impeding 23	2a	2a	138	358	1.00	4.00	NA	NA	-2.5
Impeding 24	2b	2b	112	164	1.00	2.00	0.50	0.25	0
Not Impeding13	1d	4b	64	124	1.33	2.00	2.50	0.50	-7.3
Not Impeding 14	1d	3c	116	192	1.33	2.00	1.00	0.75	-10.3
Not Impeding 15	2b	9d	NA	392	1.00	4.00	0.375	0.75	-5.4
Not Impeding 16	2b	4b	72	256	1.00	3.00	0.75	0.15	-4.8
Not Impeding 17	4b	2b	256	136	3.00	2.33	0.15	1.5	-5.9

Table 17: Characteristics of Layer Transitions Involving Rounded Grains (3)

(ρ=kg/m^3, R=scale (Fist=1, Fist+=1.33, 1F-=1.67, 1F=2.00, etc.), E=mm, T=°C, NA=Not Available)

Interface	**CrType abv**	**CrType below**	***ρ* above**	***ρ* below**	***R* above**	***R* *below***	***E* *above***	***E* *below***	***T***
Impeding 1	3b	9e	NA	NA	NA	NA	0.75	NA	NA
Impeding 2	2b	3b	136	176	2.33	3.33	1.50	1.50	-7.9
Impeding 3	3a	4b	119	204	1.67	2.00	0.15	0.28	-1.8
Impeding 4	3a	3a	336	336	3.33	2.00	0.38	0.38	-4.3
Impeding 5	3c	3b	244	332	2.00	2.67	0.75	1.25	-6.5
Impeding 6	9e	3b	378	640	4.33	3.00	1.00	0.75	-1.0
Impeding 7	9e	3b	172	378	3.67	2.00	1.00	0.75	-1.2
Impeding 8	3a	9e	280	NA	1.33	3.00	0.50	NA	-2.3
Impeding 9	3b	4c	164	240	2.00	3.00	0.50	1.00	-2.2
Impeding 10	6b	3a	460	452	2.67	3.00	0.25	0.50	0.0
Not Impeding 11	9e	3c	NA	NA	4.00	2.00	2.00	1.25	-5.5
Not Impeding 12	1d	3c	116	192	1.33	2.00	1.00	0.75	-10.3
Not Impeding 13	3c	9d	280	280	2.00	4.00	1.25	0.75	-5.6
Not Impeding 14	9d	3c	280	NA	4.00	1.67	0.75	NA	-5.6
Not Impeding 15	3c	3c	NA	NA	1.67	3.00	NA	0.75	NA
Not Impeding 16	3c	3b	NA	NA	3.00	4.00	0.75	0.75	NA
Not Impeding 17	3b	4c	332	264	2.67	2.33	1.25	1.50	-6.5
Not Impeding 18	9e	3b	378	160	4.33	3.00	1.00	0.75	-1.0
Not Impeding 19	3b	9e	160	NA	3.00	3.67	0.75	0.88	-0.4
Not Impeding 20	9e	3a	159	232	3.67	2.67	0.75	0.38	-1.9
Not Impeding 21	3a	4b	232	280	2.67	3.00	0.38	0.50	-2.3
Not Impeding 22	9e	3a	398	164	4.00	2.00	NA	NA	-2.5

Table 18: Characteristics of Layer Transitions Involving Faceted Crystals (4)

(ρ=kg/m^3, R=scale (Fist=1, Fist+=1.33, 1F-=1.67, 1F=2.00, etc.), E=mm, T=°C, NA=Not Available)

Interface	**CrType aby**	**CrType below**	***ρ* above**	***ρ* below**	***R* above**	***R below***	***E above***	***E below***	***T***
Impeding 1	9d	4a	392	240	4.00	1.00	0.75	1.00	-6.7
Impeding 2	1a	4b	64	144	1.00	2.00	2.00	0.38	-11.3
Impeding 3	4b	9e	144	NA	2.00	4.00	0.38	0.50	-2.4
Impeding 4	2b	4b	124	176	2.67	1.33	0.50	0.38	-8.4
Impeding 5	4b	4a	176	240	1.33	2.67	0.38	2.50	-7.3
Impeding 6	3a	4b	119	204	1.67	2.00	0.15	0.28	-1.8
Impeding 7	4c	4a	264	264	2.33	2.00	1.50	1.25	-4.2
Impeding 8	9d	4c	239	216	3.00	2.00	0.75	0.50	-3.5
Impeding 9	3b	4c	164	240	2.00	3.00	0.50	1.00	-2.2
Not Impeding 10	1d	4b	64	124	1.33	2.00	2.50	0.50	-7.3
Not Impeding 11	2b	4b	72	256	1.00	3.00	0.75	0.15	-4.8
Not Impeding 12	4b	2b	256	136	3.00	2.33	0.15	1.50	-5.9
Not Impeding 13	9e	4c	265	244	4.00	2.00	0.88	0.75	-3.0
Not Impeding 14	3b	4c	332	264	2.67	2.33	1.25	1.50	-6.5
Not Impeding 15	9e	4c	358	172	3.67	2.00	1.00	0.40	-1.2
Not Impeding 16	4c	9e	172	378	2.00	4.33	0.40	1.00	-1.1
Not Impeding 17	9e	4b	358	159	4.00	3.00	NA	NA	-2.5
Not Impeding 18	4b	9e	159	398	3.00	4.00	NA	NA	-2.5
Not Impeding 19	3a	4b	232	280	2.67	3.00	0.38	0.50	-2.3

Table 19: Characteristics of Layer Transitions Involving Wet Grains (6)

(ρ=kg/m^3, R=scale (Fist=1, Fist+=1.33, 1F-=1.67, 1F=2.00, etc.), E=mm, T=°C, NA=Not Available)

Interface	**CrType aby**	**CrType below**	***ρ* above**	***ρ* below**	***R* above**	***R below***	***E above***	***E below***	***T***
Impeding 1	6a	6a	265	250	3.33	2.33	0.38	0.50	0.0
Impeding 2	6b	9e	371	391	1.33	3.00	0.50	1.00	0.0
Impeding 3	6b	9e	420	420	1.67	3.33	1.75	2.00	0.0
Impeding 4	6b	9e	434	528	2.67	2.67	0.25	1.00	0.0
Impeding 5	6b	3a	460	452	2.67	3.00	0.25	0.50	0.0
Not Impeding 6	6a	9e	184	358	1.00	3.67	0.50	1.00	-1.2
Not Impeding 7	6a	9e	380	380	1.33	3.33	1.25	1.25	0.0
Not Impeding 8	6b	9e	456	NA	2.00	4.00	1.00	NA	0.0
Not Impeding 9	6b	6b	139	452	2.00	2.67	1.00	0.75	0.0
Not Impeding 10	9e	6b	380	420	3.33	1.67	1.25	1.75	0.0
Not Impeding 11	9e	6a	NA	484	4.00	2.00	NA	0.25	0.0
Not Impeding 12	6b	6b	452	440	3.00	2.67	0.75	1.25	0.0
Not Impeding 13	6a	9e	484	NA	2.00	4.00	0.25	NA	0.0
Not Impeding 14	6b	6b	440	428	2.67	3.00	1.25	0.50	0.0
Not Impeding 15	9e	6a	NA	434	4.00	3.00	NA	0.25	0.0
Not Impeding 16	6b	6b	428	460	3.00	2.67	0.50	0.25	0.0

Table 20: Characteristics of Layer Transitions Involving Crusts (9)

(ρ=kg/m^3, R=scale (Fist=1, Fist+=1.33, 1F-=1.67, 1F=2.00, etc.), E=mm, T=°C, NA=Not Available)

Interface	CrType abv	CrType below	ρ above	ρ below	R above	R below	E above	E below	T
Impeding 1	1d	9e	120	NA	1.33	4.00	1.00	2.00	-4.7
Impeding 2	9d	4a	392	240	4.00	1.00	0.75	1.00	-6.7
Impeding 3	9d	2b	144	144	1.33	1.67	0.15	0.15	-1.0
Impeding 4	3b	9e	NA	NA	NA	NA	0.75	NA	NA
Impeding 5	4b	9e	144	NA	2.00	4.00	0.38	0.50	-2.4
Impeding 6	1d	9e	53	239	1.00	4.33	1.50	2.00	-2.8
Impeding 7	9e	3b	378	640	4.33	3.00	1.00	0.75	-1.0
Impeding 8	9e	3b	172	378	3.67	2.00	1.00	0.75	-1.2
Impeding 9	9e	2b	186	112	3.67	1.00	0.75	0.50	-0.8
Impeding 10	3a	9e	280	NA	1.33	3.00	0.50	NA	-2.3
Impeding 11	9d	2b	NA	152	3.00	2.00	0.20	0.38	-6.5
Impeding 12	9d	4c	239	216	3.00	2.00	0.75	0.50	-3.5
Impeding 13	6b	9e	371	391	1.33	3.00	0.50	1.00	0.0
Impeding 14	6b	9e	420	420	1.67	3.33	1.75	2.00	0.0
Impeding 15	6b	9e	434	528	2.67	2.67	0.25	1.00	0.0
Not Impeding 16	9e	3c	NA	NA	4.00	2.00	2.00	1.25	-5.5
Not Impeding 17	2b	9d	NA	392	1.00	4.00	0.38	0.75	-5.4
Not Impeding 18	3c	9d	280	280	2.00	4.00	1.25	0.75	-5.6
Not Impeding 19	9d	3c	280	NA	4.00	1.67	0.75	NA	-5.6
Not Impeding 20	9e	4c	265	244	4.00	2.00	0.88	0.75	-3.0
Not Impeding 21	6a	9e	184	358	1.00	3.67	0.50	1.00	-1.2
Not Impeding 22	9e	3b	378	160	4.33	3.00	1.00	0.75	-1.0
Not Impeding 23	9e	4c	358	172	3.67	2.00	1.00	0.40	-1.2
Not Impeding 24	3b	9e	160	NA	3.00	3.67	0.75	0.88	-0.4
Not Impeding 25	4c	9e	172	378	2.00	4.33	0.40	1.00	-1.1
Not Impeding 26	9e	4b	358	159	4.00	3.00	NA	NA	-2.5
Not Impeding 27	9e	3a	159	232	3.67	2.67	0.75	0.38	-1.9
Not Impeding 28	4b	9e	159	398	3.00	4.00	NA	NA	-2.5
Not Impeding 29	9e	3a	398	164	4.00	2.00	NA	NA	-2.5
Not Impeding 30	6a	9e	380	380	1.33	3.33	1.25	1.25	0.0
Not Impeding 31	6b	9e	456	NA	2.00	4.00	1.00	NA	0.0
Not Impeding 32	9e	6b	380	420	3.33	1.67	1.25	1.75	0.0
Not Impeding 33	9e	6a	NA	484	4.00	2.00	NA	0.25	0.0
Not Impeding 34	6a	9e	484	NA	2.00	4.00	0.25	NA	0.0
Not Impeding 35	9e	6a	NA	434	4.00	3.00	NA	0.25	0.0

APPENDIX B

FIELD SNOW PROFILES

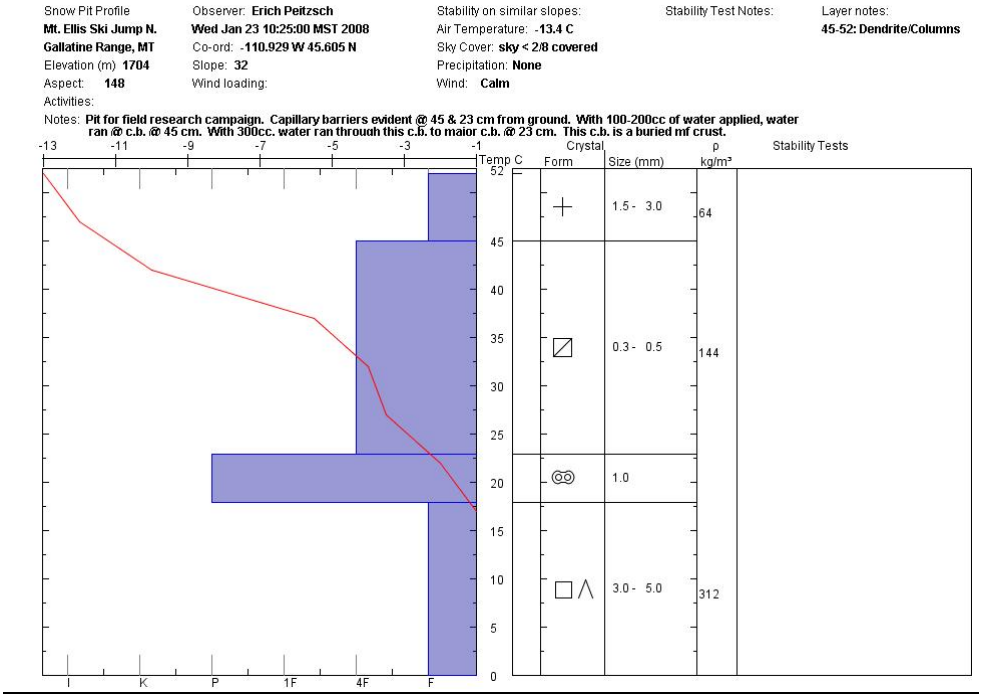

Figure 50: Pit profile #1.

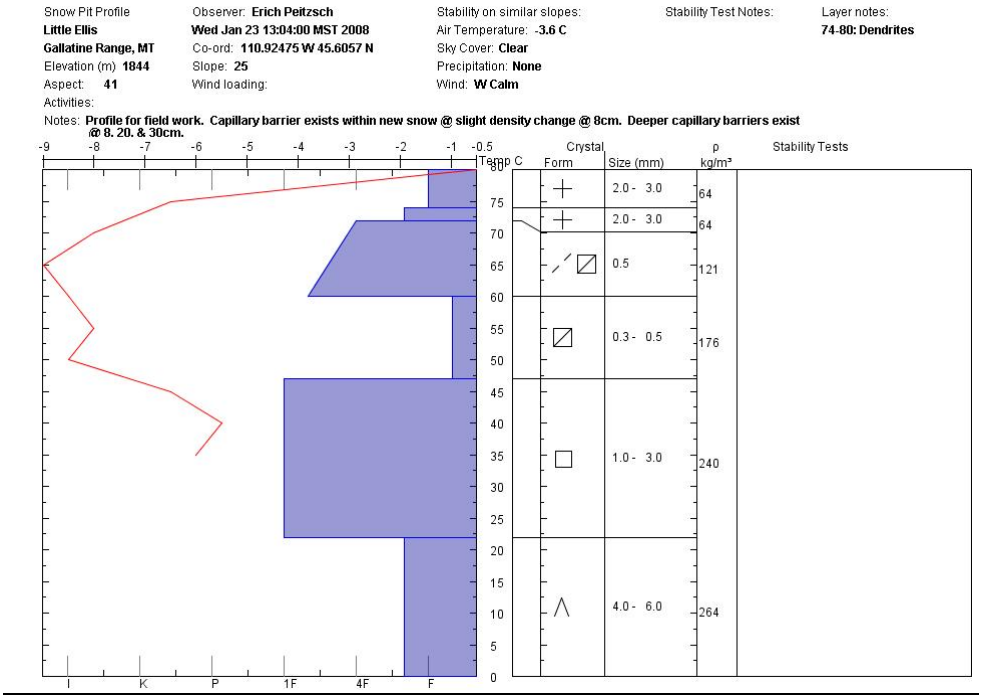

Figure 51: Pit Profile #2.

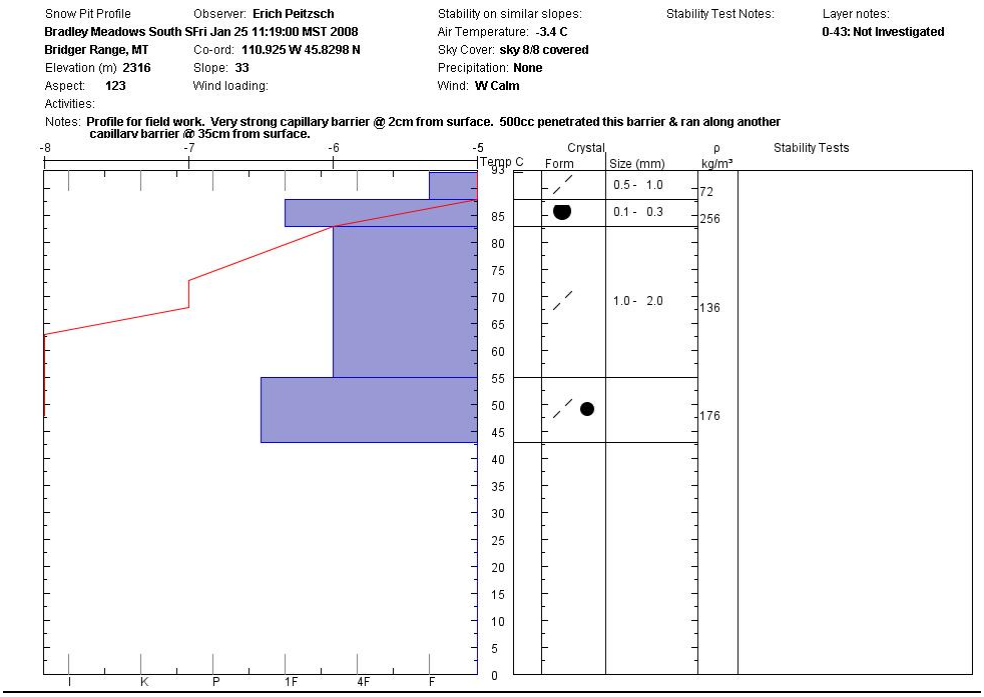

Figure 52: Pit Profile #3.

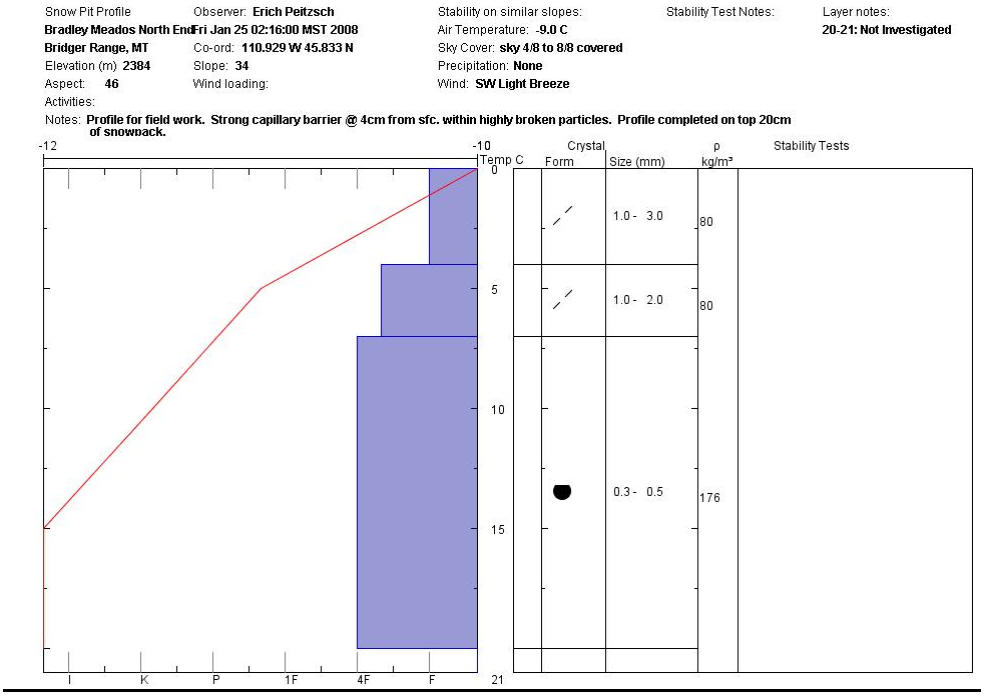

Figure 53: Pit profile #4.

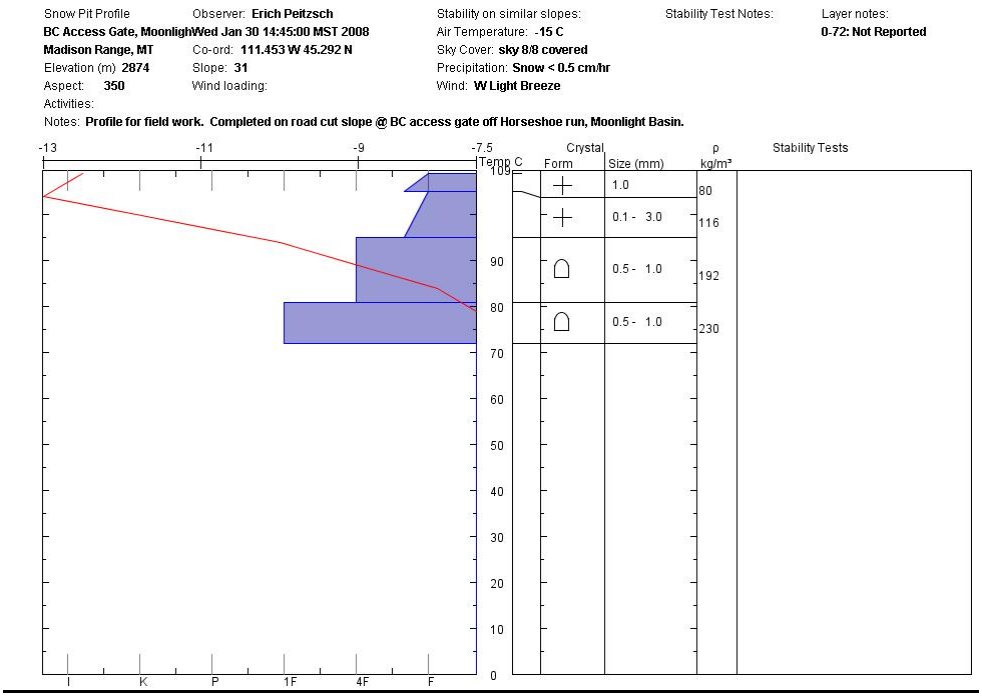

Figure 54: Pit profile #5

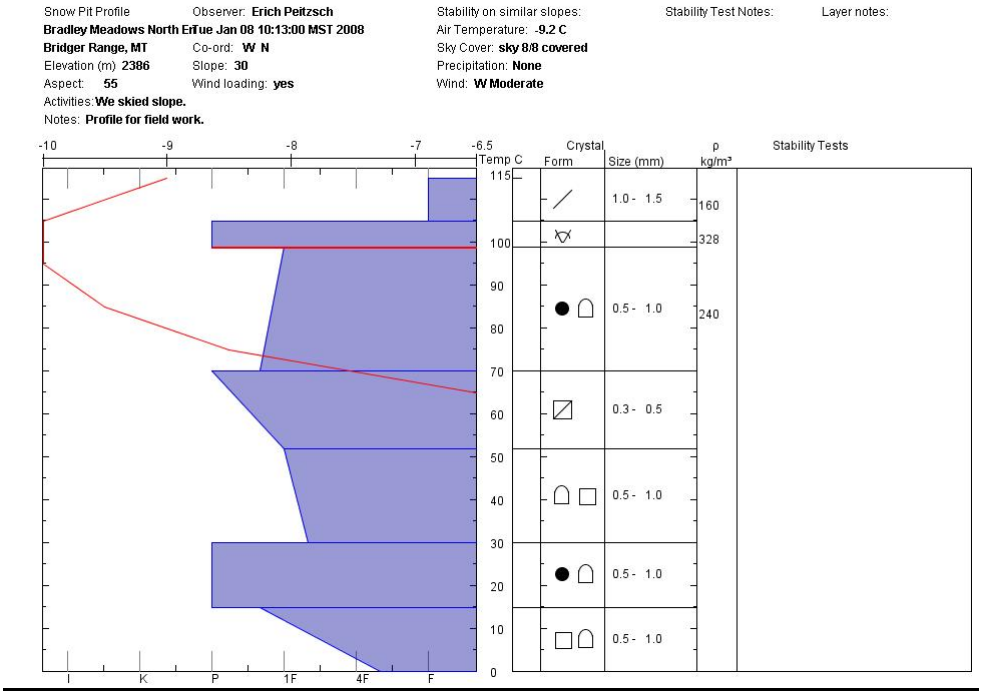

Figure 55: Pit profile #6.

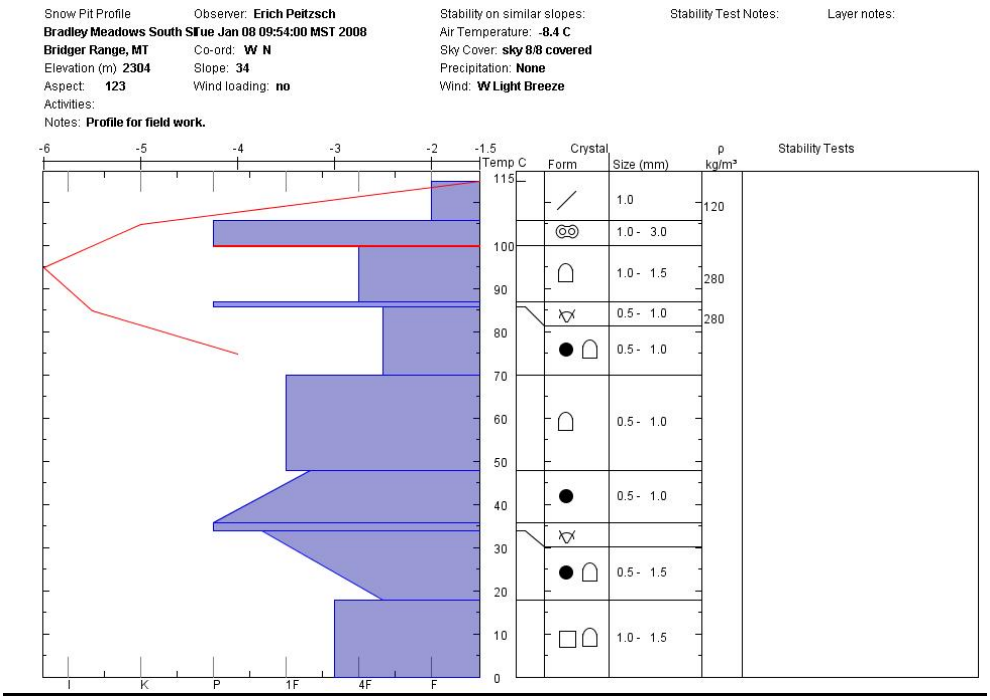

Figure 56: Pit profile #7.

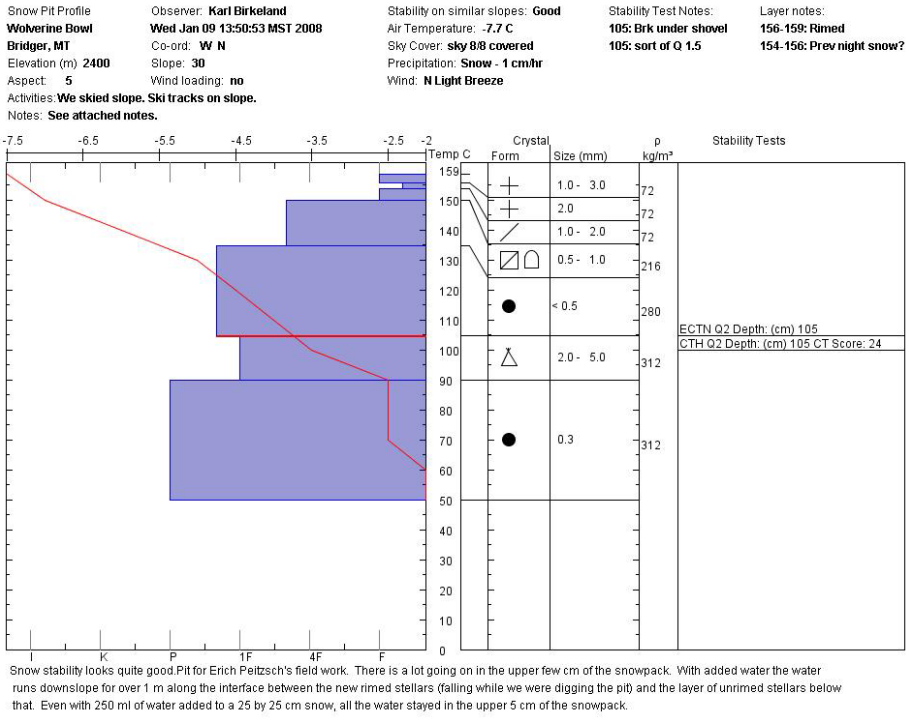

Figure 57: Pit profile #8.

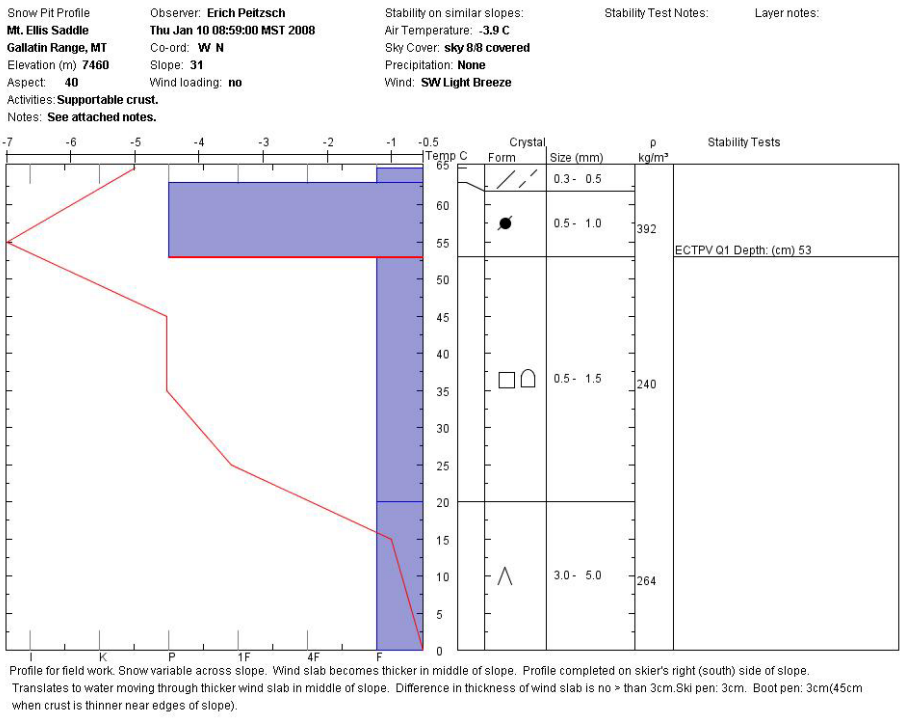

Figure 58: Pit profile #9.

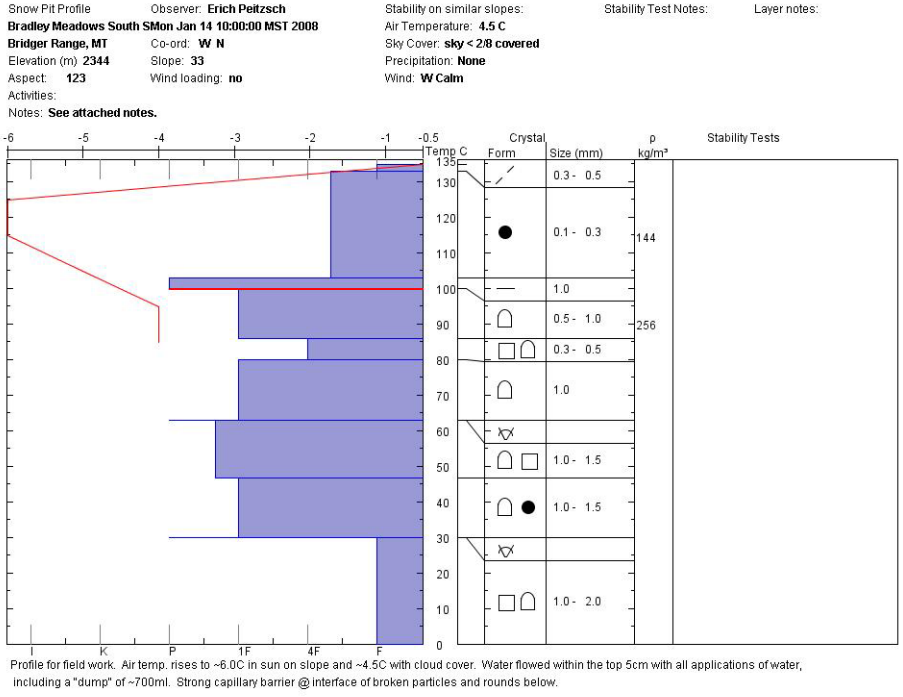

Figure 59: Pit profile #10.

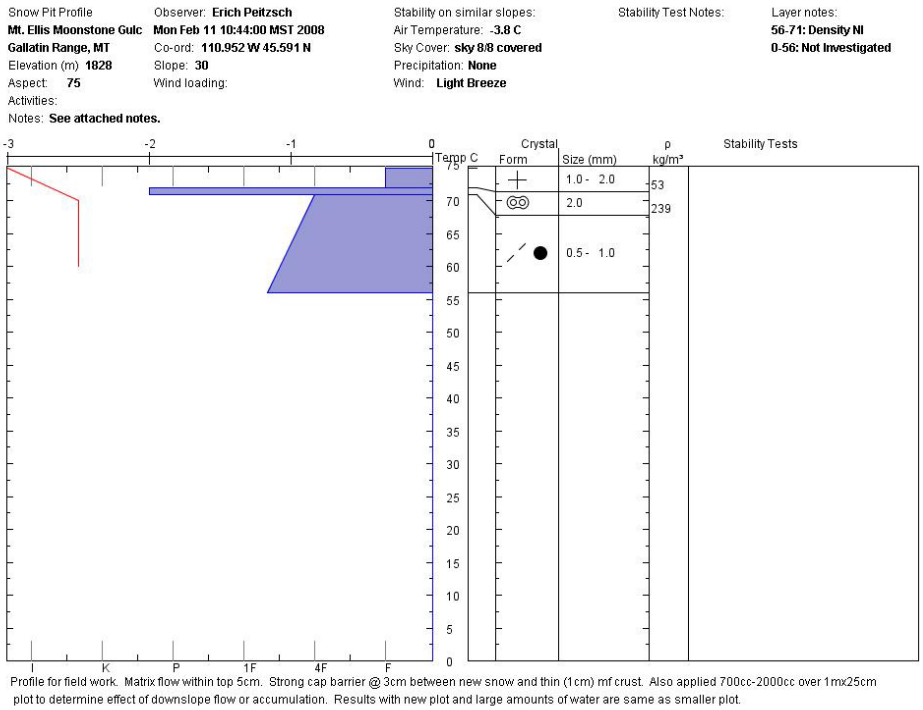

Figure 60: Pit profile #11.

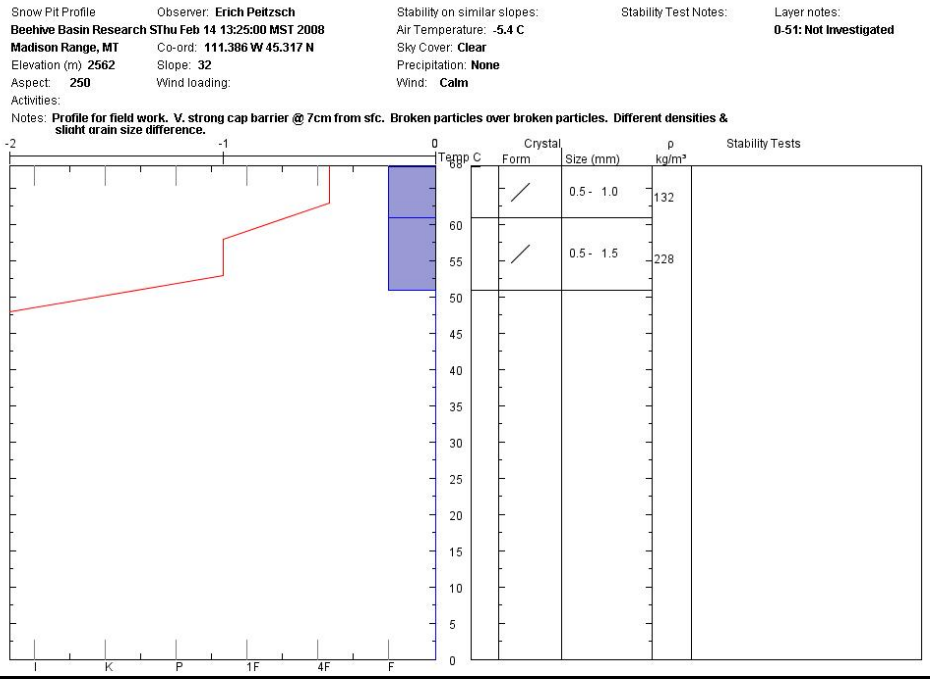

Figure 61: Pit profile #12.

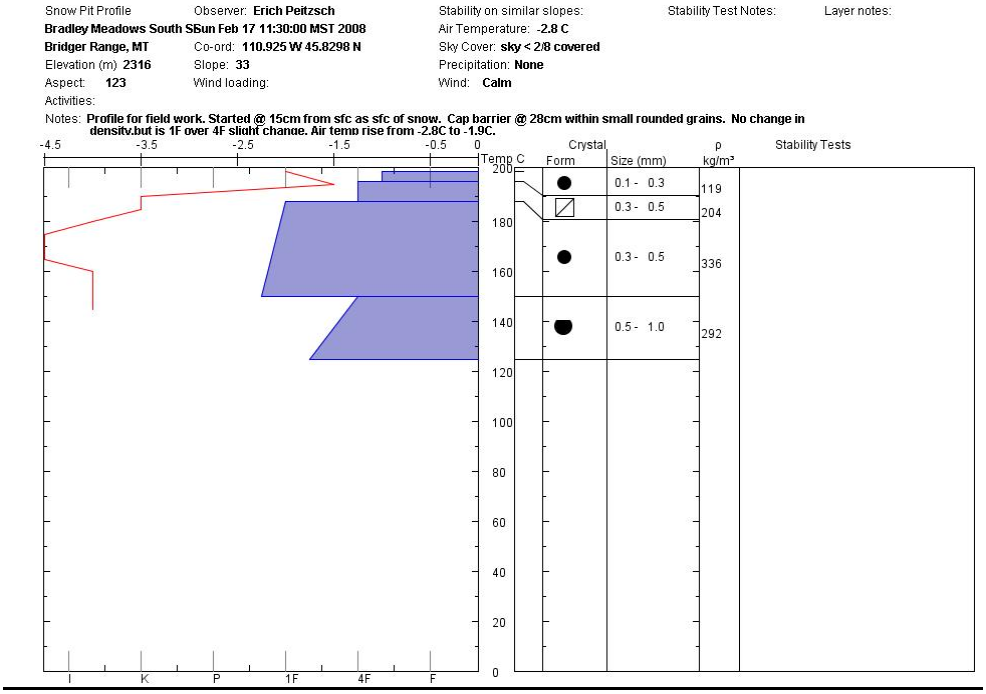

Figure 62: Pit profile #13.

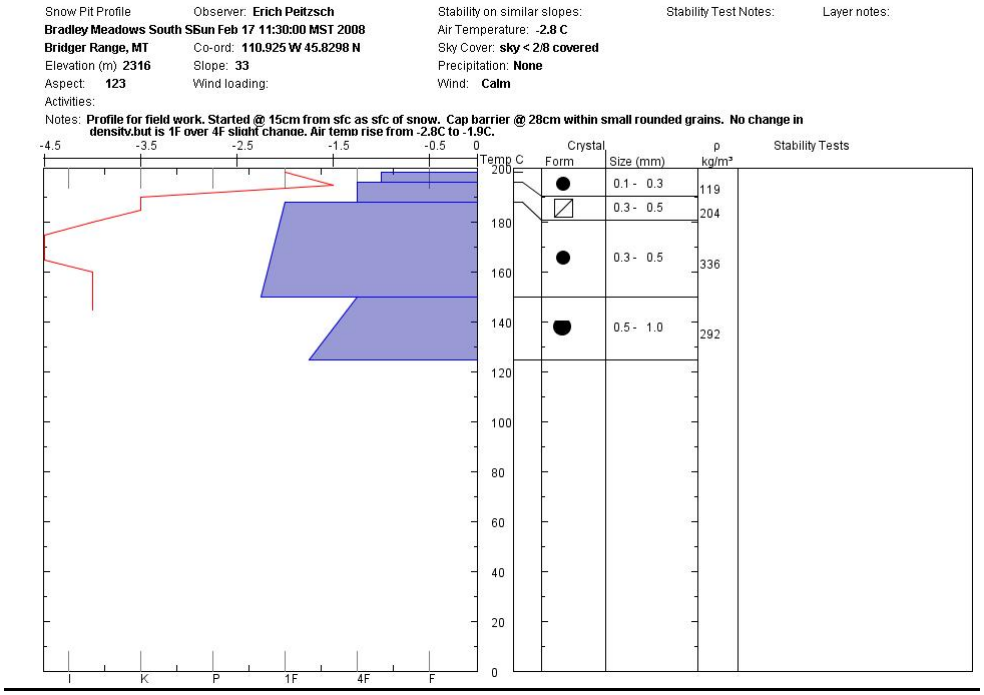

Figure 63: Pit profile #14.

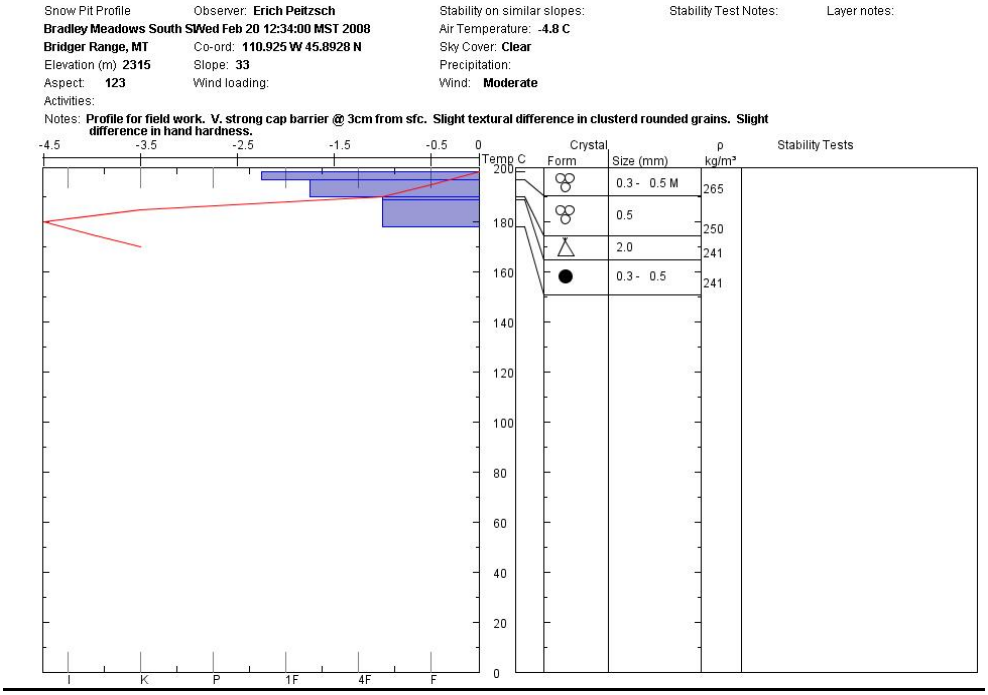

Figure 64: Pit profile #15.

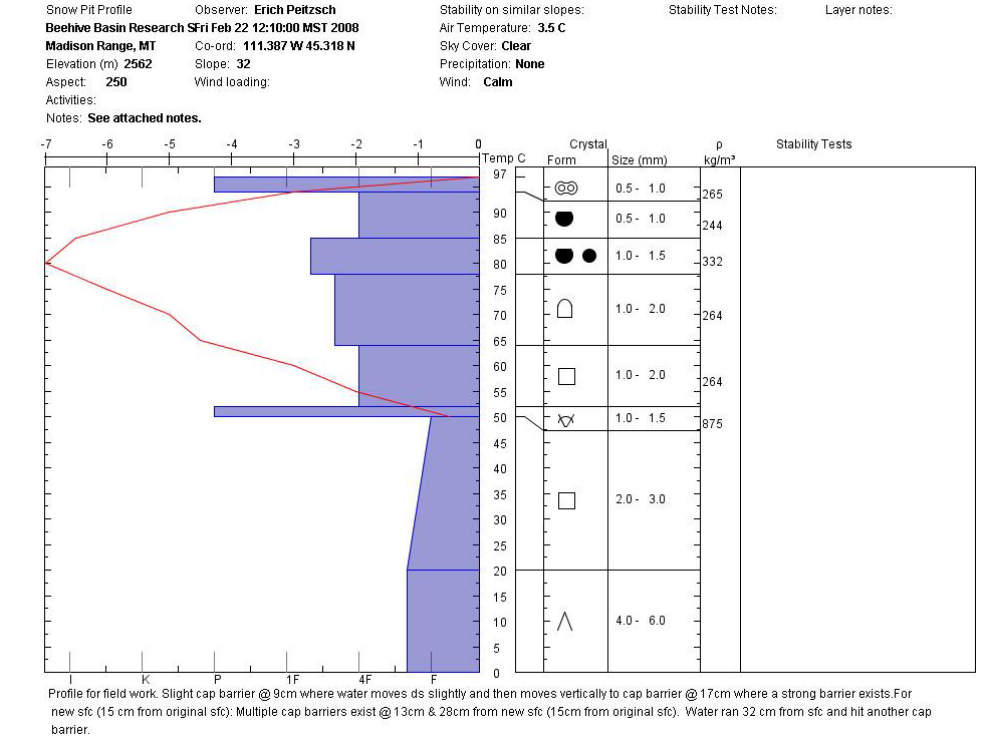

Figure 65: Pit profile #16.

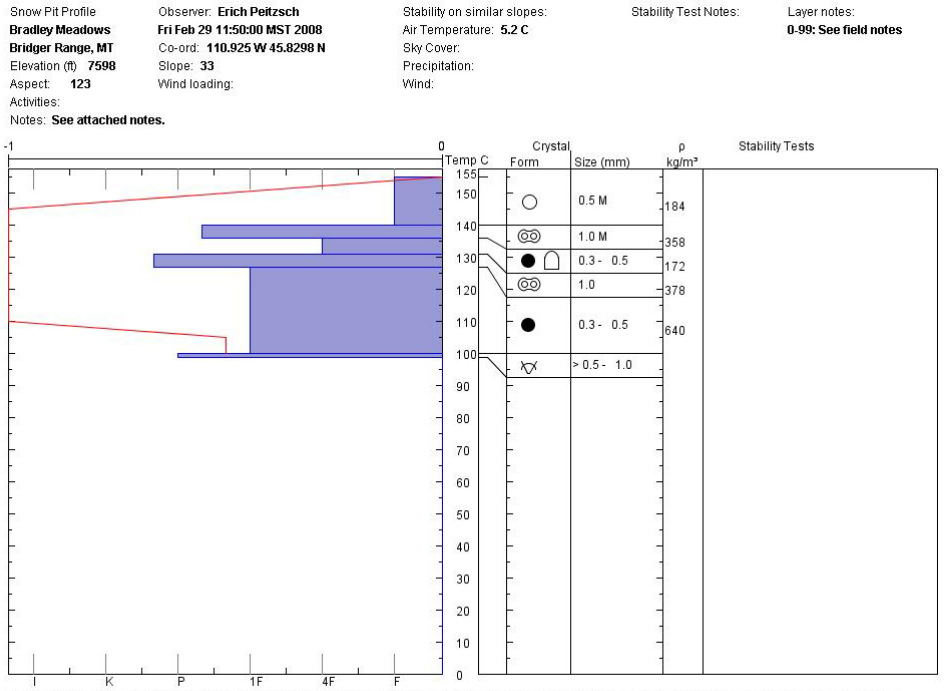

Figure 66: Pit profile #17.

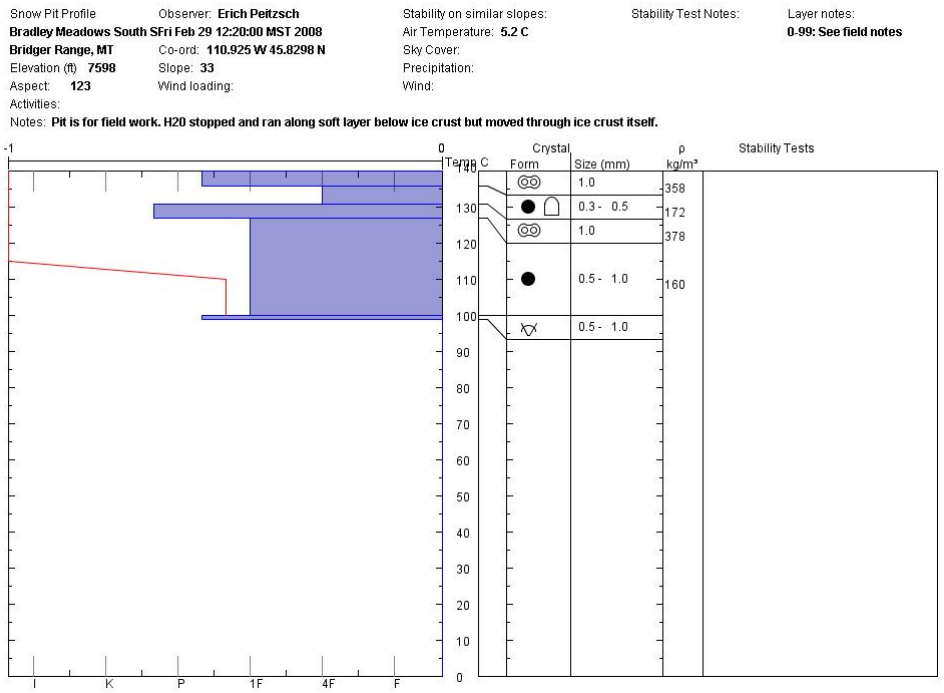

Figure 67: Pit profile #18.

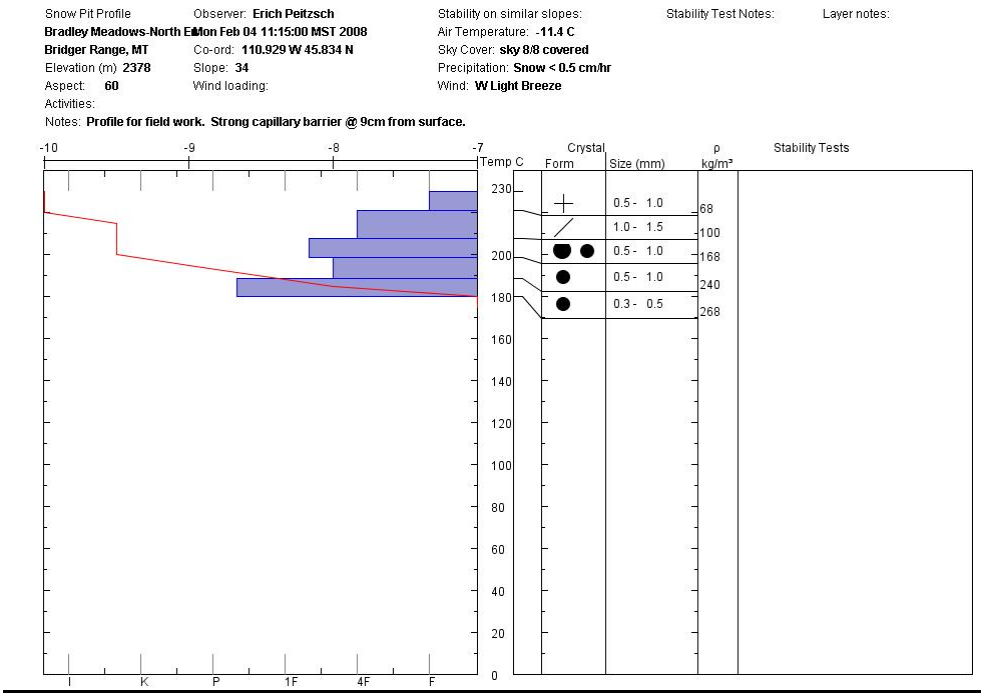

Figure 68: Pit profile #19.

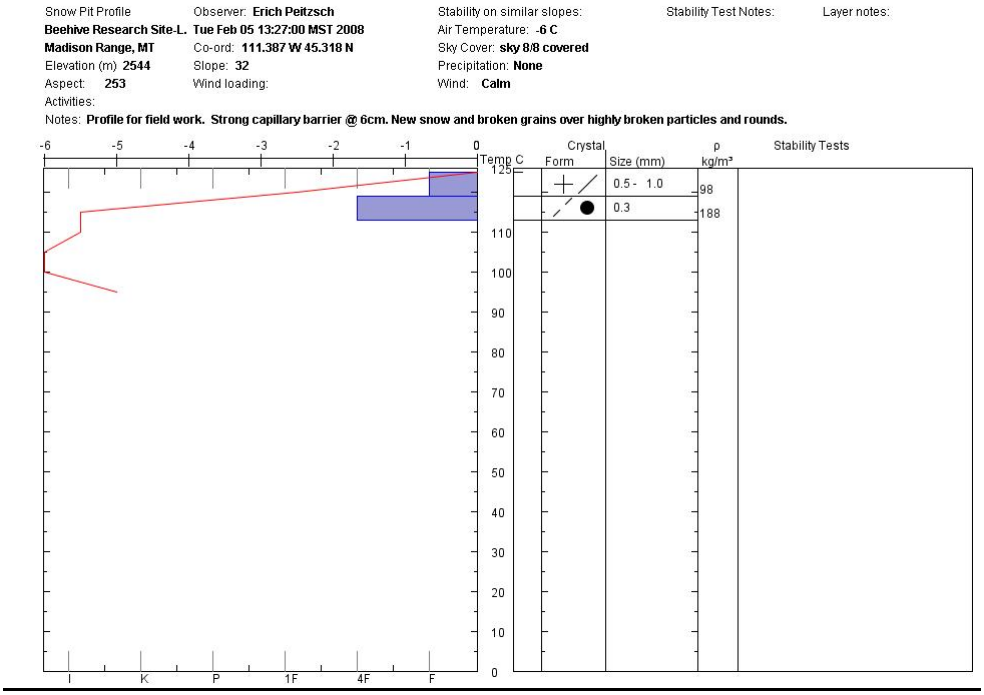

Figure 69: Pit profile #20.

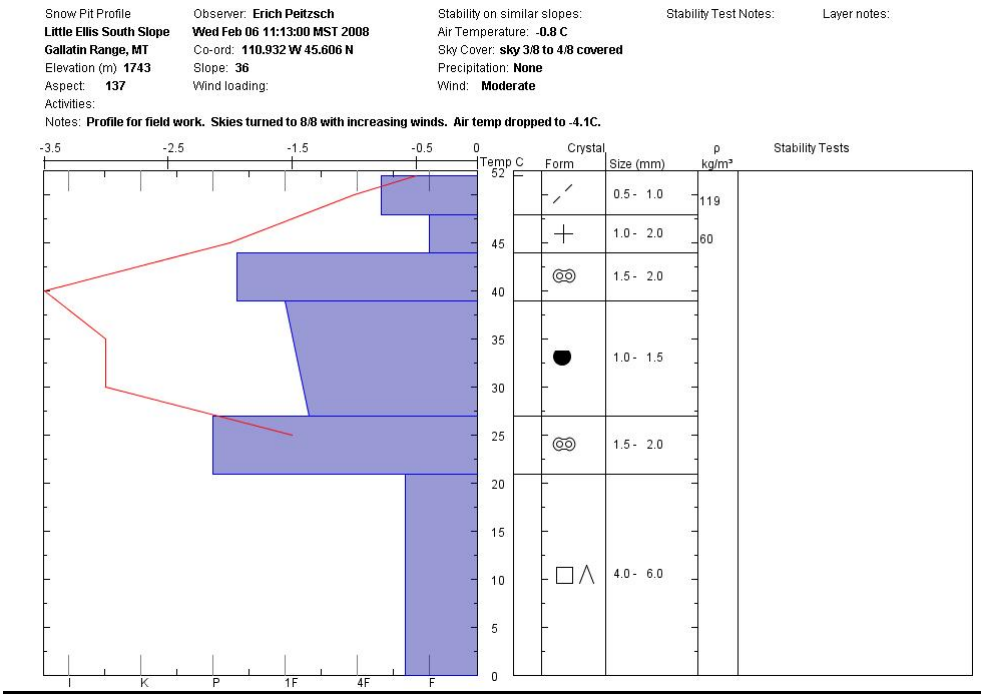

Figure 70: Pit profile #21.

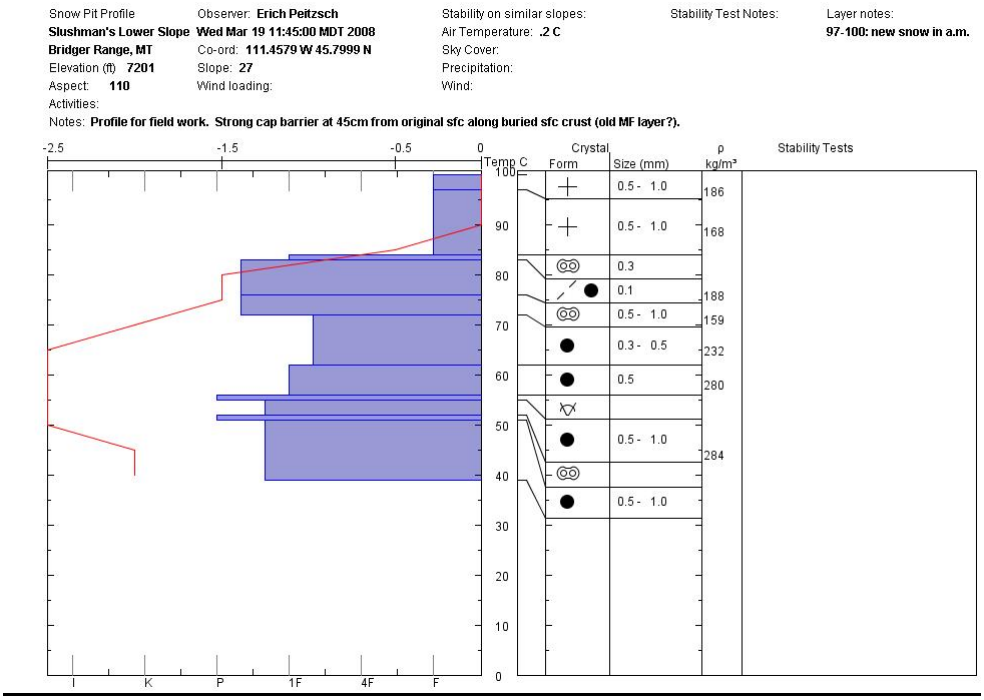

Figure 71: Pit profile #22.

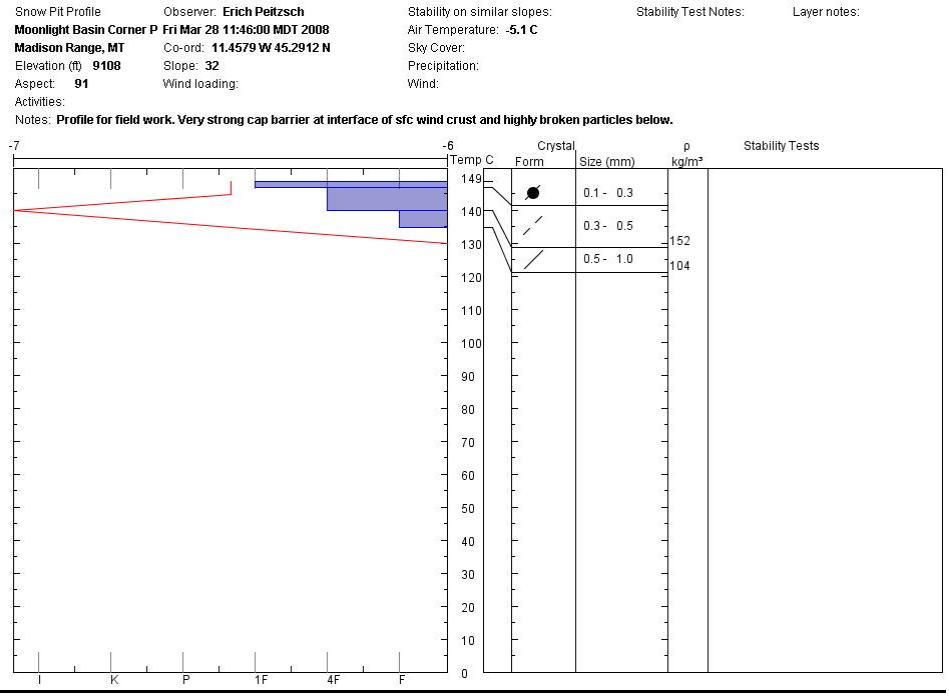

Figure 72: Pit profile #23.

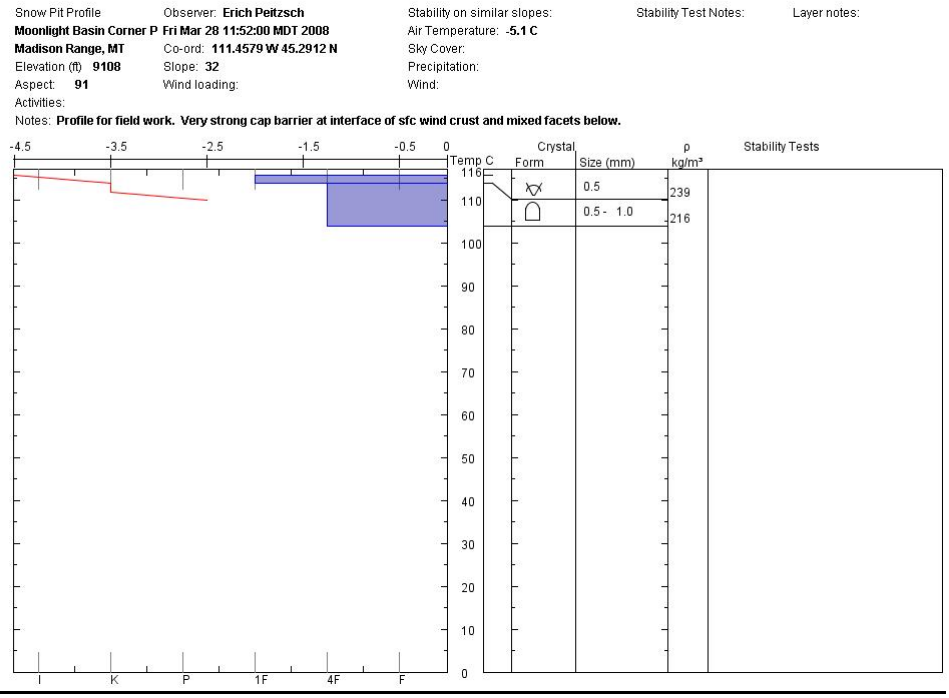

Figure 73: Pit profile #24.

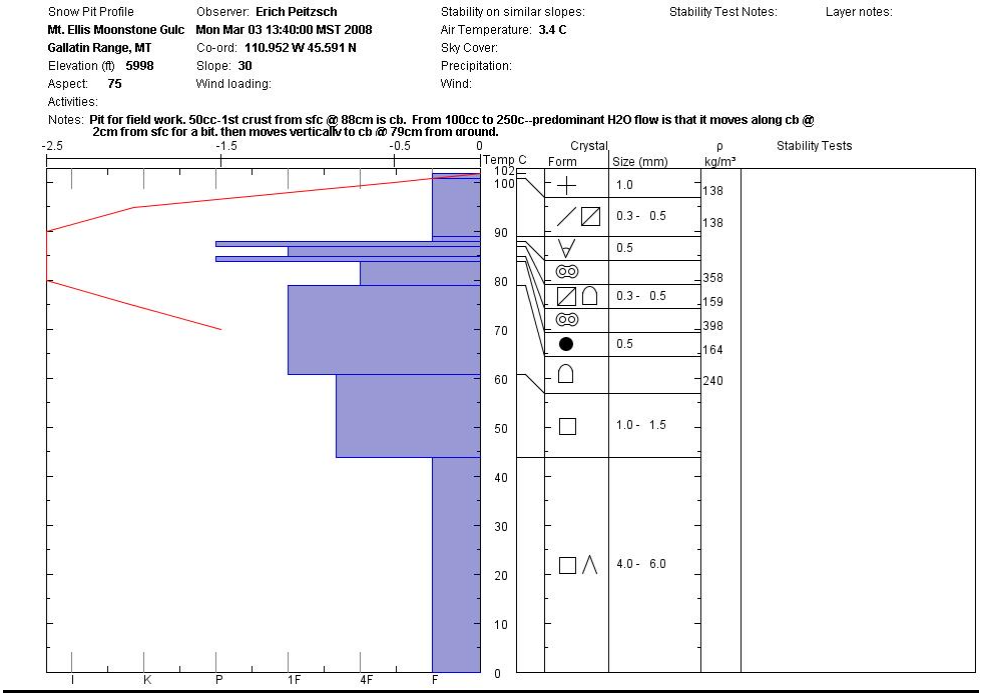

Figure 74: Pit profile #25.

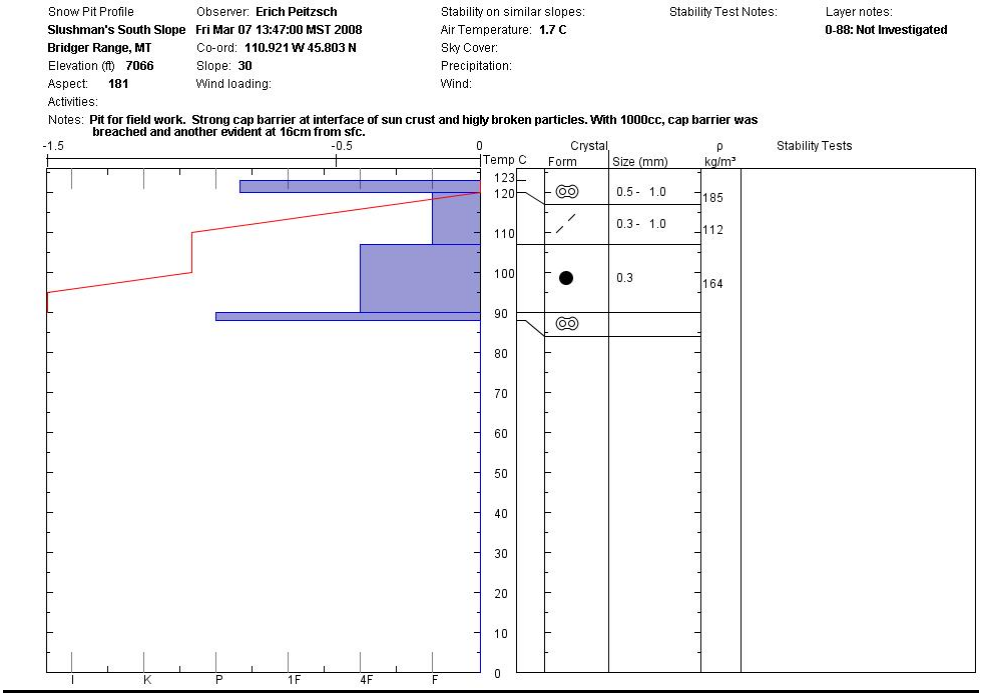

Figure 75: Pit profile #26.

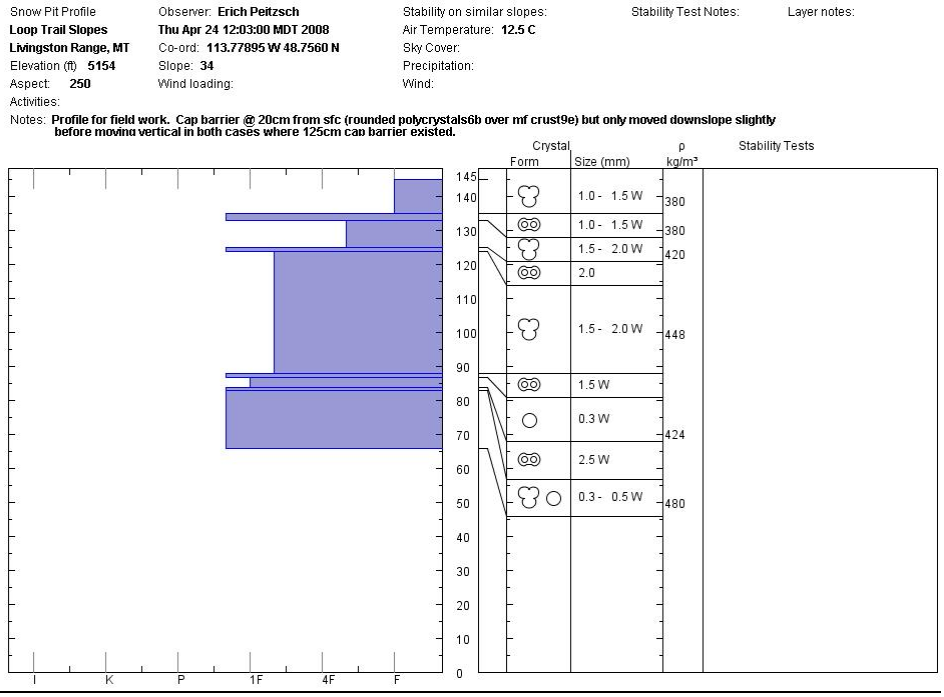

Figure 76: Pit profile #27.

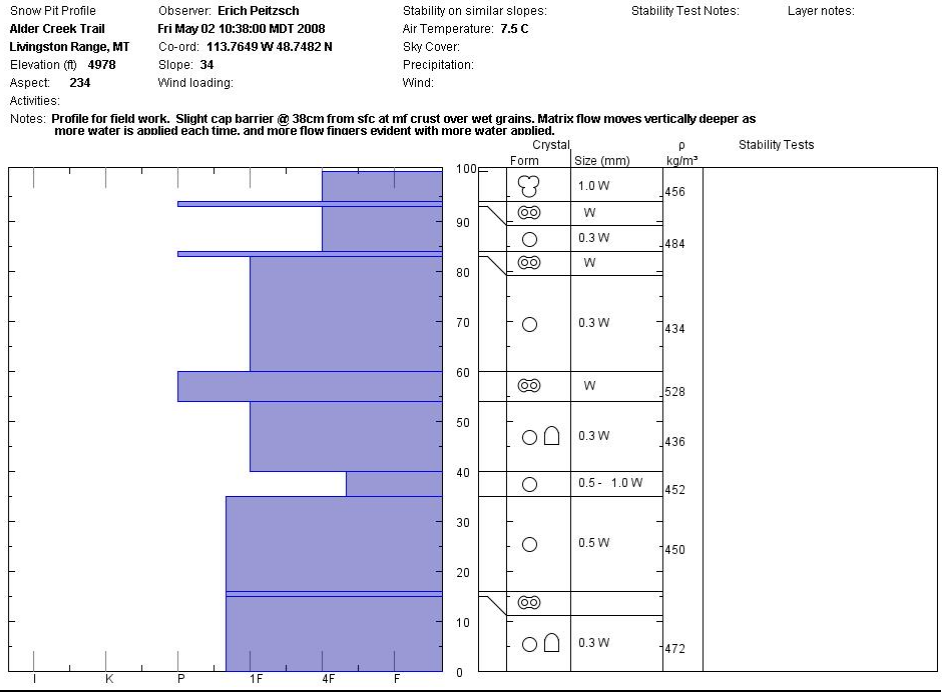

Figure 77: Pit profile #28.

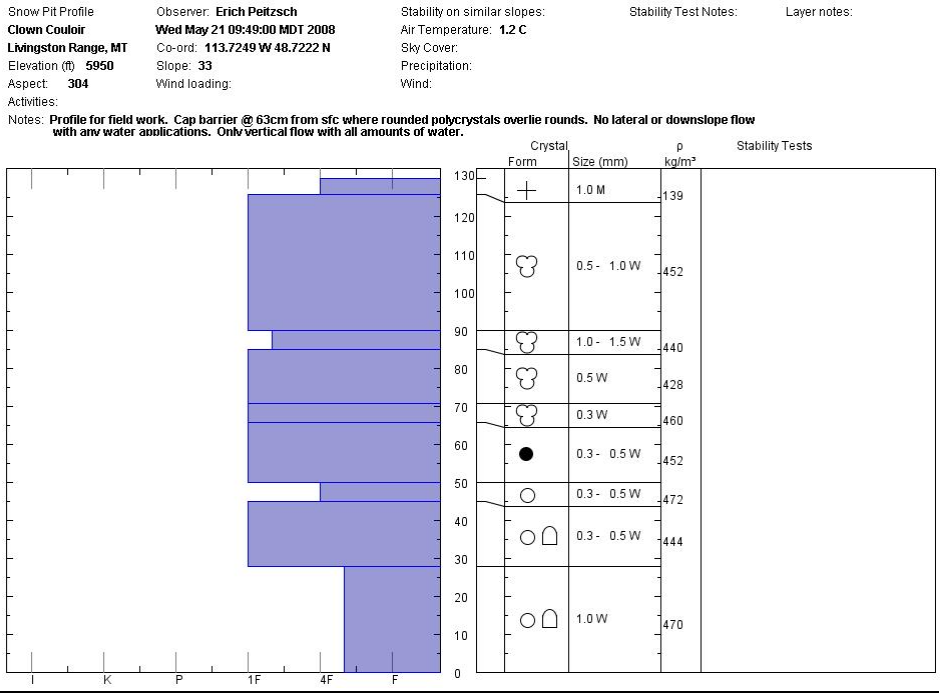

Figure 78: Pit profile #29.

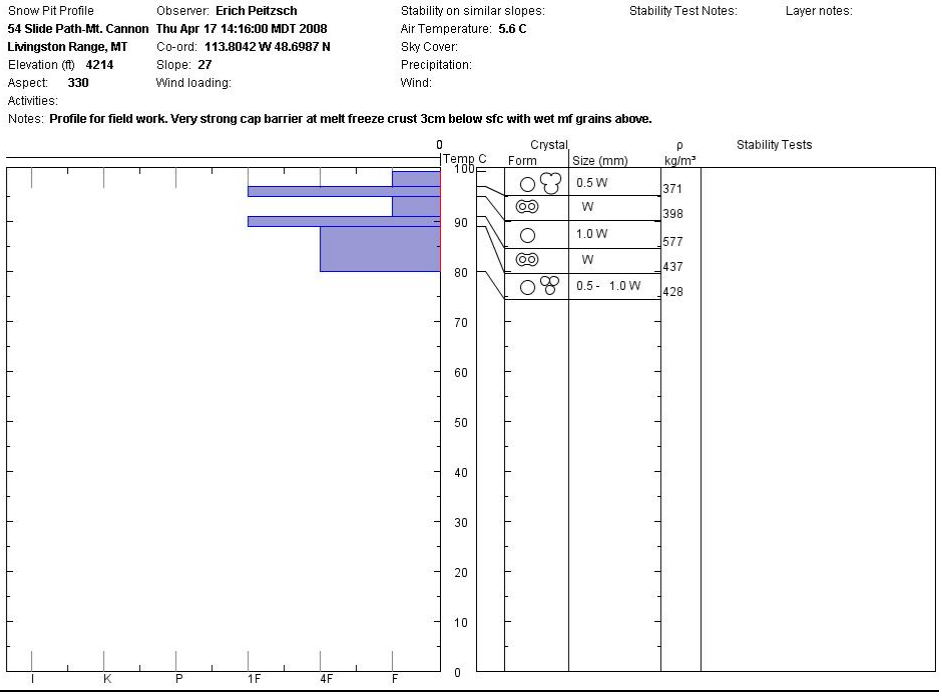

Figure 79: Pit profile #30.

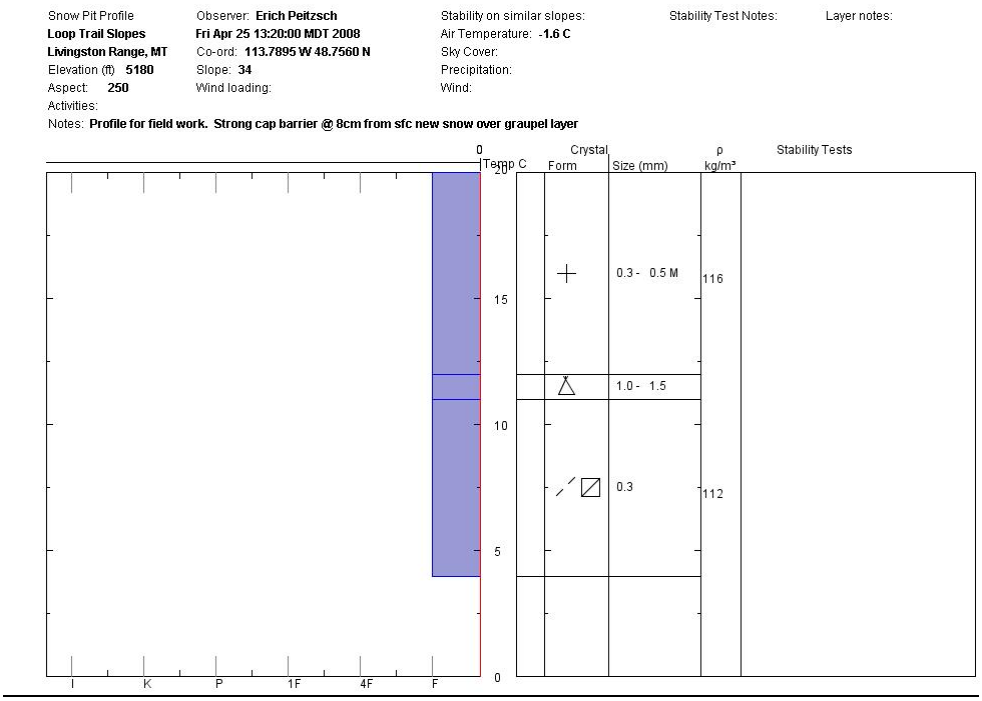

Figure 80: Pit profile # 31.

APPENDIX C

SMP PROFILES

The following SMP profiles are identified by the header above each figure with the date and file number for that day. For instance, 020508file2 signifies the second profile from 5 February 2008. The final 10 profiles, however, are labeled with file names only. These profiles are all from 28 March 2008. The graphs display mean rupture force (F) in Newtons (N), mean number of ruptures (N), and structural element length (L) in (mm). The x axis is the metric values and the y-axis is depth from the snow surface (mm). The numbered circles indicate the rank of the step change, and the numbered diamonds the rank of slope for the transitions for each profile (1=largest change). Blue indicates a decrease in value and red a positive change in the value. The gray solid lines indicate the location of peak hardness near the capillary barrier based on the manual profile, and the gray dashed lines provide a 5 mm scale on either side. The solid teal line represents the manual delineation of capillary barriers and the dashed teal lines a 5mm scale on both sides.

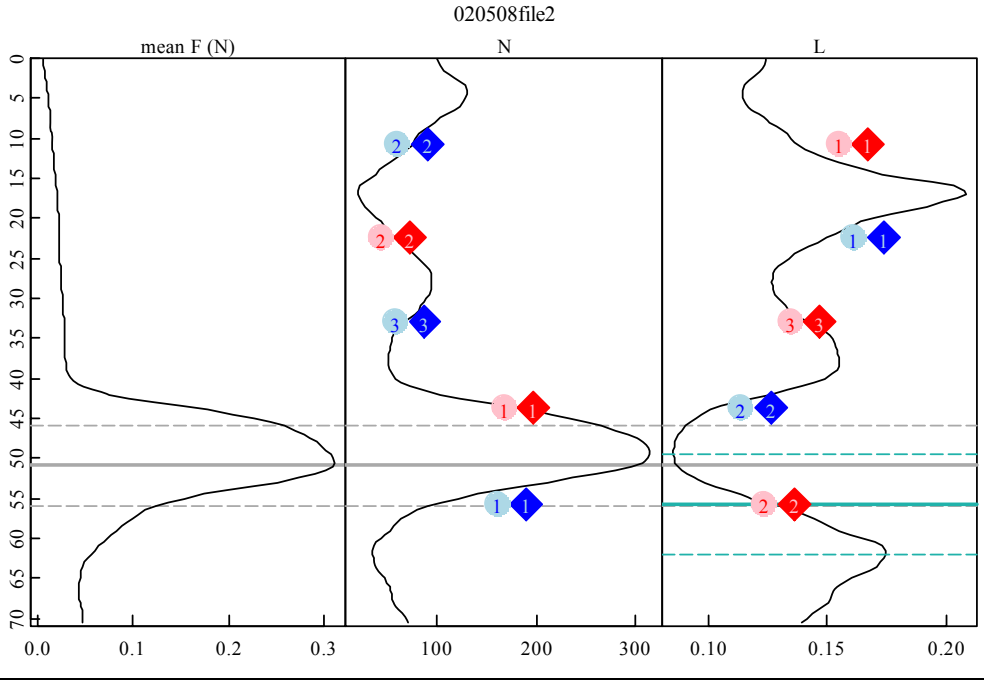

Figure 81: SMP Profile #1.

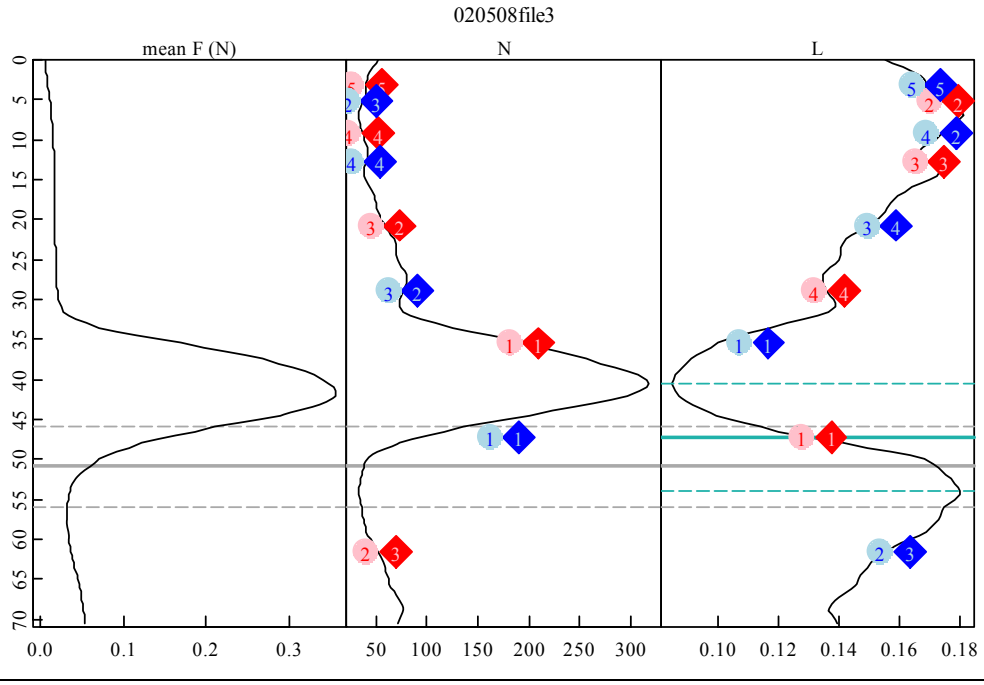

Figure 82: SMP Profile #2.

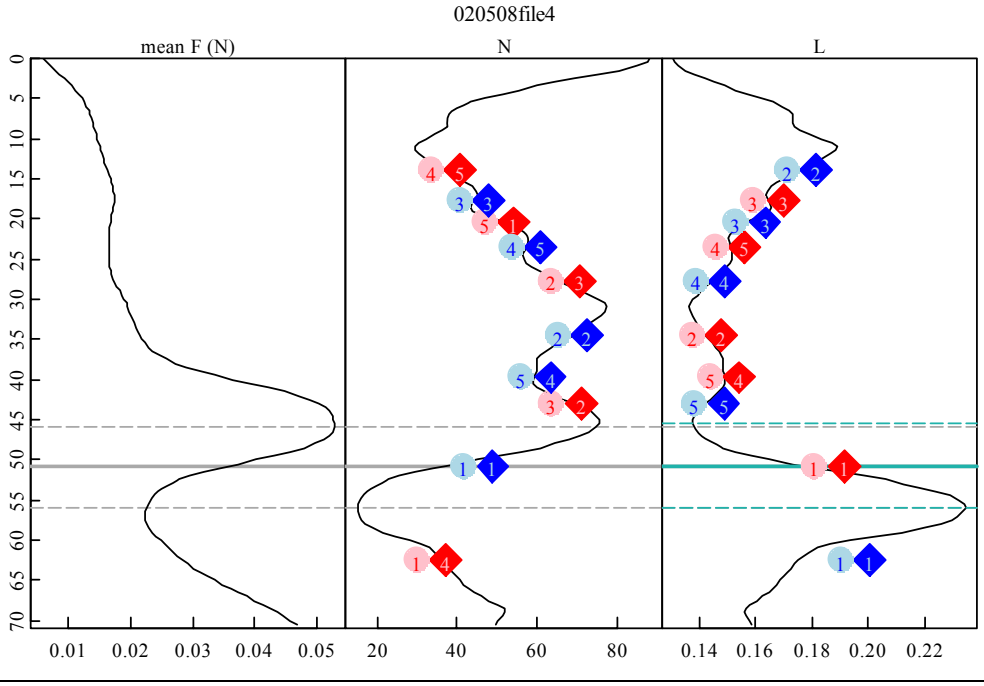

Figure 83: SMP Profile #3.

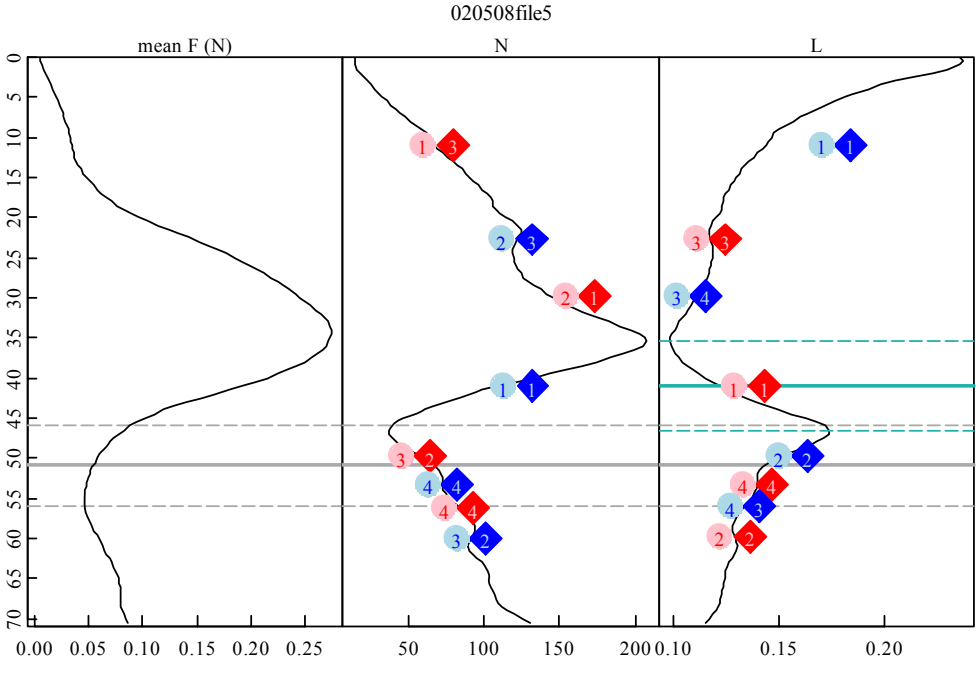

Figure 84: SMP Profile #4.

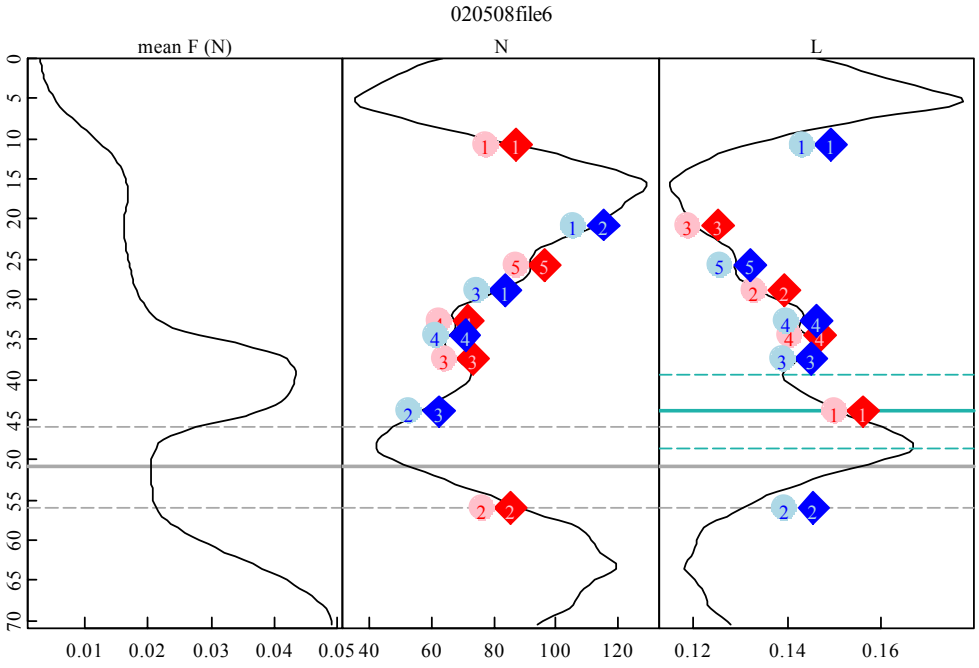

Figure 85: SMP Profile #5.

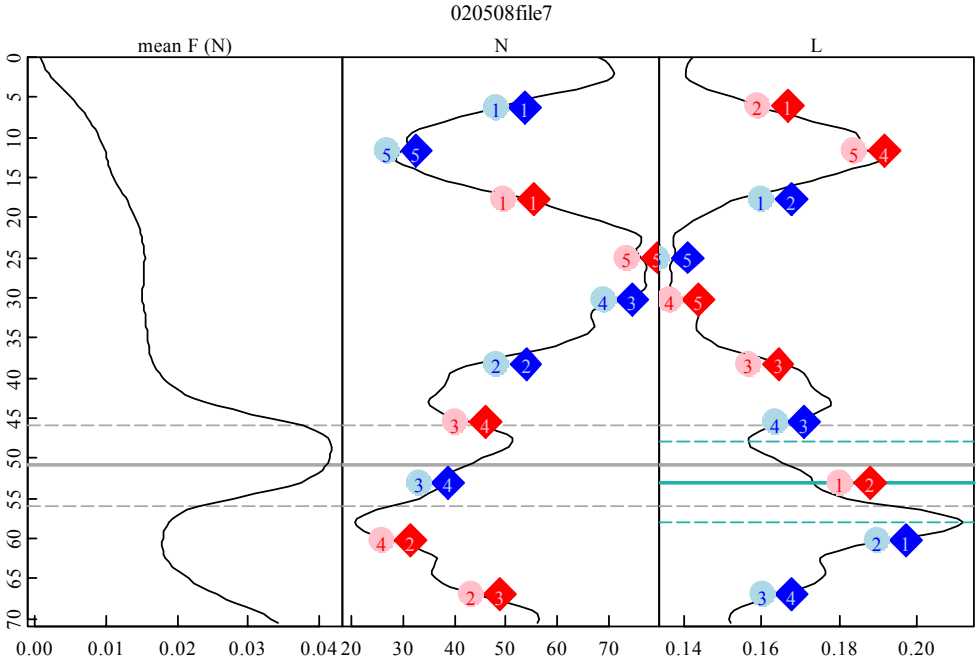

Figure 86: SMP Profile #6.

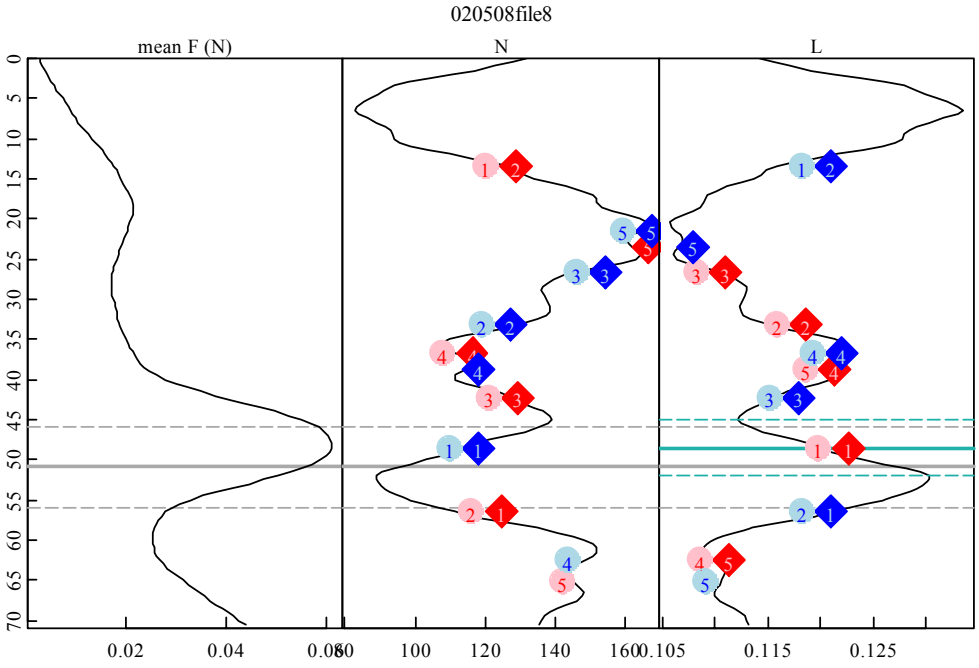

Figure 87: SMP Profile #7.

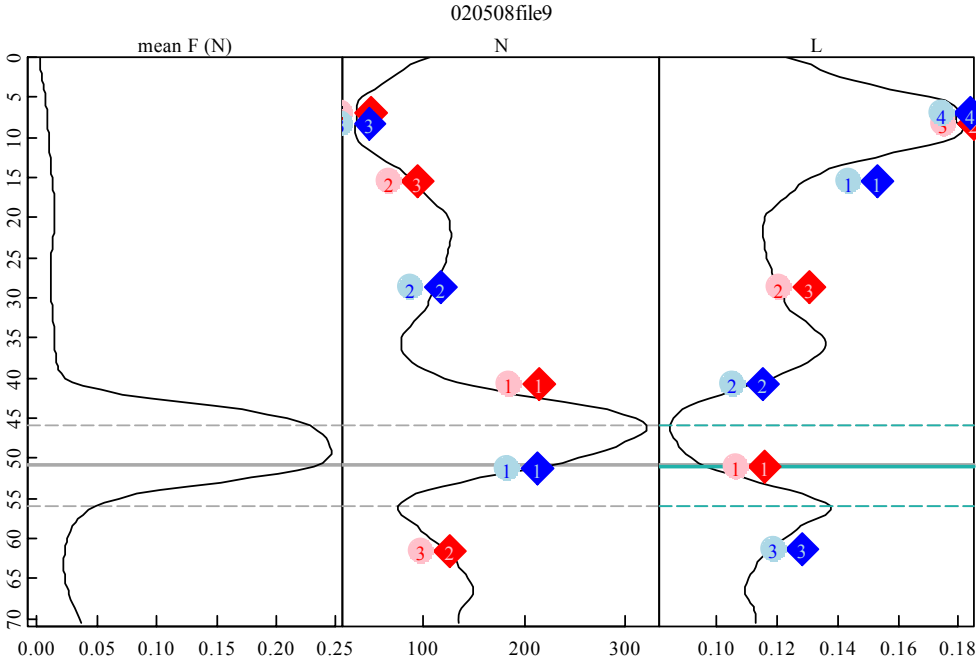

Figure 88: SMP Profile #8.

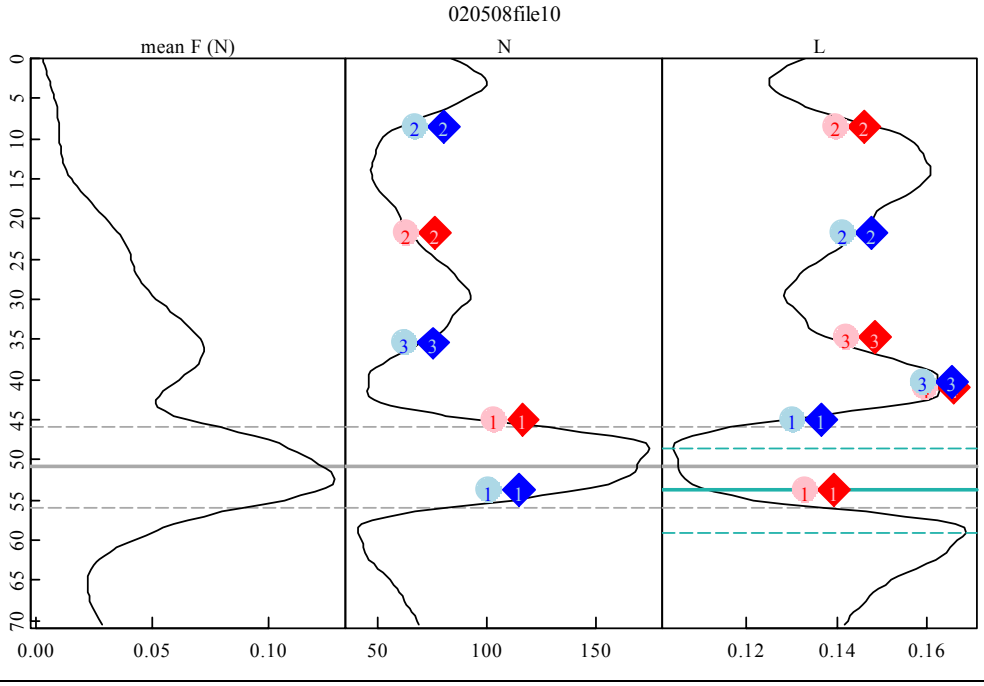

Figure 89: SMP Profile #9.

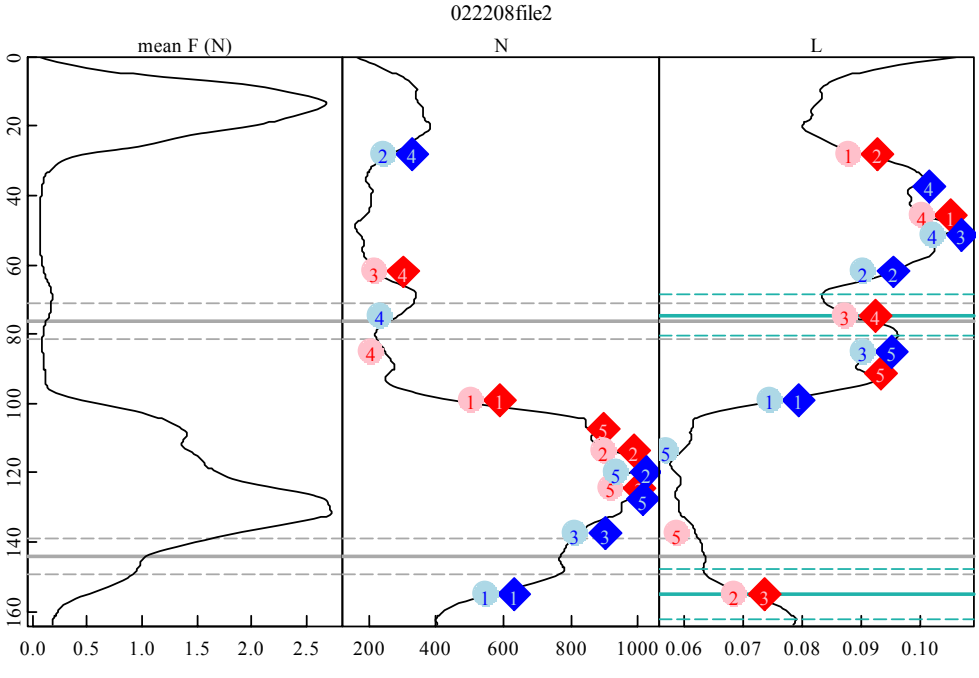

Figure 90: SMP Profile #10.

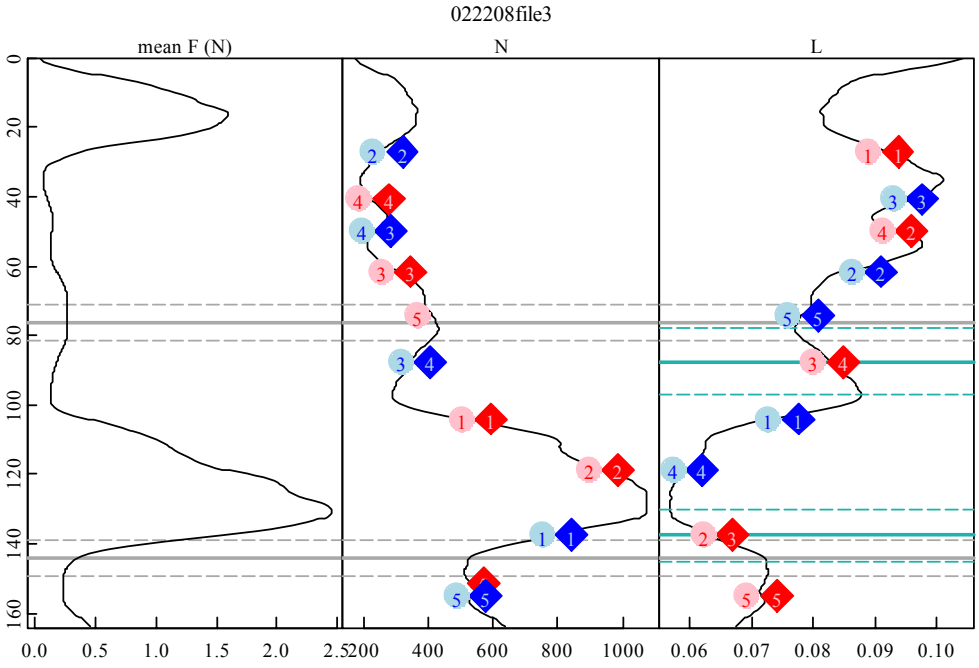

Figure 91: SMP Profile #11.

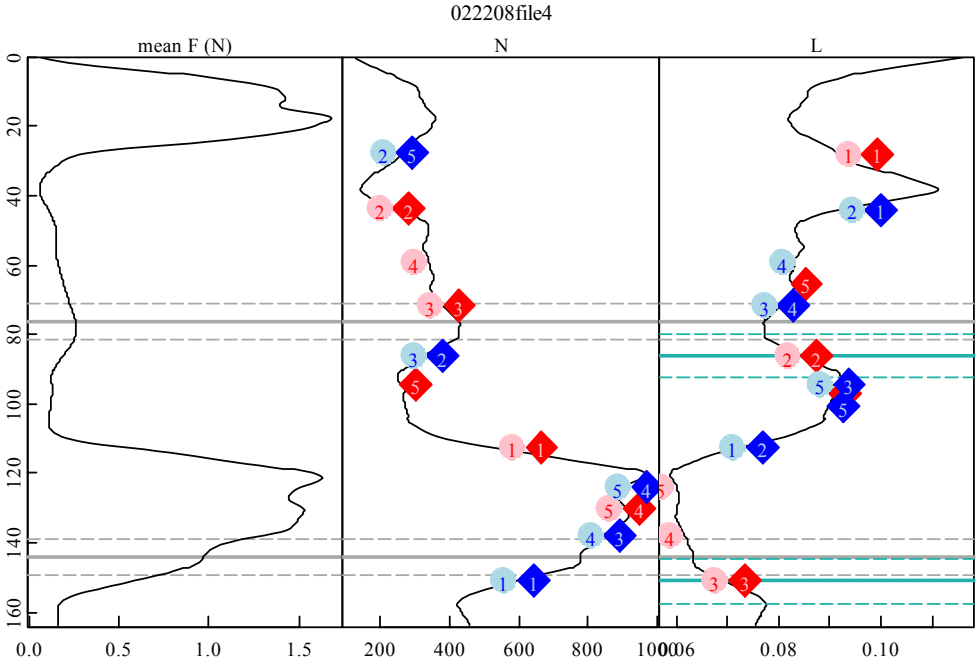

Figure 92: SMP Profile #12.

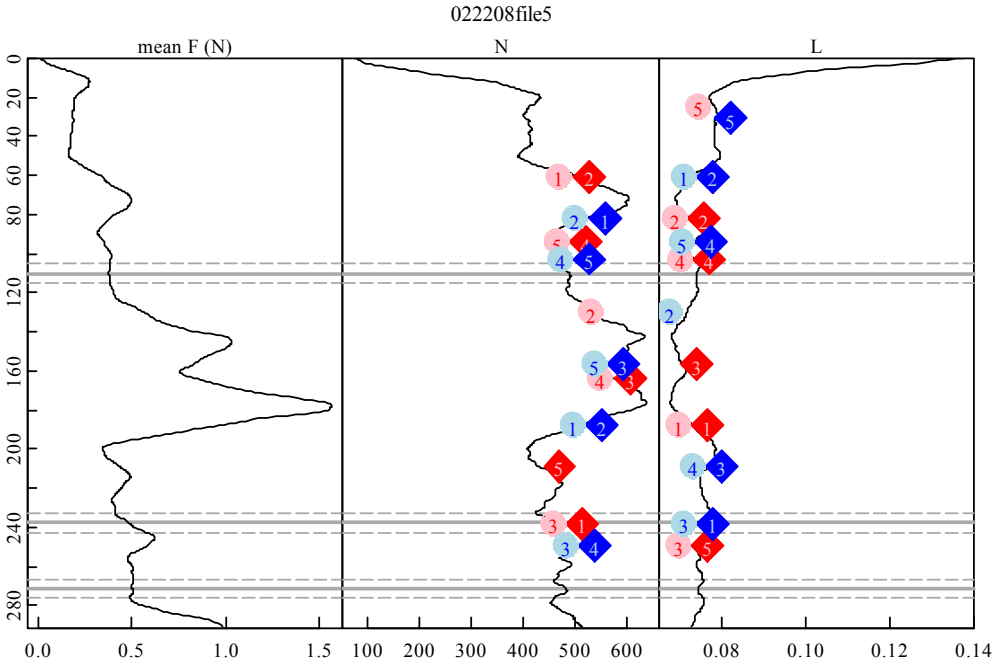

Figure 93: SMP Profile #13.

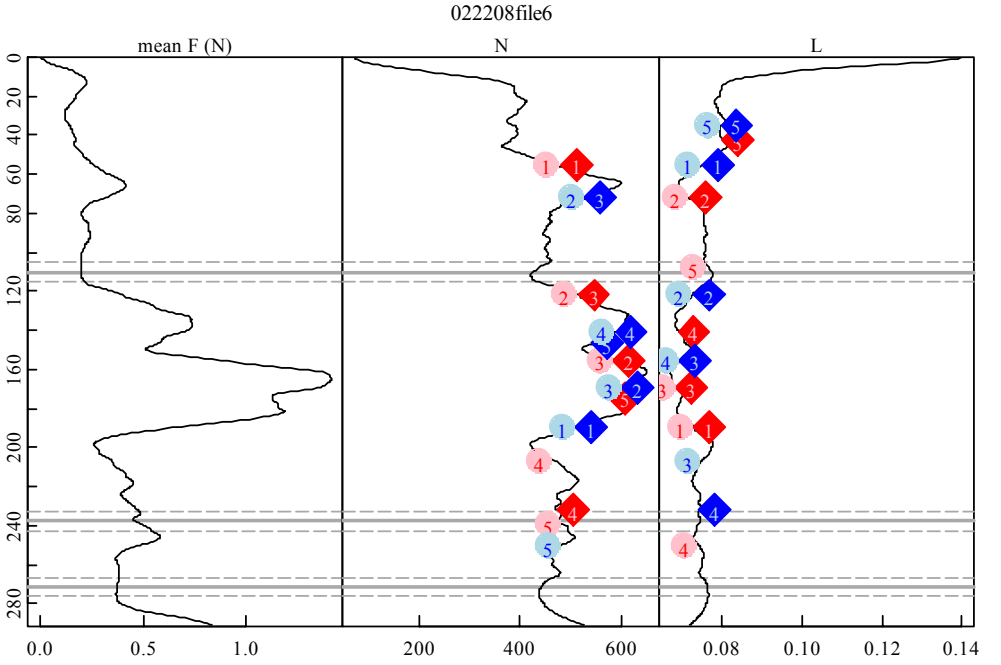

Figure 94: SMP Profile #14.

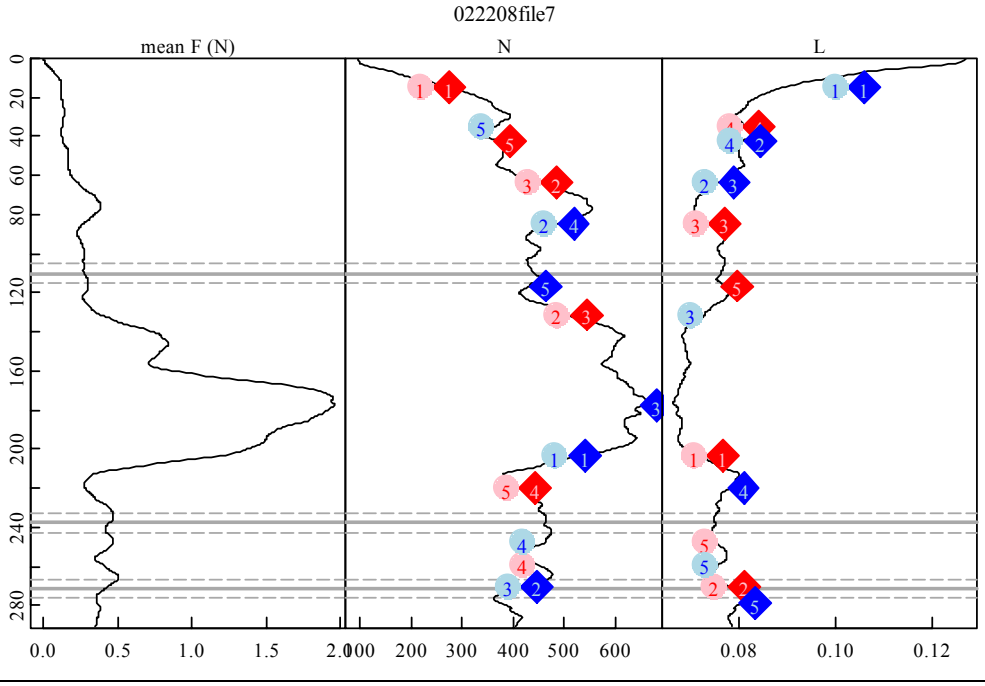

Figure 95: SMP Profile #15.

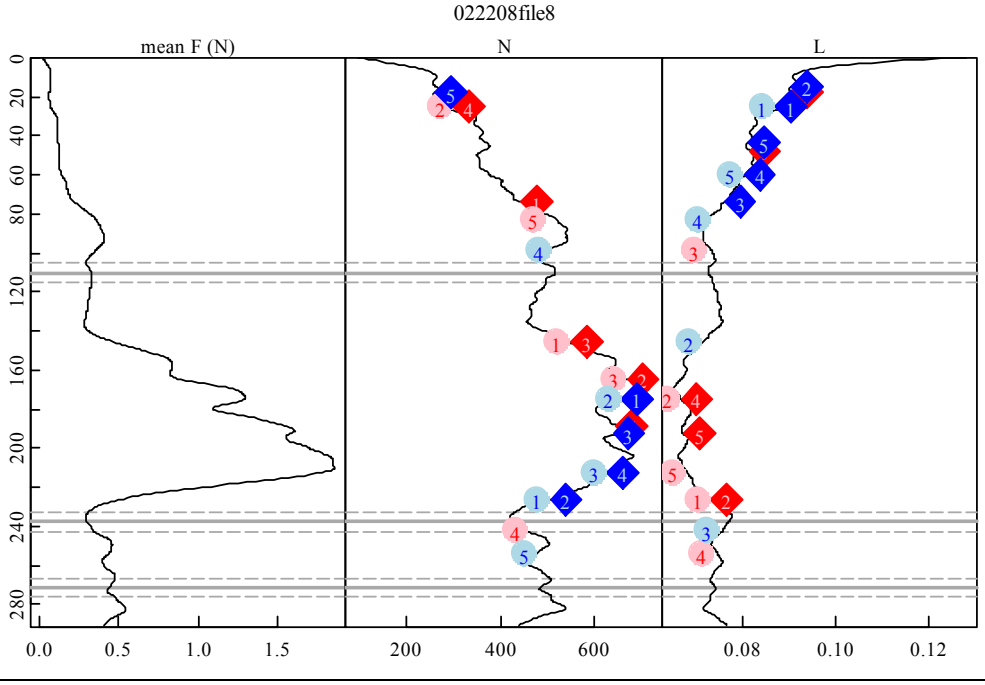

Figure 96: SMP Profile #16.

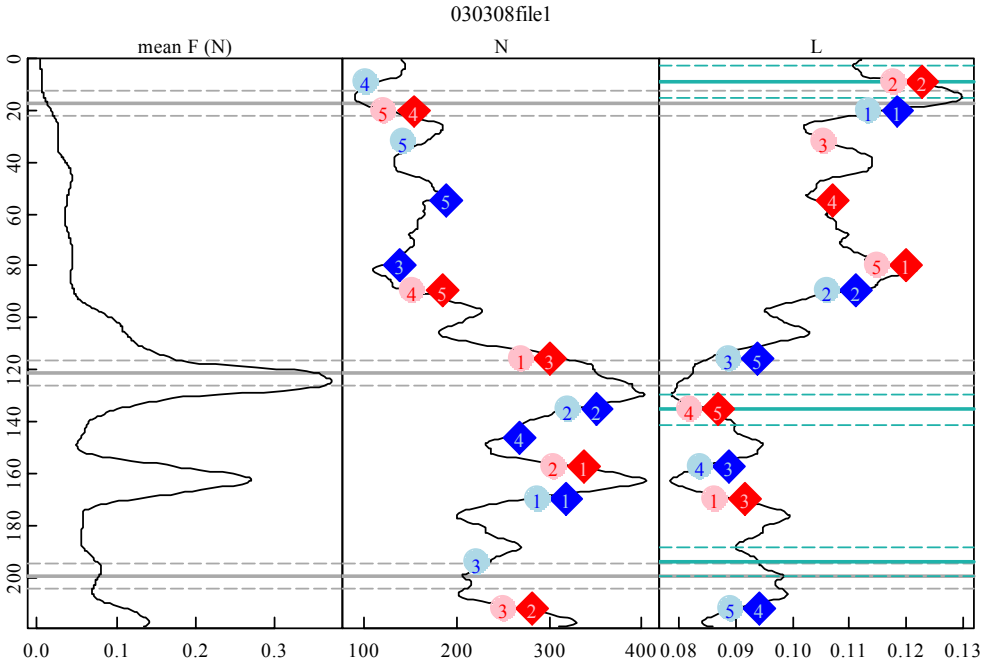

Figure 97: SMP Profile #17.

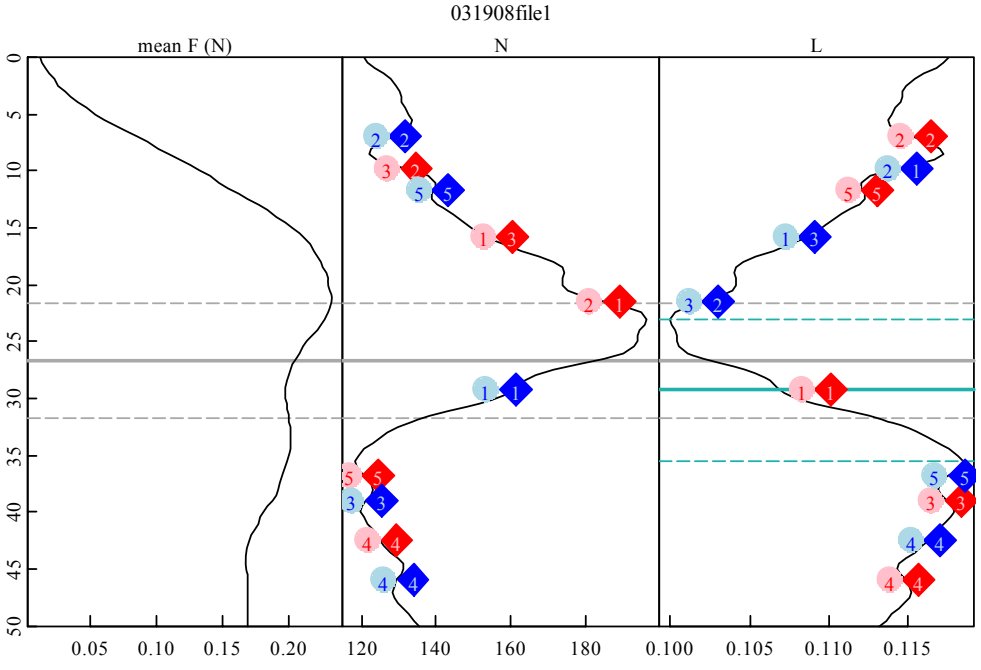

Figure 98: SMP Profile #18.

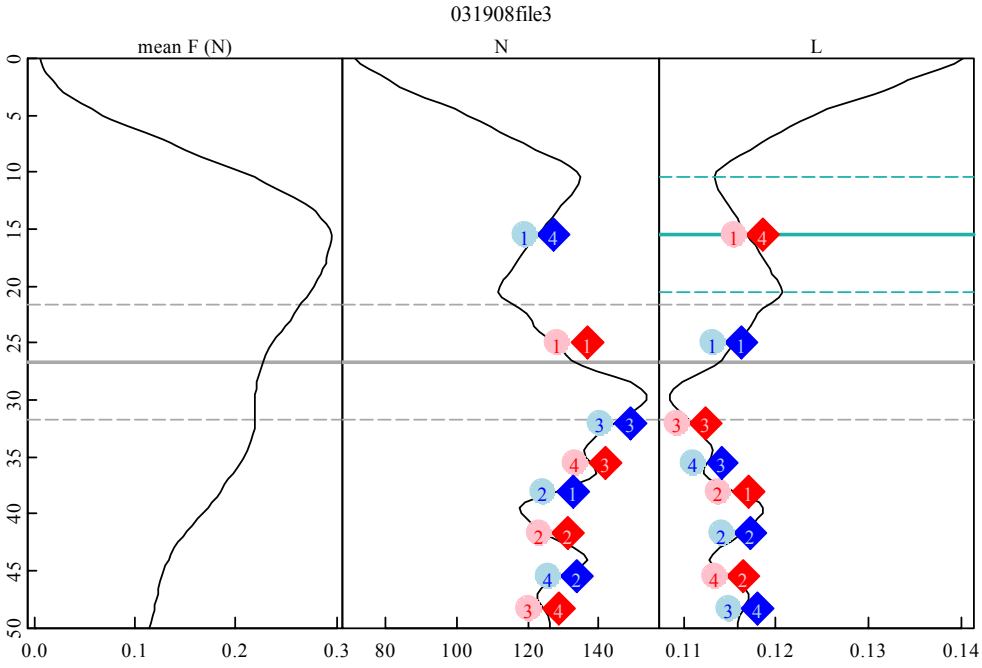

Figure 99: SMP Profile #19.

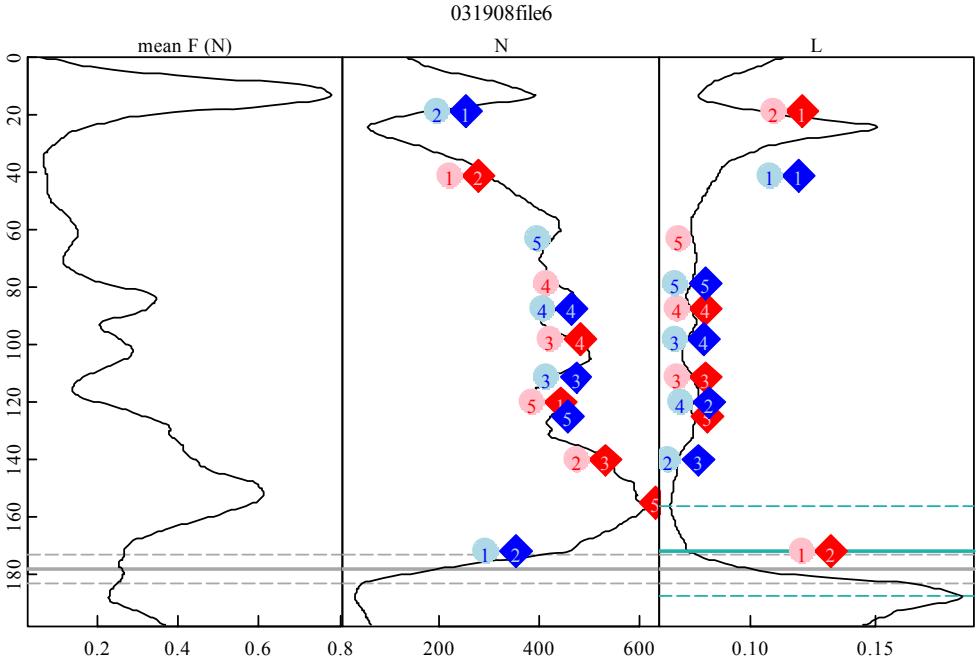

Figure 100: SMP Profile #20.

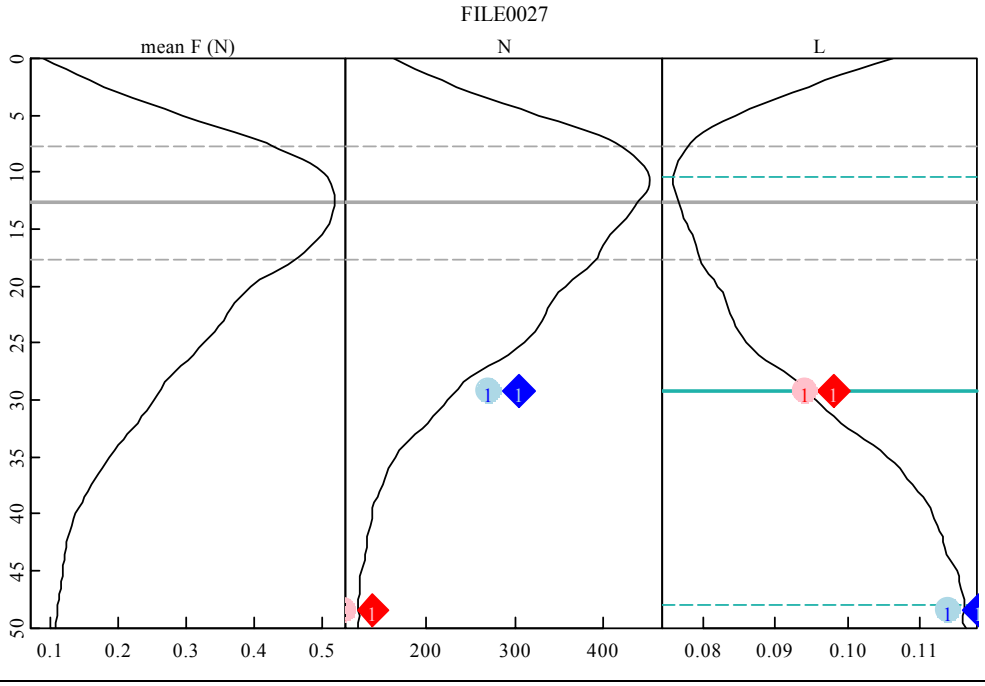

Figure 101: SMP Profile #21.

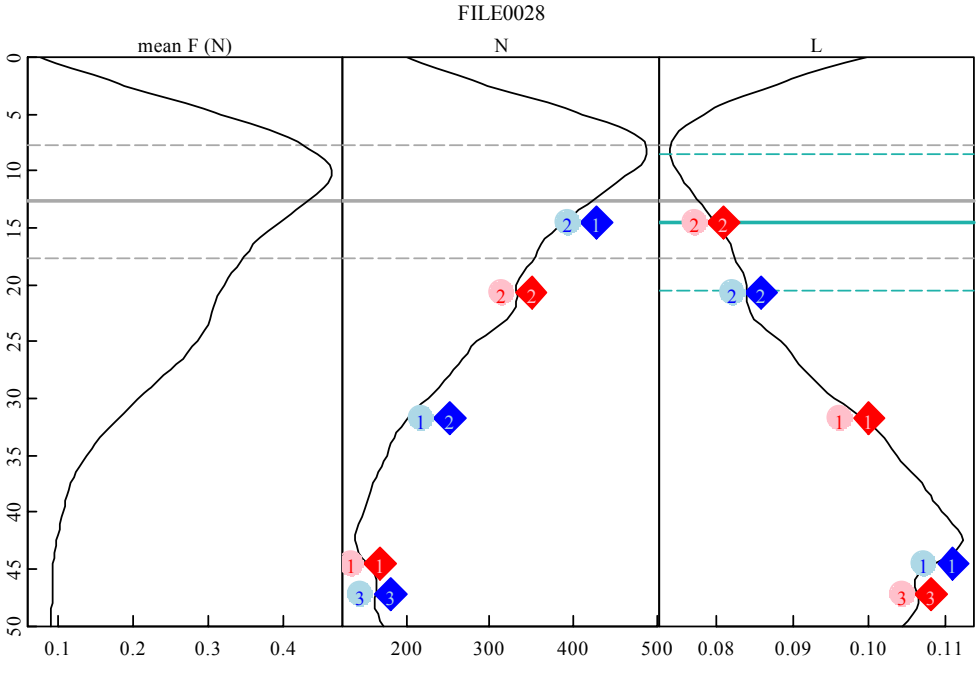

Figure 102: SMP Profile #22.

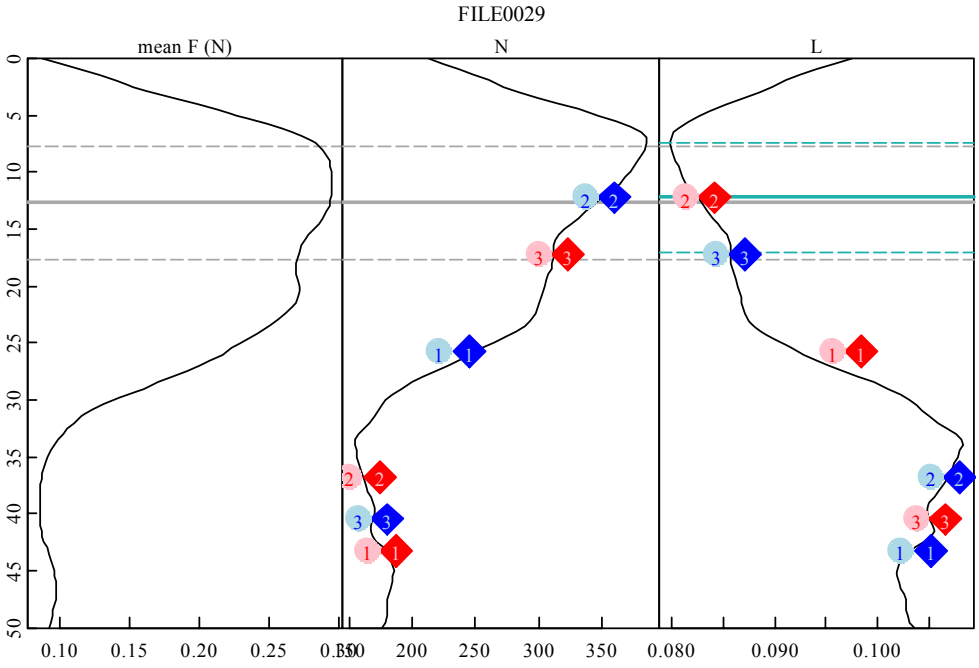

Figure 103: SMP Profile #23.

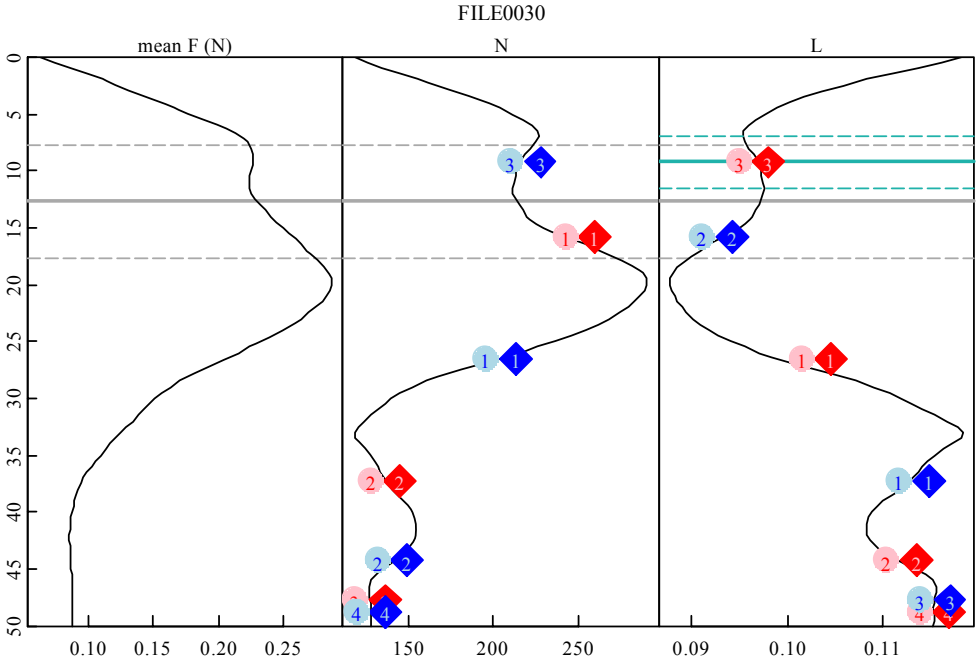

Figure 104: SMP Profile #24.

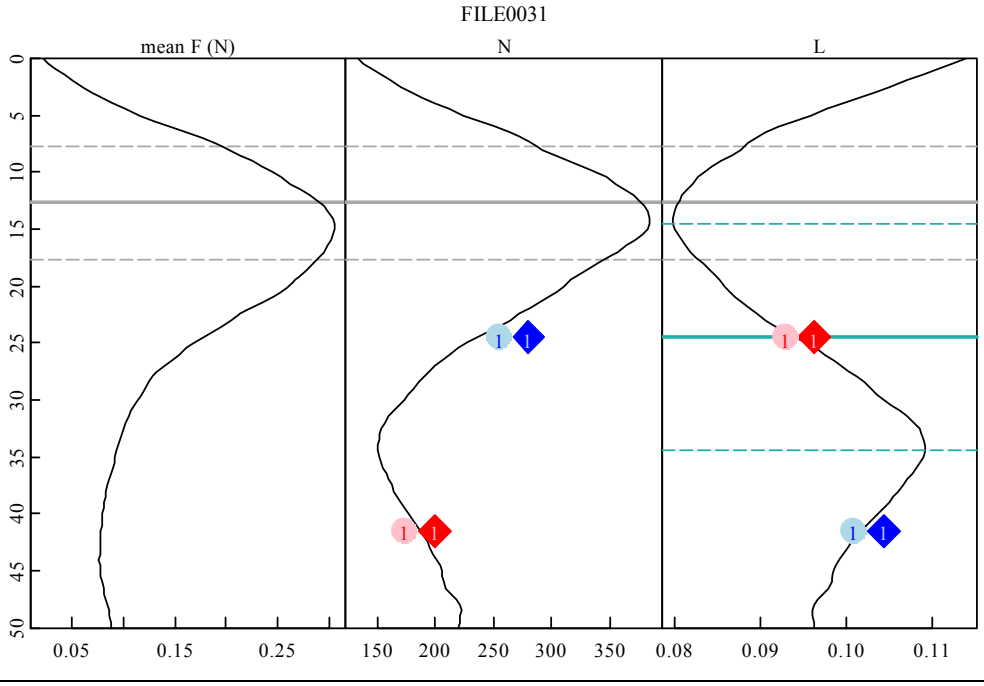

Figure 105: SMP Profile #25.

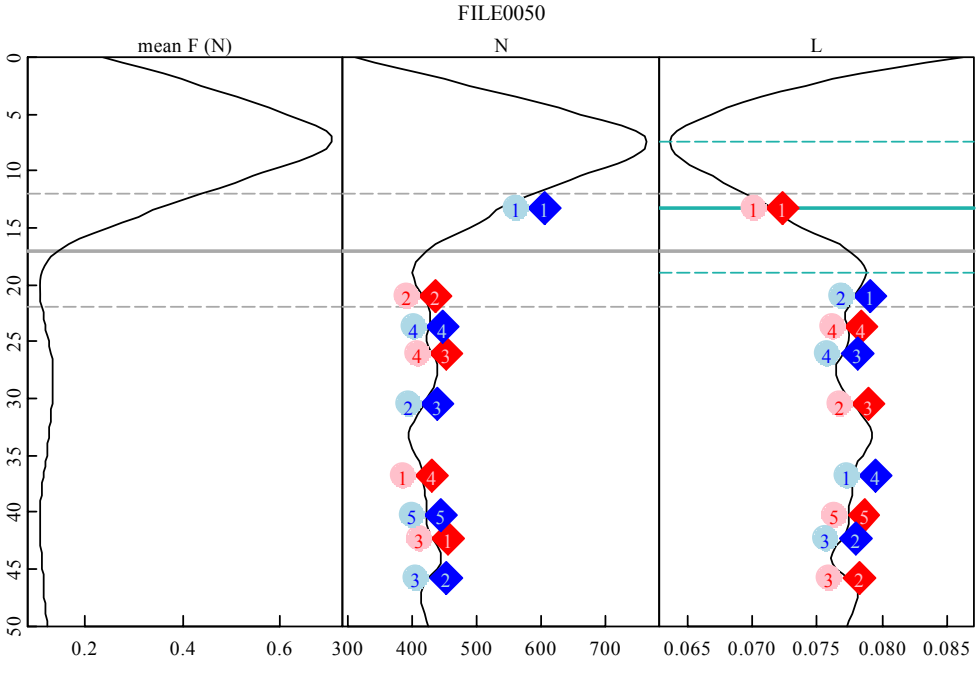

Figure 106: SMP Profile #26.

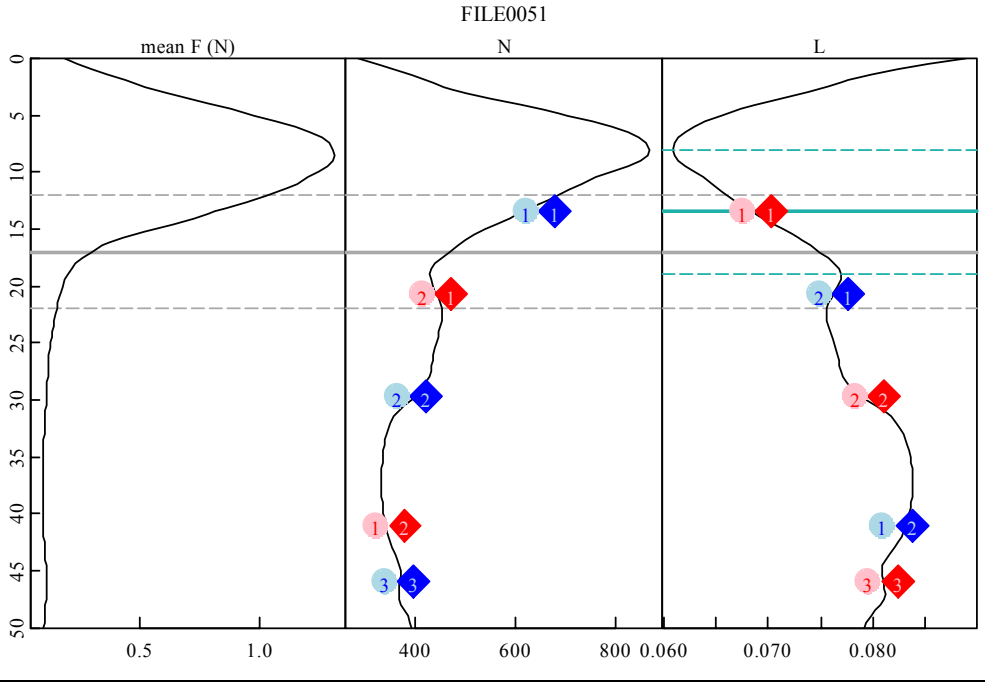

Figure 107: SMP Profile #27.

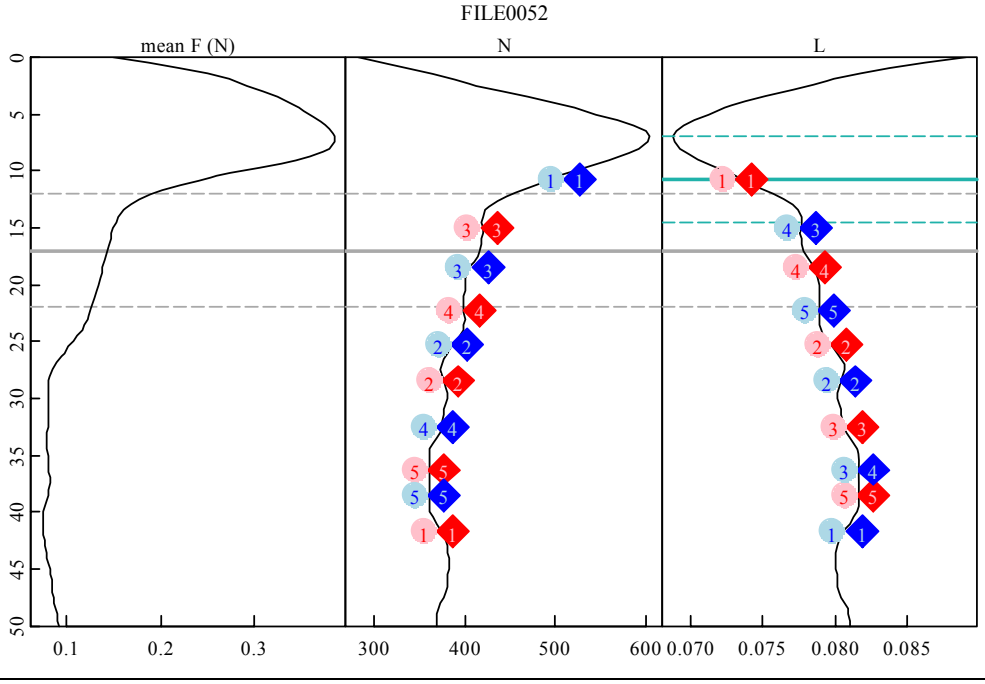

Figure 108: SMP Profile #28.

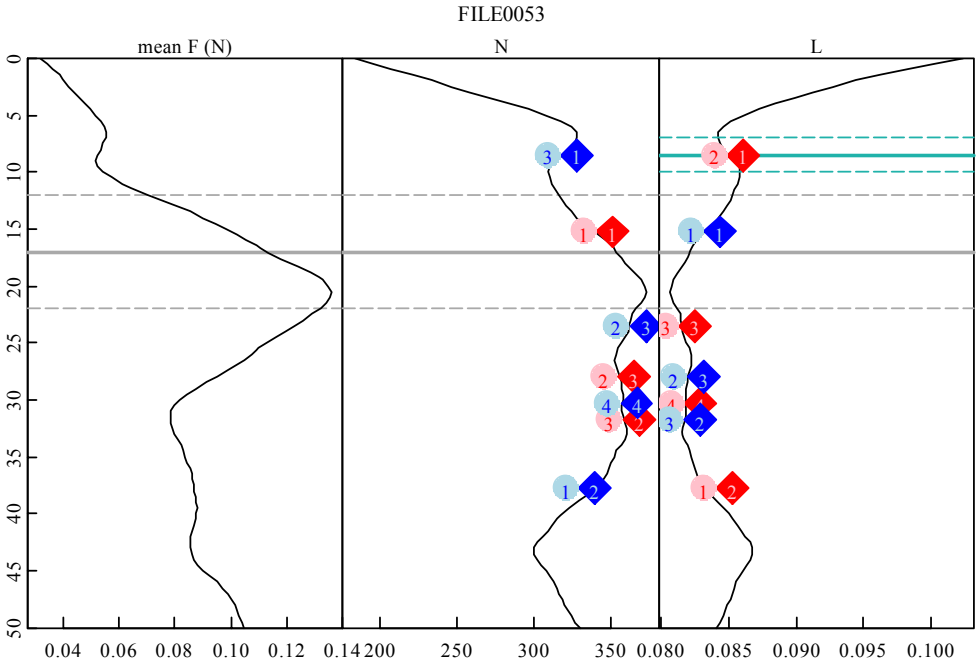

Figure 109: SMP Profile #29.

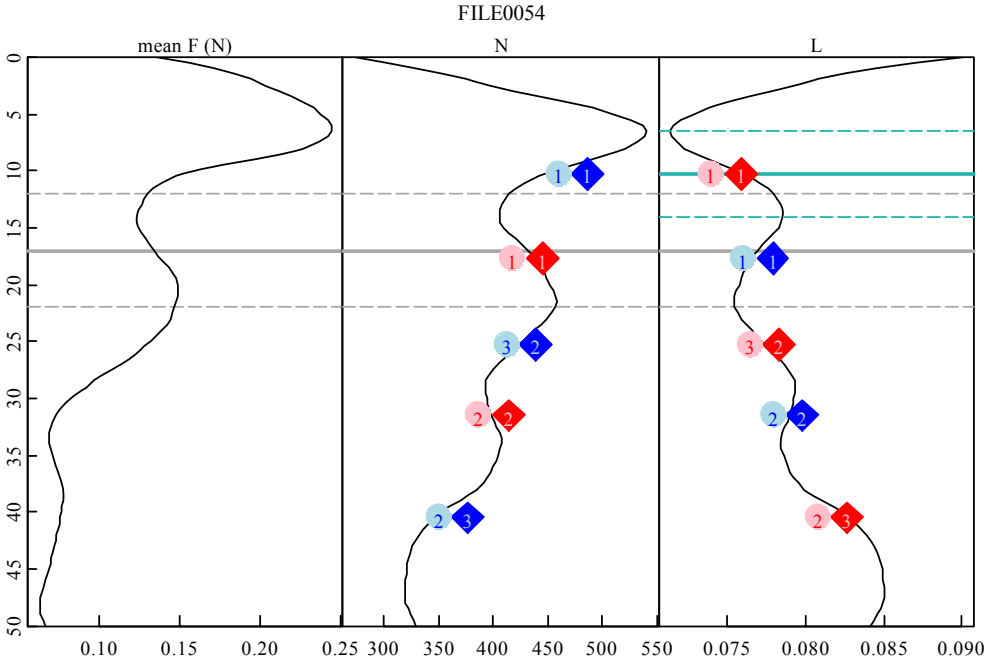

Figure 110: SMP Profile #30.